Shimane University
Interdisciplinary Faculty of Science and Engineering

Doctoral Thesis

Evolution of the fluvial systems and petrography of sedimentary rocks of the Miocene Siwalik Group, Karnali River section, Nepal Himalaya: implications for provenance, paleoclimate and Himalayan tectonics

by
Ashok Sigdel
(S109706)

Department of Materials Creation and Circulation Technology,
Shimane University, Japan

July 22, 2013

Evolution of the fluvial systems and petrography of sedimentary rocks of the Miocene Siwalik Group, Karnali River section, Nepal Himalaya: implications for provenance, paleoclimate and Himalayan tectonics

A dissertation submitted to the Department of Material Creation and Circulation Technology in partial fulfillment of the requirement for the Degree of Doctor of Science (D.Sc.)
at the Interdisciplinary Graduate School of Science and Engineering, Shimane University, Japan

by

Ashok Sigdel
(S109706)

July 22, 2013

Supervisor
Assoc. Prof. Tetsuya Sakai

Examination Committee
Prof. Hiroaki Ishiga
Prof. Yoshikazu Sampei
Prof. Toshiaki Irizuki
Assoc. Prof. Barry P. Roser

CONTENTS

CHAPTER-ONE

INTRODUCTION   1-4

CHAPTER-TWO

PREVIOUS STUDIES ON THE SIWALIK GROUP   5-10

CHAPTER-THREE

GEOLOGICAL SETTING   11-18

CHAPTER-FOUR

LITHOSTRATIGRAPHY   19-40

CHAPTER-FIVE

FLUVIAL FACIES   **41-62**

CHAPTER-EIGHT

ABSTRACT

Fluvial deposit of the Miocene Siwalik Group (4000–6500 m thick) was accumulated in the Himalaya foreland basin. The Siwalik Group is considered to be an important archive of Himalayan uplift and related climate changes. It is thought that uplift of the Himalaya affected world climate pattern. A noticeable effect was global cooling due to the absorption of carbon dioxide by the chemical weathering process induced by increased rainfall (Indian Summer Monsoon) due to uplift. Although several studies have been focused on the Siwalik Group by using different methods to reconstruct the monsoonal climate change, the lack of the studies on possible causes of the gap of the estimated timing of climate change is not yet clear. One probable cause is the effect of local climate change induced by local topography.

This study analyzes the fluvial successions of the Siwalik Group along the Karnali River, where the large paleo-Karnali River is presumed to have flowed, and in which local climatic effects should be minimal. Therefore, the Karnali River section is expected to contain a good record of regional changes in climate and tectonics. Because fluvial facies are directly affected by increased precipitation related to climate change and increase in sediment supply associated with uplift, lithostratigraphic and fluvial facies studies were conducted to understand the changes in depositional system. Petrographic analysis was also carried out to determine the sediment source area and related tectonic setting.

The newly established stratigraphy of the Karnali River section is: Chisapani Formation (equivalent to Lower Siwalik, (2045 m), Baka Formation (equivalent to Middle Siwalik, (2740 m), Kuine and Panikhola Gaun Formations (equivalent to Upper

Siwalik, 1500 m) in ascending order. The Chisapani Formation is composed of interbedded red mudstones and fine- to medium-grained sandstones. The Baka Formation is composed of medium- to coarse-grained 'salt and pepper', pebbly sandstones interbedded with greenish grey mudstones. The Kuine and Panikhola Gaun Formations consist of thick pebble, cobble to boulder conglomerates.

Based on facies analysis, six facies associations (FA1-FA6) were identified. The individual facies associations represent fine-grained meandering river systems (FA1), flood flow-dominated meandering river system (FA2), deep (FA3) and shallow (FA4) sandy braided river systems, followed by gravelly braided river systems (FA5) and a debris flow-dominated braided river system (FA6), respectively. The facies change from FA1 to FA2 is an important indicator of climate change. The change from fine-grained meandering river deposits with red soils (15.8-13.5 Ma) to the flood flow-dominated meandering river deposits with greenish grey mudstones (13.5-9.6 Ma) indicates increased water discharge after 13.5 Ma, which resulted from increased precipitation. Appearance of playa lake facies in FA2 also reflects a seasonal increase in precipitation. In contrast, the timing of this facies change ranges from 10.5 to 9.5 Ma in other Nepal Siwalik sections. The earlier facies changes in the Karnali River section at about 13.5 Ma may have been due to intensification of the Indian Summer Monsoon. Earlier uplift in the western Nepal Himalaya may also have caused higher orographic rainfall in this region. The change from a meandering river system to a braided river system at about 9.6 Ma is probably related to progradation of large alluvial fans in the ancient Indo-Gangatic Plain.

The results of petrographic analysis confirm that the sediments were mainly derived from the Higher Himalaya and the Lesser Himalaya throughout the deposition.

The Higher Himalaya was a major source terrain even in the early stage (16.0 Ma) of deposition, and Lesser Himalayan contribution increased after 13.0 Ma. This indicates the Lesser and the Higher Himalayas were deeply incised by the large paleo-Karnali River. The petrographic results along with previous studies from all Siwalik sections suggest the diachronous uplift of the Himalaya, which began earlier in far western Nepal.

The early uplift and related orographic rainfall are consistent with other studies which show extension of drier areas in western China and restriction of humid areas to southern China during the late middle Miocene (13.5 Ma). The uplift may have suppressed deep penetration of wind originating from the Indian Ocean to the Tibetan Plateau, creating a rain shadow zone in western China, and significant orographic rainfall in the frontal Himalaya.

List of Figures

Chapter 5

Chapter 6

List of Tables

Chapter 1

INTRODUCTION

1.1 Introduction

The Siwalik Group was deposited during Middle Miocene to Early Pleistocene in the Himalayan foreland basin system and is now occupied as the frontal part of the Himalayan fold thrust belt (Gansser, 1964; Johnson et al., 1983; Tokuoka et al., 1986; Burbank et al., 1996; DeCelles et al., 1998; Robinson et al., 2006). This Siwalik Group hosts about 6 km thick fluvial sediments deposited in foreland basin formed in front of the Himalaya (Prakash et al., 1980; Tokuoka et al., 1986).

The Siwalik Group is expected to be one of the good recorders of the regional changes in climate and Himalayan tectonics since 16.0 Ma. The uplift of the Himalaya then might have started to change in climate as well as changes in fluvial system. The noticeable climate change was the global cooling due to the absorption of carbon dioxide by the chemical weathering process induced by rainfall (Indian Summer Monsoon) due to uplift. Because of its great potential for elucidating the tectonics, climatic and erosional histories of the Himalaya, the Siwalik Group has been focused by numerous lithostratigraphic (Auden, 1935; Hagen, 1969; Gleinni and Zeigler, 1964; Opdyke et al., 1982; Sah et al., 1994) sedimentological (Tokuoka et al., 1986; Willis, 1993; Nakayama and Ulak, 1999) chronostratigraphic as well as isotopic studies (Quade et al., 1995; Dettman et al., 2001; Szulc et al., 2006). Carbon isotope analyses of paleosols showed that the major climatic shift occurred at 7-8 million years ago due to monsoon intensification (Quade et al., 1995). But some studies suggested that it occurred at around 10 million years ago (Tanaka, 1997). Fluvial facies studies suggested

the Monsoon intensification occurred at about 10.0 Ma (Nakayama and Ulak, 1999). Oxygen isotope studies mentioned that Indian Summer Monsoon has started at around 10.7 million years ago (Dettman et al., 2001). Recently, the age of Indian Summer Monsoon onset has been back at around 15.0 million year ago (e.g. Clift and Plumb, 2008). However, despite of these impressive previous works, there is no consensus on age gap on the timing of beginning of such climatic changes.

In my idea, the possible cause of this age gap was the effect of local climate changes by changing local topography. For the reliable depositional information and climate change, the river catchment system plays an important role. The small river system is sensitive for minor increase in water discharge due to precipitation by local topographic change. On the other hand, in large river system, the amount of discharge is not affected by the local precipitation resulted by local topography. It can minimize local precipitation reflecting regional precipitation. Therefore, the large river system should be analyzed for knowing the changing pattern of depositional environment and regional climate.

The present study analyzes the fluvial deposit of the Siwalik Group along the Karnali River (Fig 1.1), where the large paleo-Karnali River is presumed to have flowed based on previous petrographical and εNd isotopical analysis (Huyghe et al., 2005; Szulc et al., 2006), which show that the Siwalik Group of Karnali River host earlier evidence from the sediments supplied from the higher Himalaya and Lesser Himalaya. The study area has been the locus of a variety of studies (DMG, 1987, 2003; Gautam and Fujiwara, 2000; Huyghe et al., 2001; Szulc et al., 2006; Van der Beek et. al., 2006; Bernet et al., 2006). DMG (1987, 2003) examined the area on a broad scale and divided it into the Lower, Middle, and Upper Siwaliks. Gautam and Fujiwara
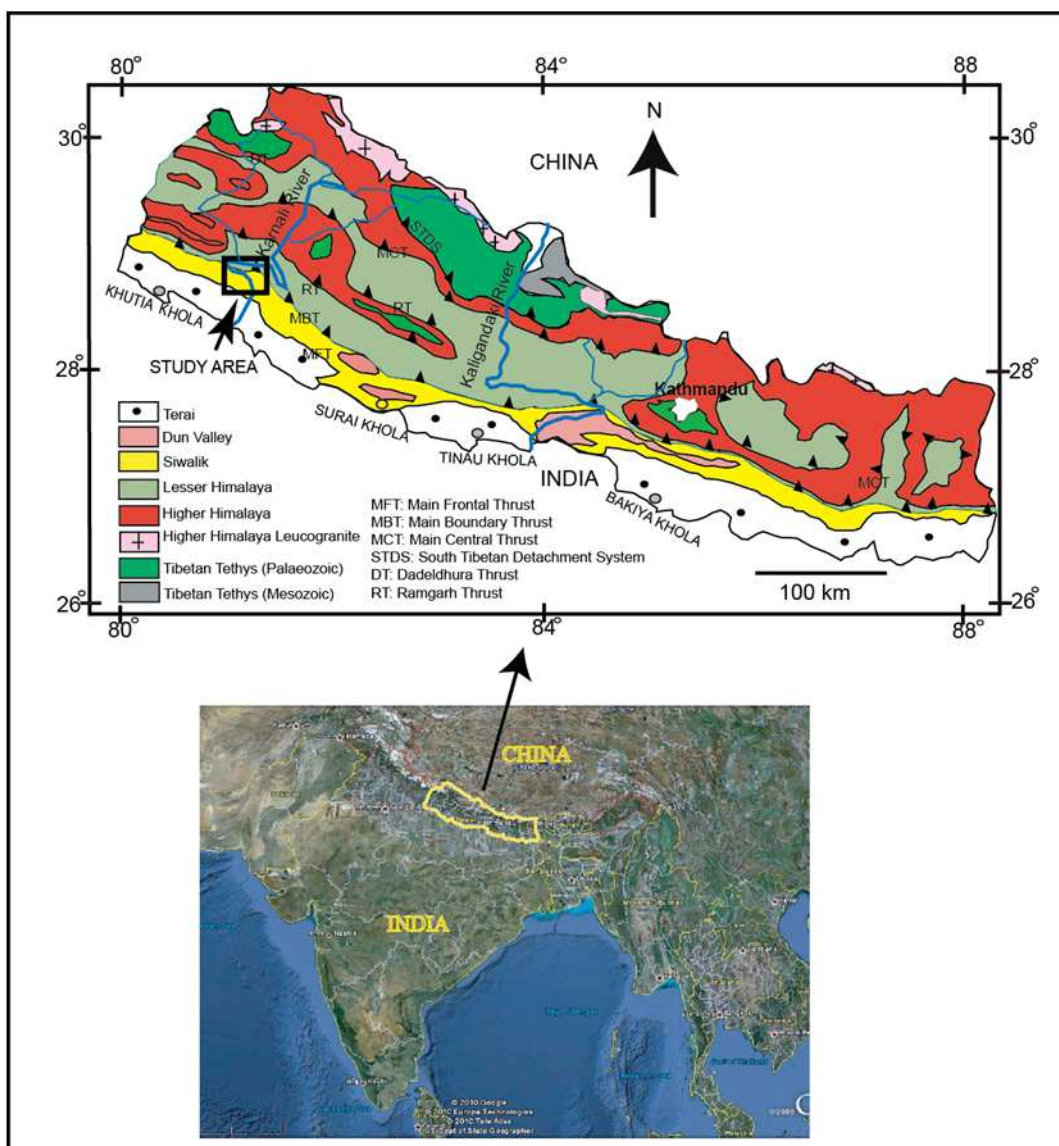
Fig. 1.1: Location map of the study area, bottom regional map taken from Google earth.

(2000) studied the magnetostratigraphy and some lithological characteristics of the sediments, and defined the Lower and Middle Siwaliks based on grain size and simply following the criteria proposed by Rösler et al. (1997) and Mugnier et al. (1998). However, they did not examine lithofacies characteristics at meter-scale and also did not define the exact Middle - Upper Siwalik boundary, and a large part of the Upper Siwalik remains unstudied and undated. Their study was thus incomplete, being focused on age,

3

and not on lithology. Huyghe et al. (2005) studied the depositional facies in broad scale and interpreted the similar order of fluvial systems with other area. However, their interpretation was limited by a lack of precise detail facies analysis at meter-scale. Szulc et al. (2006) studied the petrography of the sandstones from the limited samples, however, no detail information of detail petrographic analysis for provenance study. Although many studies have examined the petrography, εNd isotopes and age dating, no detail lithostratigraphic, and depositional facies information at meter-scale as well as petrographic data have been yet to be available for the Karnali River section.

The aims of this study are as follows:

➤ To establish a new lithostratigraphy of the area, to permit comparison and correlation among the different sections of the Siwalik Group of the Nepal Himalayas as well as and the Potwar Basin.

➤ To describe the detail depositional facies and to reappraise the fluvial facies classification of Huyghe et al. (2005).

➤ Detailed petrographic analysis to reveal the provenance, tectonic setting as well as catchment basin size and their change through time.

➤ To compare the lithostratigraphy, fluvial systems and provenance data with other Siwalik sections.

➤ To discuss the climatic change and Himalayan tectonics from the Siwalik Group sediments.

Chapter 2

PREVIOUS STUDIES ON THE SIWALIK GROUP

2.1 Lithostratigraphy

Stratigraphically, the Siwalik Group has been traditionally divided into Lower, Middle and Upper Siwaliks on the basis of lithological similarities to the type locality in the Potwar Basin (Piligram, 1913; Auden, 1935; Lewis, 1937; Hagen, 1964; Gleinni and Zeigler, 1964). The earliest lithological and paleontological observations of Siwaliks were made in Pakistan Siwaliks where tripartite subdivision based on lithology and six fold faunal zone nomenclature. The faunal zones (corresponding lithofacies) are Kamlial and Chinji (Lower Siwaliks) Nagri and Dhok Pathan (Middle Siwaliks) and Tratrot and Pinjor (Upper Siwaliks) along with several magnetostratigraphic works in the Potwar Plateau (Barry et al., 1985; Johnson et al., 1982, Burbank, 1996). These studies didn't differentiate either between lithostratigraphic, biostratigraphic or chronostratigraphic nomenclature to use of formation names. Several other subsequence studies established the stratigraphy based on proportion of sandstone and mudstone and are divided into Kamlial, Chinji, Nagri Dhok Pathan, Tetrot and Pinjor Formations (Fatmi, 1973; Johnson et al., 1982; Raza, 1983) which are now used as a standard stratigraphic nomenclature in Pakistan. In India, a classification based on the similar sequence of the Potwar Plateau has been broadly followed (Johnson et al., 1983; Tandon et al., 1984; Ranga Rao et al., 1988; Sangode et al., 1996; Kumarvel et al., 2005). The lithostratigraphy of the Siwalik Group in Nepal Himalaya has been studied by many authors (Auden, 1935; Glennie and Ziegler, 1964; Hagen 1969; Sharma, 1977; Yoshida and Arita, 1982; Tokuoka et al., 1986, 1990; Corvinus and Nanda 1994; Sah et

al., 1994; Dhital et al., 1995). The well-established three fold classification (Lower, Middle and Upper Siwaliks) was applied to the Nepalese Siwalik Group from beginning of geological survey (Auden, 1935; Hagen, 1969; Yoshida and Arita, 1982). But these divisions and correlations were mainly based on lithofacies, and individual formation boundaries were established based on changes in vertebrate fossils. Unfortunately, the Nepalese Siwaliks, unlike those type localities in Potwar region, are poor in vertebrate fossils therefore biostratigraphy has not been applied in Nepal Siwaliks sections for correlation. This paucity of biostratigraphic marker, lithological variability, lateral changes in facies and the varying degree of tectonic dissection have made tripartite division provisional, informal and inadequate for detailed mapping. Later, Tokuoka et al. (1986, 1990) established the four fold classification (Arun Khola Formation (A), Binai Khola Formation (B), Chitwan Formation (C) and Deorali Formation (D) in the Arung Khola-Tinau Khola area, west central Nepal. This classification was based on particle size (mudstone, sandstone and conglomerate) and more importantly proportion of sandstone and mudstone with some colour variability of mudstones and formation boundaries were given by magnetic polarity studies. They divided the upper Siwalik into two separate formations based on grain size. The debris flow deposit which lies in the upper most part of upper Siwalik considered as separate formation (Deorali Formation). The similar type of criteria was used for classification in Hetauda-Bakiya Khola area central and eastern Nepal (Harrison et al., 1993; Sah et al., 1994; Ulak and Nakayama, 1998) but nomenclature is different. Subsequently, Cornivus and Nanda (1994) established the lithostratigraphy and biostratigraphy of the Surai Khola area. Their classification and correlation mainly based on lithology and fossils. Subsequently, Dhital et al. (1995) retained the whole Siwalik belt around the Surai Khola area, western

Nepal and divided into five formations. According to Dhital et al. (1995), the lithological based criteria developed by Tokuoka et al. (1986, 1990) are not suitable in this area and their (Dhital et al.,1995), divisions were based on grain size, bed thickness, sedimentary structures and petrography of sandstones. From previously published lithostratigraphic works, it is clear that many difficulties and problems are encountered in establishing the stratigraphy and correlation of the Siwalik Group of Nepal Himalaya. The paucity of the fossils in all section of the Siwaliks from eastern to western part of Nepal causes difficulties for correlation. The lithologies are not similar (cf. Dhital et al., 1995) in all sections. Therefore, it is not easy to apply the distinct characteristics followed by previous researchers for classification in all sections as well as direct correlation is not possible due to diverse lithological criteria adapted in the different sections of the Siwalik Group.

2.2 Magnetostratigraphy

The paleomagnetic age data are not consistent in all area. For example, Tokuoka et al. (1986) established first paleomagnetic stratigraphy in the Tinau Khola section and correlated with the Potwar region Pakistan. But later, Gautam and Appel (1994) revised the magnetic polarity stratigraphy and modified the age boundaries of the formations in same locality. Several researchers also had attempt to established age boundaries of the formations in the Surai Khola (Appel et al., 1991; Appel and Rosler 1994) in different time periods. Similarly, Gautam and Fujiwara, (2000) established the age of Siwalik Group along the Karnali River section and mentioned the oldest section among the Nepal Siwaliks. Recently, Ojha et al. (2001, 2009) also established the new paleomagnetic age of the Khutia Khola and Surai Khola areas. From previously

published age data, it is difficult to fix the exact age boundaries of formation due to inconstancy which pose the difficulties in correlation.

2.3 Depositional facies

Studies on the fluvial facies in the Siwalik Group have been done by several researchers to interpret changes in the fluvial depositional systems in several sections in Pakistan, India as well as those in Nepal (Willis, 1993; Khan et al., 1997; Zaleha, 1997; Kumar et al., 2003; 2004; Tokuoka et al. 1986, 1990, 1994; Hisatomi and Tanaka, 1994; Nakayama and Ulak, 1999; Ulak and Nakayama, 2001; Huyghe et al., 2005). These studies reconstructed the meandering, sandy braided and gravelly braided river systems and revealed that order of appearance of the fluvial systems is consistence among the Siwalik sections but the timing of appearance of these changes differs among the sections.

2.4 Provenance and tectonics setting

Petrologic, thermochronologic, and geochemical analyses can provide a great deal of information on sediment provenance, source rock lithology, and the rate and timing of exhumation (e.g. Dickinson, 1985; McLennan et al., 1993; Garver et al., 1999). In the case of the Himalaya, the Siwalik Group holds important information on the late Tertiary exhumation history of this mountain belt and provenance of the sediments. For the central part of the Himalaya, most research in recent years was focused on sections of exposed Siwalik Group rocks in India and western and central Nepal, resulting in large datasets on the sediment petrology and zircon U–Pb

geochronology (e.g. Copeland & Harrison, 1990; DeCelles et al., 1998, 2000, 2004; White et al., 2001; Najman et al., 2004), apatite and zircon fission track and white mica ^{40}Ar–^{39}Ar thermochronology (Bernet et al., 2006; Szulc et al., 2006; Van der Beek et al., 2006; Chirouze et al., 2012), and εNd isotope geochemistry (Robinson et al., 2001; Huyghe et al., 2001, 2005). These researchers indicate that the sediments of the Siwaliks Group were mainly supplied from the Higher and Lesser Himalayan rocks and sediments composition varies in space and time. Their results suggested that the diachronous uplift and erosional unroofing may have caused the variations of sediments compositions among the areas.

2.5 Paleoclimate

Many proxy data are now available to interpret the Middle to Late Miocene monsoon climate in south Asia. Quade et al. (1989) documented the late Miocene shifts in δ^{13}C and δ^{18}O towards more positive values from the northern Pakistan. They interpreted the shift of δ^{13}C results as recording the shift from C3 to C4 type vegetation, i.e. forest to grassland, given that plant-respired CO_2 is the main source of carbon in pedogenic carbonate. The spread of C4 grasslands was in turn taken to represent onset of strong monsoon conditions in the region. Harrison et al. (1993) found a similar shift in δ^{13}C in pedogenic carbonates from the southeast Nepal at 7.0 Ma. Quade et al. (1995) also reported a positive shift in δ^{18}O of paleosols from the Nepalese sections, occurring at 6.0 Ma, i.e. about 2.0 Myr younger than in Pakistan. But some analyses suggested that the climatic change was occurred around 10 million years ago from isotopic analysis of the paleosols (Tanaka et al., 1997). Nakayama and Ulak (1999) and Ulak and Nakayama (2001) documented the climatic change occurred at 10 Ma from the fluvial

facies studies in Nepal. Dettman et al. (2001) analyzed δ^{18}O of freshwater bivalve shells and mammal teeth to study seasonal variation of surface waters in the late Miocene and Pliocene. The change in values over this period inferred an intense monsoon and high plateau must have been present at least before 10.7 Ma, with the implication that the Tibetan plateau was high and wide enough through this time to create a monsoon system similar to the present day. Increase in δ^{13}C and decrease in δ^{18}O values of soil carbonate nodules in India were interpreted by Sanyal et al. (2004) to indicate (i) a switch from C3 to C4 type vegetation, and (ii) monsoon onset by 6 Ma, with a possible earlier peak at 10 Ma. Ganjoo and Shaker (2007) documented the geochemical and micromorphological studies of the paleosols from the India (Ramnagar member) and suggested the paleosols formation under wet and humid climatic conditions due to the early uplift of the Tibetan Plateau/Himalaya resulted in a contemporaneous change in precipitation and monsoonal climate conditions within the Indian region beginning in Middle Miocene. Singh et al. (2012) also studied the paleosols which reconstructed the progressive increase in aridity from ~12 Ma to Recent excluding a short term increases in rainfall or monsoon intensity at around 10 Ma, 5 Ma and 1.8 Ma. However, despite of these impressive previous works, there is no consensus on timing of beginning of such climatic changes.

Chapter 3

GEOLOGICAL SETTING

3.1 Geology of Nepal Himalaya

The Nepal Himalaya is one of the important parts of entire Himalayan Range. In the entire 2400 km long Himalayan Range, it is about 800 km long and occupies the central part (Fig 3.1). It is generally accepted that the youngest and highest peaks were formed by collision of the northward moving Indian continent with the Eurasian plate, started at about 60 Ma (Patriat and Achache, 1984; Chen et al. 1993; Bordet, 1955, 1972). The collision activity is manifest in the present day northward movement of India at the rate of 5 cm per year (Seeber and Armbruster, 1981; Jackson and Bilham, 1994; Pandey et al., 1995). This movement is accommodated within the Himalayas by activities of various thrusts and folds, nappes regional metamorphism and generation of leucogranite plutons (Le Fort, 1975, 1996; Vanney and Hodges, 1996; Harrison et al., 1998; Hodges, 2000). The basic framework of the Himalaya is controlled by the three major thrusts that extend throughout the Himalaya range longitudinally. These are the Main Central Thrust (MCT), the Main Boundary Thrust (MBT) and the Main Frontal Thrust (MFT). The MCT was the first thrust to break the Indian crust. The MCT separates the highly metamorphosed Higher Himalayan rocks from the less metamorphosed Lesser Himalayan rocks. It was active at about 22 Ma (Hubbard and Harrison, 1989) and reactivated around 15.0 and 12.0 Ma, again 6.0 and 8.0 Ma (Harrison et al., 1998)
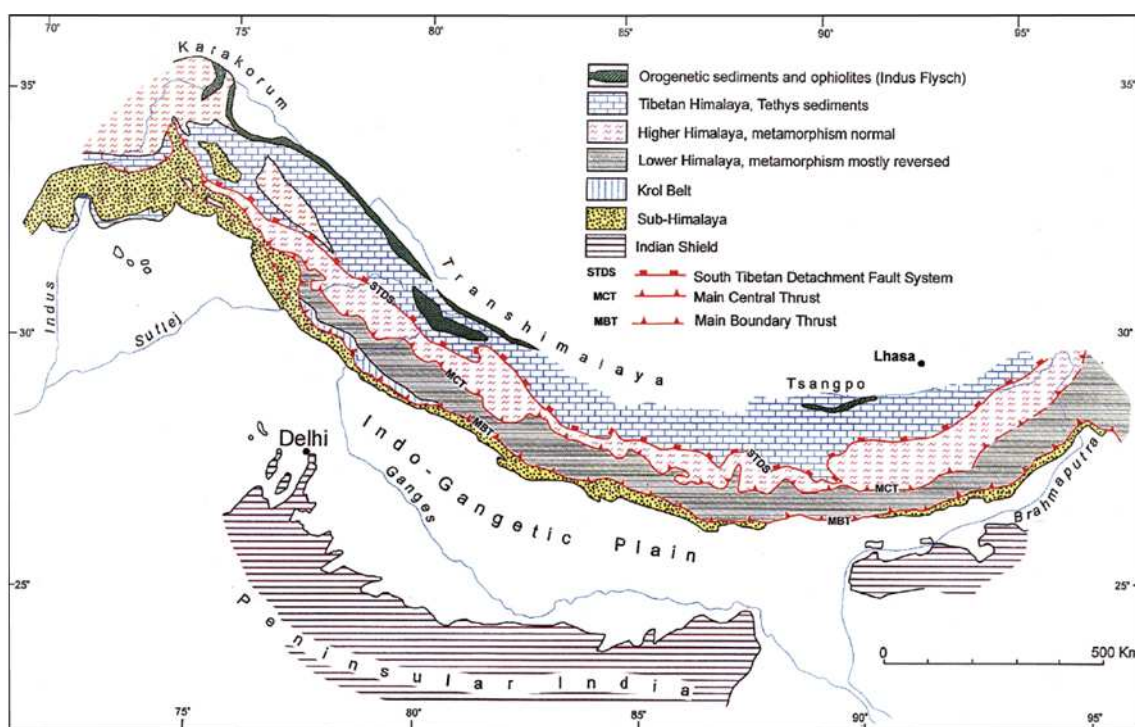
Fig. 3.1: Physiographic subdivision of the Himalayan arc (after Gansser, 1964).

The MBT is separating the synorogenic sediments of the Siwalik Group from the Lesser Himalayan rocks. The MFT brought the Siwalik Group over the Gangetic Plain (Valdiya, 1998). Tectonically, Nepal Himalaya is divided into the following five major tectonic zones (Fig. 3.2) from the north to south.

1. Tibetan-Tethys Zone

2. Higher Himalayan Zone

3. Lesser Himalayan Zone

4. Sub-Himalayan Zone (Siwaliks or Churia)

5. Terai Plain

3.1.1 Tibetan-Tethys Zone

The northernmost tectonic zone of the Himalayas occupies a wide belt consisting of sedimentary rocks known as the Tibetan Tethys Zone. The Tibetan Tethys Zone lies between the South Tibetan Detachment System (STDS), a north dipping normal fault and the Indus-Tsangpo Sutures Zone (ITS). It has undergone very little metamorphism, except at its base where it is close to the Higher Himalaya Zone. The rocks of this zone consists of thick and nearly continuous lower Paleozoic to lower Tertiary marine, highly fossiliferous sedimentary successions including slate, sandstone and limestone. The rocks are considered to have been deposited in a part of the Indian passive continental margin (Liu and Einsele, 1994).

3.1.2 Higher Himalayan Zone

Heim and Gansser (1939) firstly identified and described the Central Himalaya Crystalline Zone in Kumaon area in India and mapped it along the entire Himalaya Range. Geologically, the Higher Himalaya Zone in Nepal represents the Central Crystalline Zone and lies to the north of, and above the Main Central Thrust (MCT) and below the Tibetan Tethys Zone (Upreti, 1999). The metamorphism occurred due to the intrusion of leucogranites after the collision of the continents as a result of the formation of the MCT (Le Fort, 1975). The Higher Himalaya Zone is composed of various gneisses, schists and migmatites extend continuously along the entire length of the Nepal Himalaya. The thickness of this zone is about 6 to 12 km. It is now generally accepted that the series of STDS fault separated the Higher Himalaya Zone from the Tibetan Tethys Zone (Burchfiel et al., 1992). This zone has been divided into four main

units, the kyanite-sillimanite gneiss, pyroxenic marble and gneiss, banded gneiss, and augen gneiss in the ascending order (Bordet et al., 1972).
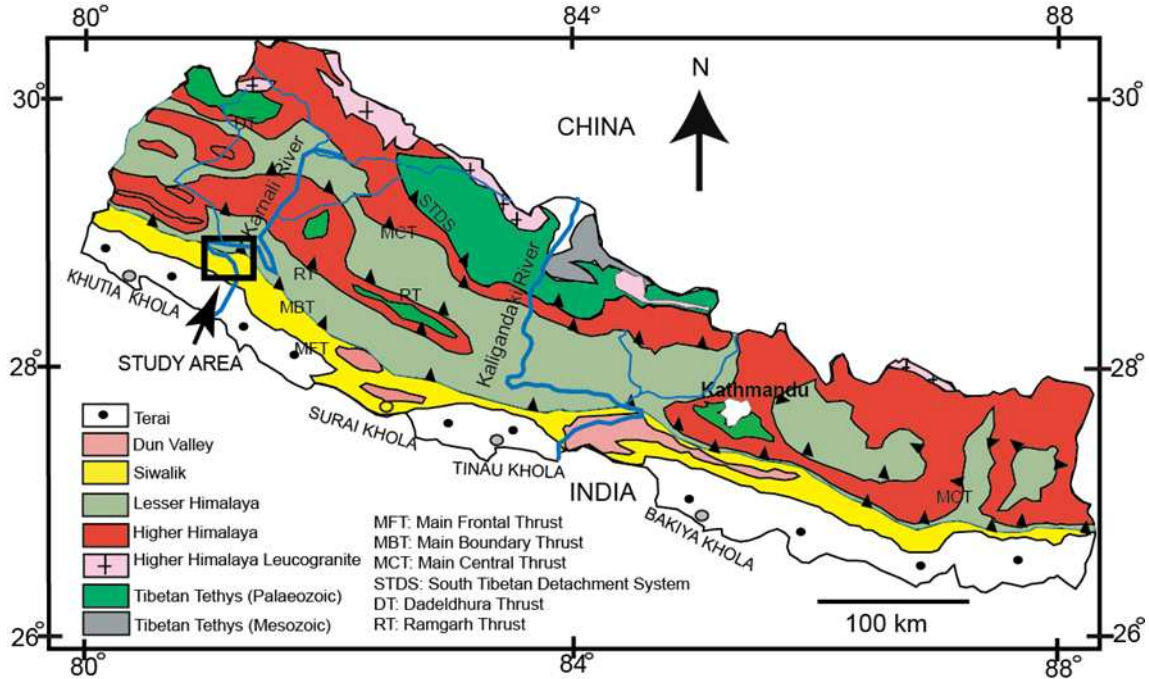
Fig. 3.2: Generalized geological map of the Nepal Himalaya (modified from Amatya and Jnawali, 1994).

3.1.3 Lesser Himalayan Zone

The Lesser Himalaya Zone lies between the Sub-Himalaya and Higher Himalaya, which is separated by the Main Boundary Thrust (MBT) and the Main Central Thrust (MCT) in south and north respectively. Tectonically, this zone is composed of low grade metasedimentary rocks, with overriding crystalline nappes and klippes (Upreti, 1999). The total width ranges from 60-80 km. The Lesser Himalayan rocks are divided into two groups (Upreti, 1999). Older Lesser Himalaya Formation and younger Lesser Himalaya Formation are separated by major unconformities (Valdiya, 1995, 1998). The older formation is Precambrian in age (from 1800-2000 Ma to 570 Ma) (Perrish and Hodges, 1996). The younger formations are the Gondwana

14

sedimentary rocks in Permo-carboniferous age through to marine rocks in the early Cretaceous to Eocene age (Sakai, 1983, 1985), and finally capped by the fluvial Dumri Formation (late Oligocene to early Miocene). It is also composed of unfossiliferous sedimentary and metasedimentary rocks including slate, phyllite, schist, quartzite, limestone, and dolomite etc. The geology of this zone is complicated due to folding, faulting and thrusting.

3.1.4 Sub-Himalayan Zone (Churia or Siwalik)

The Sub Himalayan Zone is occupied by the Himalayan foreland basins deposits. The zone forms the largest foreland basin accumulated on the Earth, and consists of the Neogene fluvial sediments in the southernmost hills in Nepal, i.e. Churia hills. It is delimited by the Main Frontal Thrust (MFT) to the south and the Main Boundary Thrust (MBT) to the north. The Lesser Himalaya metasedimentary rocks have been thrust southward over the Churia rocks along the MBT, and a large part of the Churia Group rocks are burried beneath the cover of the overthrusting Lesser Himalayan rocks to the north (Upreti, 1999). The Siwalik Group consists of very thick (4000 to 6500 m) molasse-like fluvial sedimentary deposits. Detailed geology and stratigraphy is described in section 3.2.

3.1.5 Terai Plain

This zone represents the northern border of the Indo-Gangetic alluvial plain and forms the southernmost tectonic zone of the Nepal Himalaya. It is delimited by the Main Frontal Thrust (MFT) to the north, which is exposed at many places. At many places along this thrust, the Churia rocks are exposed over the Terai sediments. The

Terai plain gradually rises from 60 m above the sea level in the south to more than 200 m in the north. It is covered by Quaternary to Recent sediments which is about 1500 m thick. The recent alluvium is mainly derived from the Churia Hills (Siwaliks) and also from the Lesser Himalaya by the river systems.

3.2 General geology and stratigraphy of the Siwalik Group

The Siwalik Group represents ancient Gangetic plain deposits. The sediments were supplied from the north as a result of upliftment and erosion of the Himalaya. Its thickness varies laterally (4,000 – 6,500 m thick), becoming thinner to the east (DeCelles et al., 1998; Mugnier et al., 1999; Ojha et al., 2000). The mudstones are dominated in the Lower Siwalik, sandstones are dominated in the middle Siwalik and conglomerates are dominated in the Upper Siwalik. The age of the Siwalik Group in Nepal ranges from 15.8 to 1 Ma on the basis of paleomagnetic studies along the Khutia Khola, Karnali River, Surai Khola section, Tinau Khola section, and Hetauda Bakiya Khola section The generalized stratigraphy and correlation of the Siwalik Group summarized in Table 3.1.

Auden (1935)	Glennie & Ziegler (1964)	Hagen (1969)	Sharma (1973)	Yoshida & Arita (1982)	Tokuoka et al. (1986, 1988)	Sah et al. (1994), Ulak and Nakayama (1998)	Corvinus & Nanda, (1994) and Dhital et al. (1995)	DMG(1987, 2003) Ojha et al.(2000), Gautam and Fujiwara (2000), Robinson et al. (2006),	Present study
1	2	3	4	5	6	7	8	9	10
Upper Siwalik	Conglomerate facies	Upper Siwalik	Upper Churia Group	Upper Siwalik	Deorali Formation	Churia Mai Formation	Dhan Khola Formation	Upper Siwalik	Panikhola Gaun Formation
					Chitwan Formation	Churia Khola Formation	Dobata Formation		Kuine Formation
Middle Siwalik		Middle Siwalik		Middle Siwalik	Binai Khola Formation	Amlekhganj Formation	Surai Khola Formation	Middle Siwalik	Baka Formation
	Sandstone facies		Lower Churia Group				Chor Khola Formation		
Lower Siwalik		Lower Siwalik		Lower Siwalik	Arung Khola Formation	Rapti Formation		Lower Siwalik	Chisapani Formation
							Bankas Formation		

1) Udaipur Garhi-Anraha and Amlekhganj-Sanotar areas; 2) Kali Ganga, Sarda river, Taptakunda, Koilabas, Butwal, Kaligandaki, Amlekhganj, Hetauda and Saptakoshi areas; 3) Various parts of Nepalese Siwaliks; 4) Dang, Koilabas, Butwal, Amlekhganj, Trijuga and Kankai River areas; 5) Surai Khola, Patharkot, Banganga, Butwal, Narayani River and Hetauda areas; 6) Arung Khola, Tinau Khola, Binai Khola areas; 7) Amlekhganj, Hetauda, Bakiya Khola areas; 8) Surai Khola; 9) Far western Nepal around the Khutia Khola and Karnali River 10) Karnali River

Table 3.1: Classification of the Siwalik Group of the Nepal Himalaya.
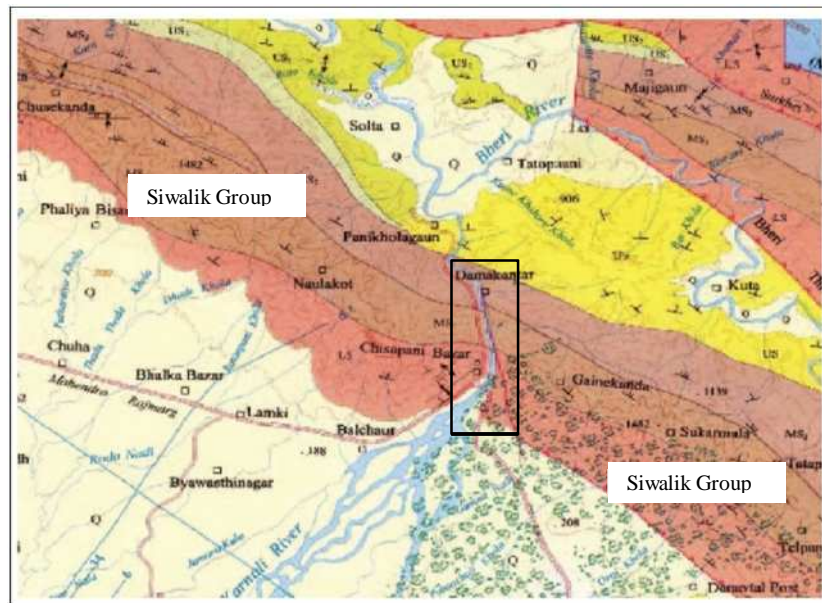
Fig. 3.3: Regional geological map of the far western Nepal (DMG, 2003). The Enclosed rectangle indicates the study area.

3.3 Geological setting along the Karnali River area

The tripartite lithological division (Lower, Middle and Upper) has previously been applied to the Siwalik Group in the Karnali area (DMG 1987, 2003, Mugnier et al., 1998, 1999) (Fig. 3.3). The age range up to the Middle Siwalik (15.8 to 5.2 Ma) was obtained by paleomagnetic study (Gautam and Fujiwara, 2000). Structurally, this section consists of two large belts separated by the MDT, which is an extensive and major and intra-Siwalik thrust (Mugnier et al., 1999) (Fig. 3.4). The southern belt is about 12 km N-S wide. The previous work indicated that this belt contains all three lithologic units (Lower, Middle and Upper Siwaliks), and had a total thickness of 4-6 km (Mugnier et al., 1998). The northern belt is about 6 km in width. This study focuses on the southern belt, because of the presence of good exposures from the lowermost to the uppermost part of the Siwalik Group, between Chisapani Bazaar in the south, and Panikhola Gaun Village in the north. The northern belt is mostly covered by forest, and exposure is poor. It is thus excluded from this study.
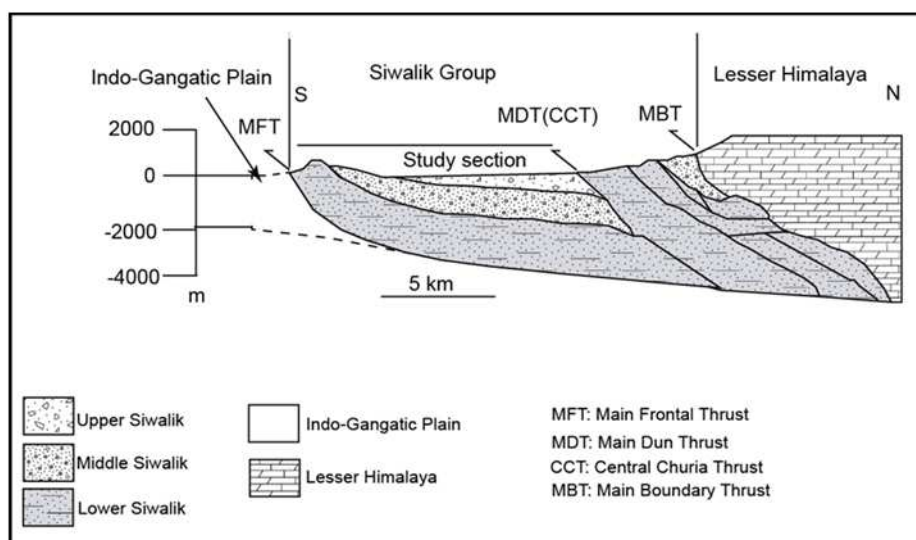
Fig. 3.4: Cross-section along the Karnali River section showing relation between the northern and southern belts of the Siwalik Group (modified from Mugnier et al., 1999).

Chapter 4

LITHOSTRATIGRAPHY

4.1 Introduction

The Karnali River section of the far western Nepal has been the locus of a variety of studies (Gautam and Fujiwara, 2000; Huyghe et al., 2005; Szulc et al., 2006; Van der Beek et. al., 2006; Bernet et al., 2006). These studies focused on petrography, isotopes and age dating. DMG (1987, 2003) examined the area on a broad scale and divided it into the Lower, Middle, and Upper Siwaliks. Gautam and Fujiwara (2000) studied the magnetostratigraphy and some lithological characteristics of the sediments, and defined the Lower and Middle Siwaliks based on grain size. However, they did not examine lithofacies characteristics at meter-scale and also did not define the exact Middle - Upper Siwalik boundary, and a large part of the Upper Siwalik remains unstudied and undated. Their study was thus incomplete, being focused on age, and not on lithology. To define the lithostratigraphy, the typical characteristics (type locality, lithofacies, fossils, marker beds) of particular sections need to be assessed individually, rather than simply being based on comparison with adjacent areas, and following the divisions made at those sites. Consequently, previous stratigraphic work in the Karnali River section does not adequately follow the international stratigraphic nomenclature. Furthermore, those studies did not address detailed meter-scale variations of lithology and grain size in the area, which is required for the future work on paleoclimate and tectonic evolution. It is thus difficult to correlate with other sections of the Siwalik Group in Nepal where four or five-fold classifications (along with several subdivisions) have been adopted (Table 3.1). This study aims to build a new lithostratigraphy of the

area, to permit comparison and correlation among the different sections of the Siwalik Group of the Nepal Himalayas, and with the Potwar Basin in Pakistan. This will establish a template for future research on the tectonic evolution and paleoclimate of the Himalaya and surrounding regions.

4.2 Methods

This study is based on geological traverses only along the river sections. Survey could not be expanded to nearby areas because restricted access areas of the Bardiya National Park extend to the east, and dense forest covers most of the area to the west. Classification of the rock units into formations and members was made based on grain size, color, and thicknesses of sandstone, mudstone and conglomerate beds. The thicknesses of the individual beds, colour (Munsell colour chart), and grain size changes within the beds were measured in detail, and the data compiled as columnar sections. Existing paleomagnetic data (Gautam and Fujiwara, 2000) permits regional correlation with other Siwalik sections of Nepal.

4.3 Stratigraphy

The Siwalik Group in the Karnali River section is here newly divided into four mappable lithostratigraphic units. These are named the Chisapani, Baka, Kuine and Panikhola Gaun Formations, in ascending order. A new geological map and cross-section are given in Fig. 4.1.
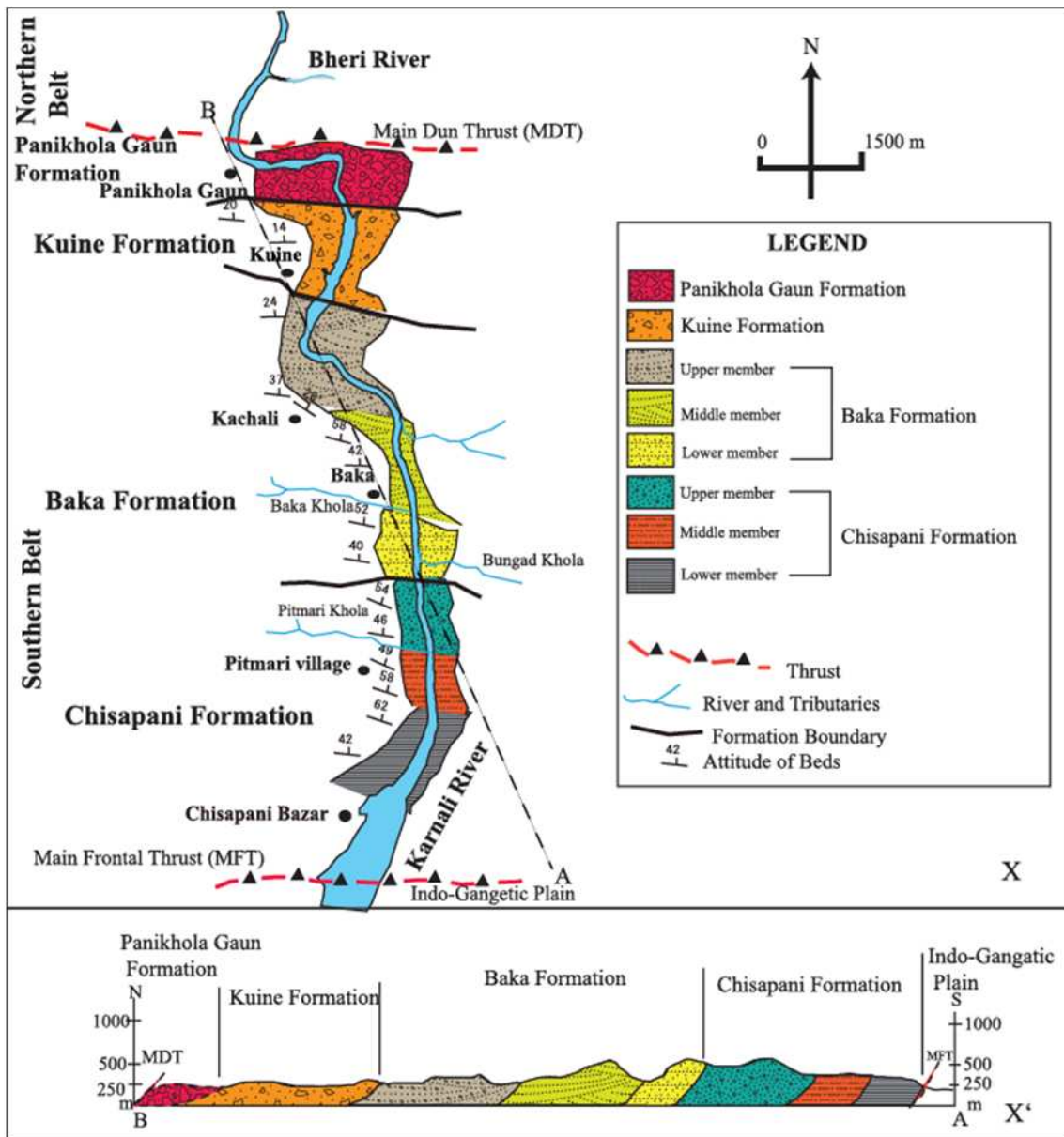
Fig. 4.1: Geological division of the Siwalik Group along the Karnali River section (X). X' indicates the cross section along the line A-B.

4.3.1 Chisapani Formation (Lower Siwaliks)

4.3.1.1 Type locality

Along Karnali River, in exposures north of Chisapani Bazaar.

4.3.1.2 Lithology

The Chisapani Formation is represented by alternations of very fine- to medium-grained, greenish-grey to reddish-brown sandstones, and variegated reddish-brown bioturbated mudstones (Fig. 4.2). The lower part is dominated by mudstones and the upper part by sandstones. The total thickness of this formation is 2045 m. This formation is well exposed along the Karnali River from Chisapani Bazaar in the south to Bungad Khola in the north (Fig. 3.1). The Chisapani Formation is subdivided into lower, middle, and upper members based on the thickness ratios of sandstone and mudstone, colour, and sandstone grain size.

4.3.1.2.1 Lower member

The sediments of this member are exposed from north of Chisapani Bazaar to Pitmari Village. The total thickness of this member is 340 m. This member is composed of alternating variegated mudstone and grey sandstone (Figs. 4.2 A, 4.2 B). Colour of the mudstones ranges from greenish-grey (GLEY1 7/10Y, GLEY1 7/5G) to greyish-brown (2.5Y 7/3, 10R 6/2, 2.5Y 4/4, 10YR 5/2). Thicknesses of the mudstones range from 0.2 m to 5 m, whereas sandstone thicknesses range from 0.2 m to 10 m. The mudstones contain rootlets, burrows, nodules, and concretions, characteristics typical of paleosols (Fig. 4.3I). The mudstones are generally rooted, bioturbated, and are intercalated with very fine to fine-grained, variegated and purple to greenish-grey sandstones (Figs. 4.2A, 4.2B). Successions of sandstones 4 to 10 m in thickness consist of fine- to medium-grained sand, and contain parallel lamination or trough- or planar cross-stratifications in their basal parts, and very fine-grained sandstones containing ripple laminations in their upper parts (Fig. 4.3I). The successions show fining-upward

trends. The bases of the fining-upward successions are marked by erosional surfaces, upon which mud clasts are scattered. The frequency of thicker sandstone successions tends to increase up-section in this member.
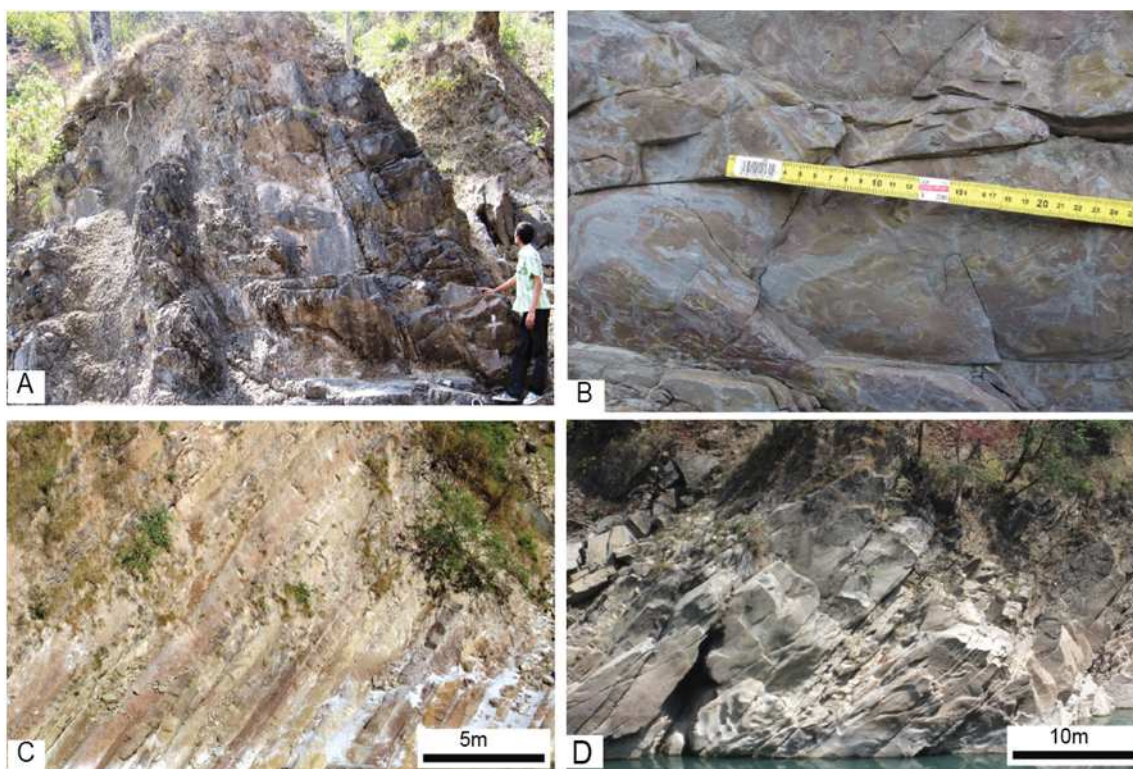
Fig. 4.2: Outcrop photographs of the Chisapani Formation A) Mudstone-dominated interval in the lower member. Person for scale (1.7 m). B) Variegated, rooted and bioturbated mudstone in the lower member. The scale is 25 cm long. C) Red mudstone - dominated interval in the middle member. D) Thicker sandstones in the upper member.

4.3.1.2.2 Middle member

The middle member has a total thickness of about 580 m, and is well exposed around Pitmari Village. It is characterized by fine- to coarse-grained sandstones and bioturbated, reddish-brown (5YR5/4, 5YR 5/3) to brown (7.5YR 5/3) or grey mudstones (GLEY 1 7/10Y).
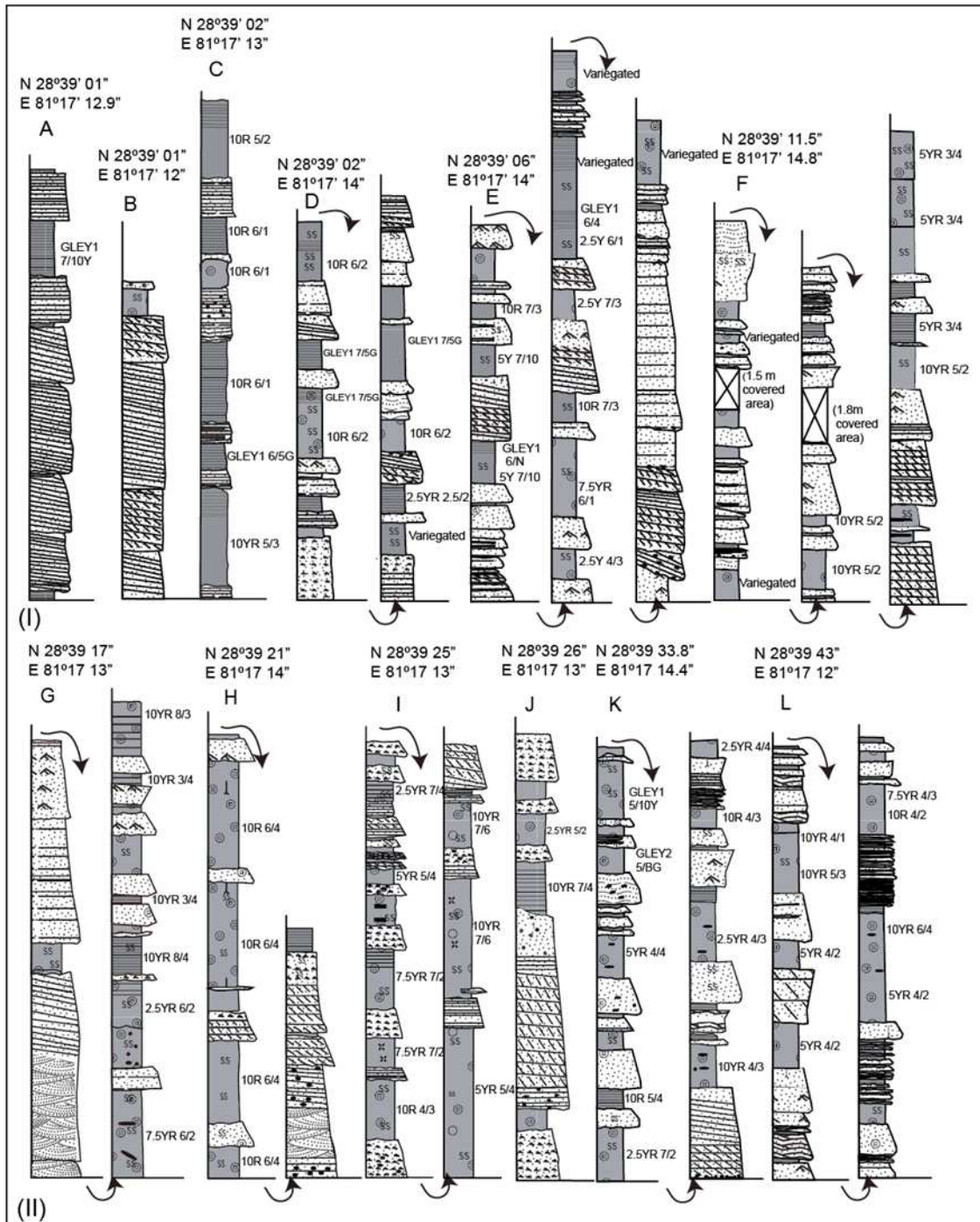
Fig. 4.3: Typical columnar sections of the Chisapani Formation. I) Lower member II) Middle member. Letters A, B, C… Q (with latitude and longitude) at the top of each column indicate the locations of the measured sections.

The red mudstones (10YR 4/6, 2.5YR 5/4, 7.5YR 5/4, 7YR 5/3, 5YR 5/3, and 5YR 3/2) contain rootlets, burrows, nodules, and concretions typical of paleosols, and are frequently interbedded among the sandstones in this member (Figs. 4.2C, 4.3II). The nodules within the red mudstones consist mostly of calcium carbonate and iron oxides (Fig. 4.3II). The sandstone beds are thin (0.5-1m) and interbedded with red mudstones. These sandstones exhibit parallel and ripple lamination (Fig. 4.3II). The thicknesses of the individual sandstone and mudstone beds range from 0.2 to 12 m. The ratio of sandstone and mudstone is roughly equal in the lower half of this member, but the proportion of sandstone increases up-section. Medium- to coarse-grained sandstones first appear in the upper boundary of this member. This type of sandstone is referred to as "salt and pepper" sandstone, because it contains significant amounts of a black mineral (biotite) interspersed with white minerals such as quartz and feldspar (Nakayama and Ulak 1999). Generally, sets of sandstones form fining-upward successions. The thickness of the fining-upward successions ranges from 6 to 12 m. The fining-upward successions contain trough and planar cross-stratification, with parallel lamination in the lower part and ripple laminations in the upper part, grading upward into mudstones. The bases of the successions are almost flat, or feature shallow erosional depressions up to 0.5 m in relief.

Fig. 4.4: (Contd.): Typical columnar sections of the Chisapani Formation. III) Upper member. Letters A, B, C... Q (with latitude and longitude) at the top of each column indicate the locations of the measured sections.

4.3.1.2.3 Upper member

The upper member is well exposed between Pitamari Khola and Bungad Khola along the Karnali River and road sections. Total thickness is about 1125 m. The upper member consists mainly of medium- to coarse-grained, thick bedded, grey sandstones and laminated mudstone interbeds. The laminated mudstones range from greenish-grey (GLEY1 5/10Y, GLEY1 5/10GY, GLEY1 5/N) to yellowish-brown (10YR 5/3, 10YR 5/4, 2.5YR 4/2), and contain rootlets, burrows, nodules and concretions characteristic of paleosols. Thicknesses of the sandstone and mudstone beds range from 0.5 to 15 m and 0.1 m to 4 m, respectively. The reddish-brown mudstones are less frequent than in the lower and middle members. Sets of sandstone beds (up to 15 m thick) show fining-upward trends more commonly than the lower and middle members (Fig. 4.2D). The basal parts of the successions are dominated by trough cross-stratifications or parallel laminations which are followed by planar cross-stratifications and ripple laminations (Fig. 4.4, locs. M, N, O). The thinly-bedded, fine-grained sandstones (0.5 to 1 m) contain parallel laminations and ripple lamination or climbing ripples. Some of these thinly-bedded sandstones are massive and grade upward into the overlying mudstones (Fig 4.4, loc. Q). The bed bases in the lower part of the fining-upward successions are erosional, and mud clasts are scattered upon them. Coarse-grained sandstones ("salt and pepper") also occur at the base of this member, and are interbedded at 300 m intervals in the lower part. The mudstone-dominated intervals contain thin sandstones and have sheet-like geometry. These mudstones are about 4 m thick, whereas thickness of the sandstone interbeds ranges from 0.2 to 1 m. The sandstone interbeds feature parallel lamination and ripple and climbing-ripple lamination, mostly in the upper half of the member.

4.3.1.3 Age

The age of this formation ranges from 15.8 to 9.6 Ma, based on magnetic polarity (Gautam and Fujiwara 2000). The ages of the lower, middle and upper members are 15.8 - 15.2 Ma, 15.2 – 13.2 Ma and 13.2 - 9.6 Ma, respectively.

4.3.1.4 Stratigraphic relationship

Chisapani Formation almost corresponds to the Lower Siwalik as proposed by Gautam and Fujiwara (2000), but differs from that by DMG (1987, 2003). DMG placed the boundary between the Lower and Middle Siwalik near Pitmari Khola. However, this is actually the boundary between the lower and middle members of the Chisapani Formation (Lower Siwalik) based on our present study. We also confirmed that the boundary between the Lower and Middle Siwalik is situated near Bungad Khola, where first appearance of continuous thick "salt and pepper" sandstones is found. The appearance of the interval dominated by red mudstone is defined as the boundary between the lower and the middle members, and the first appearance of "salt and pepper" sandstones is defined as the boundary between the middle and upper members. The Main Frontal Thrust (MFT) forms the lower limit of this formation. The upper boundary is conformable with the overlying Baka Formation (Fig. 4.1).

4.3.2 Baka Formation (Middle Siwaliks)

4.3.2.1 Type Locality

The type locality of this formation is around Baka Village.

4.3.2.2 Lithology

The Baka Formation is distributed between Baka Village in the south and Satbaseri-Kuine Villages in the north. Total thickness is about 2740 m. Baka Formation is composed of thickly bedded, medium- to very coarse-grained sandstones and pebbly sandstones, along with mudstone interbeds (Fig. 4.5). All of the sandstones contain abundant biotite, quartz, and feldspar, and hence exhibit "salt and pepper" characteristics. These sandstones are interbedded with greenish-grey, olive-brown to grey laminated mudstones (GLEY1 7/10Y, GLEY1 6/5GY, GLEY1 7/5GY, 5Y 5/6, 2.5Y 4/3, GLEY1 4/N, GLEY2 5/10G). The Baka Formation is also subdivided into lower, middle and upper members.

4.3.2.2.1 Lower member

The main exposures of this member are distributed from Bungad Khola to Baka Village (Fig. 3). Total thickness of this member is about 540 m. It is characterized by thick medium- to coarse-grained "salt and pepper" sandstones (Fig. 4.5A). Thickness of individual sandstone successions ranges from 3 to 17 m, whereas mudstone intervals range from 0.2 to 2 m in thickness. Individual sets of thick sandstone successions overlying mudstone beds show fining-upward trend (Fig. 4.6 I). The bases of these successions are erosional, with mud clasts scattered on these surfaces. The basal parts of the thick sandstone successions generally feature trough and planar cross-stratification, followed by ripple laminated beds, and massive beds in the upper parts of the successions (Figs. 4.6I, locs. R, S, T). Thinner sandstone beds (0.5 to 3 m) contain either parallel or ripple and climbing ripple laminations. The mudstones are laminated and are greenish-grey (GLEY1 7/10Y, GLEY1 6/5GY, GLEY1 7/5GY) to

greenish-brown (2.5Y 6/4). Olive brown (2.5Y 5/6 2.5Y 4/3) mudstones containing

rootlets, concretions and nodules characteristic of paleosols occur frequently in this

member (Fig. 4.6 I).

Fig. 4.5: Outcrop photographs of the Baka Formation. A) A "salt and pepper" sandstone, in which white grains are quartz and feldspar and black grains are mica. The compass is 7 cm long. B) Thick amalgamated sandstone in the middle member. C) Pebbly sandstones in the upper member. The hammer is 30 cm long. D) Boundary (black line) between the Baka and Kuine Formations.
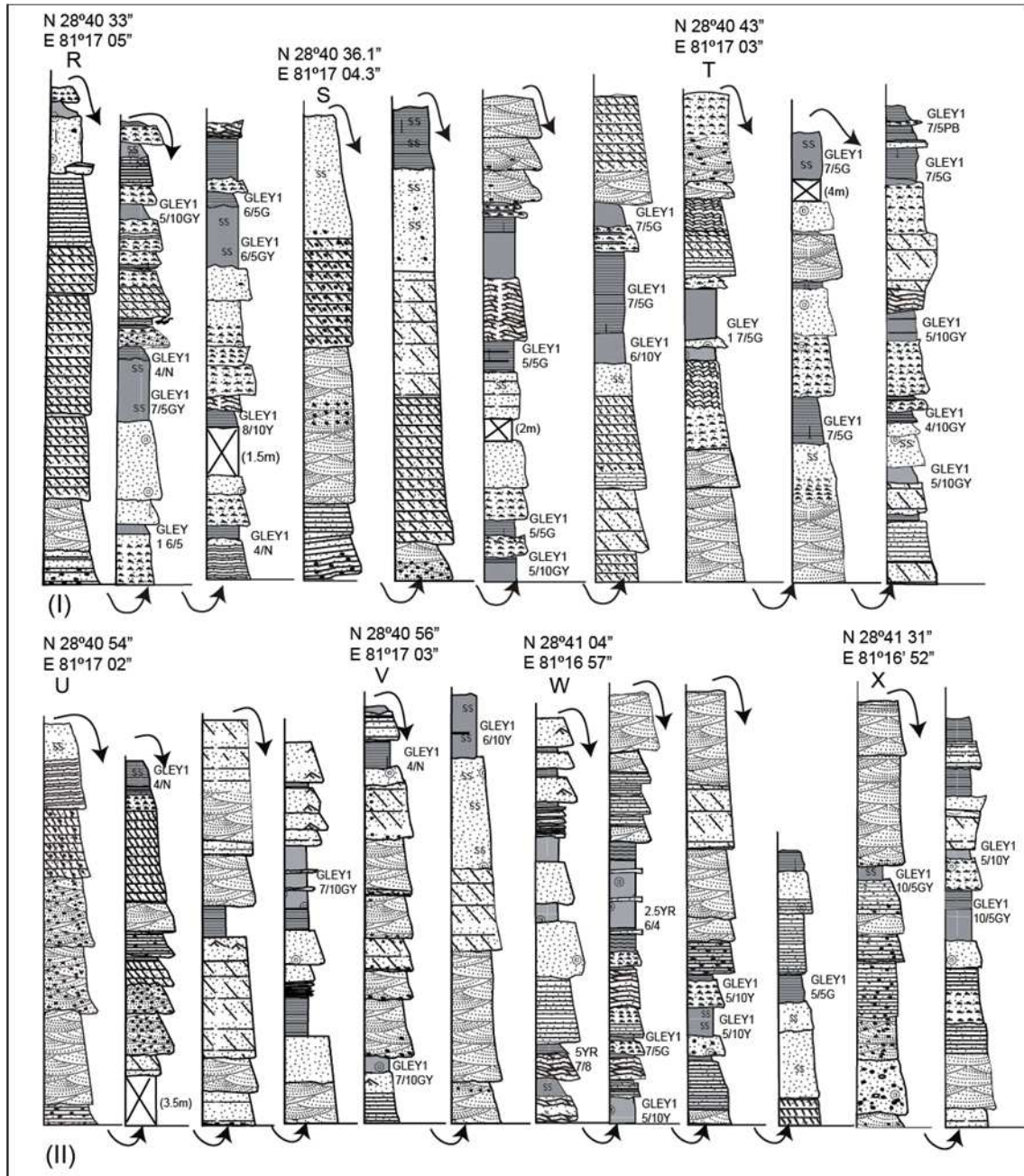
Fig. 4.6: Typical columnar sections of the Baka Formation. I) Lower member, II) Middle member, Letters R, S, T… Z* (with latitude and longitude) at the top of each column indicate the locations of measured sections.

4.3.2.2.2 Middle member

The middle member of the Baka Formation is distributed between Baka Village and Kachali Village, reaching about 650 m in thickness. This member is composed of thickly bedded, coarse- to very coarse-grained sandstone and mudstone interbeds. The sandstone beds are commonly trough and planar cross-stratified. The interbedded mudstone are greenish-grey (GLEY1 7/10GY, GLEY1 6/10GY, GLEY1 7/5GY, GLEY1 4/N) to olive grey (5Y 6/2, 5Y 4/2, 5Y 6/4), to olive brown (2.5YR 5/3, 2.5YR 6/2) (Fig. 4.6II). The thickness of individual sandstone successions reaches 25 m, showing upward-fining trend, whereas mudstone beds typically 0.3 to 2 m thick (Fig. 4.5B). Abundant mud and sand clasts are scattered within the sandstone beds, and pebbles of pre-Siwalik or Lesser Himalayan rocks also occur in places (Fig. 4.6II). In some places, 0.5 m thick coal seams are interbedded within the mudstones (Fig. 4.6II, locs. V, X).

4.3.2.2.3 Upper member

This member is well exposed around Kachali Village. Total thickness is about 1550 m. The upper member consists of coarse- to very coarse-grained, pebbly sandstones and thin mudstone interbeds (Figs 4.5C, 4.7). The long axes of the pebbles have lengths ranging from 1 to 8 cm. The pebbles are mainly quartzite. The sandstones display trough and planar cross-stratification, and thickness of individual sandstone successions reaches 25 m (Fig. 4.7, locs. Z, Z*). Sandstone successions in this member show a faint fining-upward trend, starting from trough cross-stratification at the base, followed by planar cross-stratification, succeeded by rare mudstones beds at the top. These successions are bounded by major erosional surfaces that are laterally continuous in large outcrops (Fig. 4.7). Pebbles and mud clasts are scattered throughout the

sandstone beds. The mudstones are thinly laminated, with colour ranging from greenish-black (GLEY1 4/N, GLEY2 5/10G) to greenish-grey (GLEY 1 7/10Y, GLEY 1).
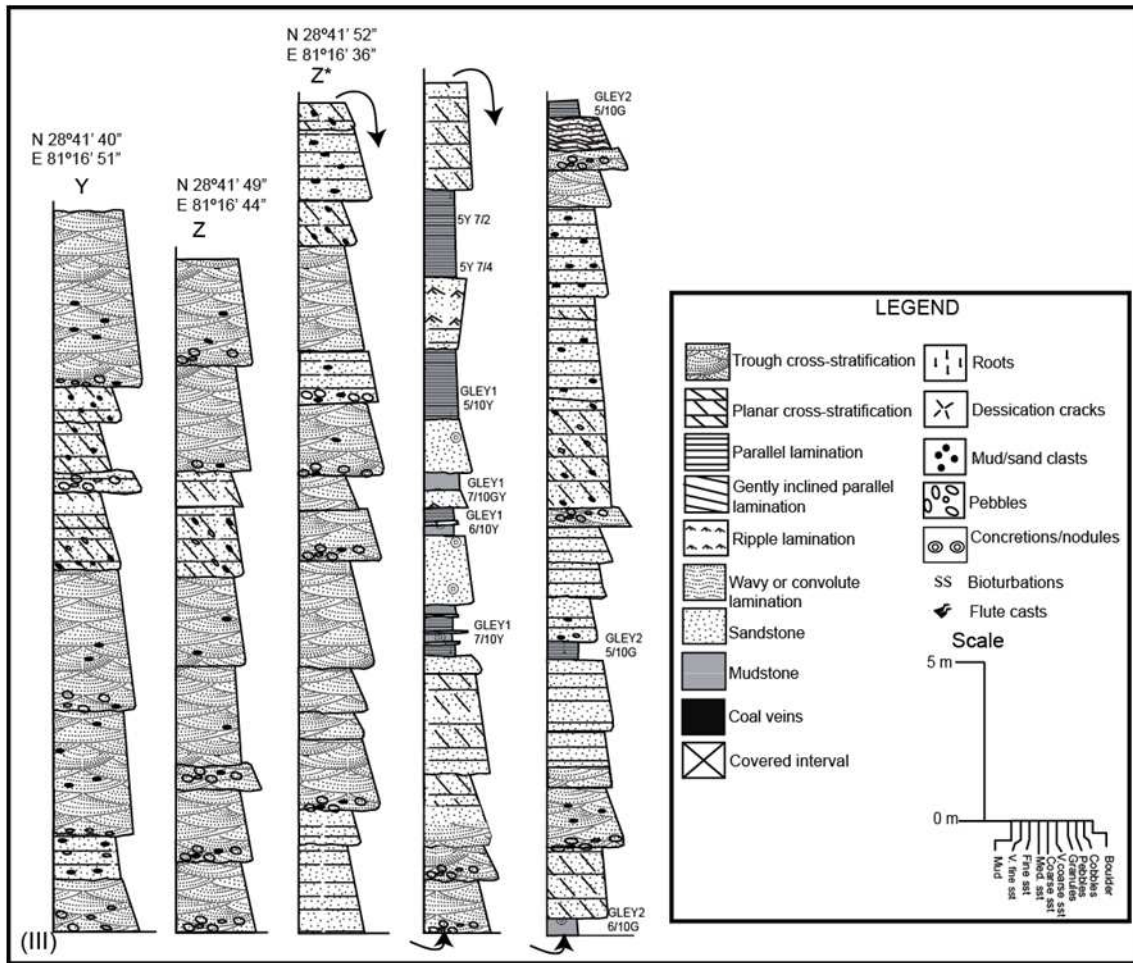
Fig. 4.7: Typical columnar sections of the Baka Formation. III) Upper member. Letters R, S, T… Z* (with latitude and longitude) at the top of each column indicate the locations of measured sections.

4.3.2.3 Age

The age of the Baka Formation has been established by Gautam and Fujiwara (2000), up to the lower half of the upper member. Although the specific age of the uppermost boundary has not been yet been obtained, it is expected to be around 3.9 Ma, based on calculated sedimentation rate. The age ranges of the individual members are 9.6-8.6 Ma, 8.6-6.0 Ma and 6.0-~3.9 Ma (lower, middle, and upper, respectively).

4.3.2.4 Stratigraphic relationship

The upper stratigraphic position of the formation is the same as that proposed by DMG (2003) for the Middle Siwaliks. Gautam and Fujiwara (2000) did not precisely define the Middle - Upper Siwalik boundary, but expected it to be slightly younger than 5.2 Ma. The first appearances of the thick coarse-grained "salt and pepper" sandstones mark the boundary between the Chisapani Formation and the lower member of the Baka Formation. The appearance of coarse- to very coarse-grained sandstones containing abundant mud and sand clasts mark the boundary between the lower and middle members. The pebbly sandstone distinguishes the boundary between the middle and upper members of this formation. The Baka Formation is conformably overlain by the Kuine Formation (Fig. 4.5D).

4.3.3 Kuine Formation (Upper Siwaliks)

4.3.3.1 Type locality

The type locality of this formation is defined in riverside exposures in the Karnali River near Kuine Village.

Fig. 4.8: Outcrop photographs of the Upper Siwalik conglomerates. (A) A well-sorted imbricated pebble to cobble conglomerate of the Kuine Formation. Person for scale (1.7m). (B) Poorly-sorted, matrix-supported boulder conglomerate of the Panikhola Gaun Formation. The scale (compass) at lower left is 15 cm long.

4.3.3.2 Lithology

The Kuine Formation is well exposed from Kuine Village in the south to Panikhola Gaun Village in the north (Fig. 4.1). Total thickness is about 1000 m. The Kuine Formation consists of thick-bedded, imbricated, well-sorted, clast-supported, cobble- and pebble-sized conglomerates (Fig. 4.8A). The gravels consist mainly of

quartzite and carbonate rocks with some metamorphic rocks. Clasts range from 1 to 10 cm in diameter. Sandstones and mudstones are interbedded as lenses within the conglomerate beds. The conglomerate beds are 5 to 30 m thick, whereas thicknesses of the sandstone and mudstone lenses range from 0.5 to 3 m.

4.3.3.3 Age

This formation has not been dated.

4.3.3.4 Stratigraphic relationship

The sudden appearance of thick conglomerate beds marks the boundary between the Baka and Kuine Formations. The stratigraphic relationship between the Baka and Kuine Formations is the same as that between the Middle and Upper Siwaliks, as proposed by DMG (2003) near Kuine Village. Gautam and Fujiwara (2000) did not define the exact boundary position, thickness and characteristics of the Upper Siwalik in this section. The Kuine Formation conformably underlies the Panikhola Gaun Formation.

4.3.4 Panikhola Gaun Formation (Upper Siwaliks)

4.3.4.1 Type locality

Exposures near Panikhola Gaun village are defined as the type locality of the formation.

4.3.4.2 Lithology

This formation is well exposed around Panikhola Gaun and Karawa Gaun

villages, where it reaches about 500 m in total thickness. The Panikhola Gaun Formation consists of matrix-supported pebble, cobble, to boulder conglomerates, and coarse- to very coarse-grained sandstone and mudstone interbeds. Gravels are mostly angular to sub-rounded, and are composed of quartzite and occasional Siwalik Group sandstone clasts (Fig. 4.8B). The gravels are 1 to 10 cm (pebbles/cobbles) and 25 to 30 cm (boulder) in diameter. The conglomerate beds range from 8 to 30 m in thickness, whereas individual sandstone and mudstone interbeds range from 1 to 2 m thick.

4.3.4.3 Age

The formation has not yet been dated.

4.3.4.4 Stratigraphic relationship

The boundary between the Kuine and Panikhola Gaun Formations was not delineated by Gautam and Fujiwara (2000). The boundary between US, US1 and US2 defined by DMG (1987, 2003) which is very similar to the Kuine and Panikhola Gaun boundary defined in our present study. Based on our study, the first appearance of boulder sized-conglomerates bed marks the boundary between the Kuine and Panikhola Gaun Formations. The Panikhola Gaun Formation is truncated at its top by the Main Dun Thrust (MDT) (Fig. 4.1).

4.4 Correlation with the Potwar Basin

Direct lithological correlations of Nepalese Siwalik sections with the Siwalik sections in the Potwar Basin of Pakistan are difficult, due to the prominent lithological variations within the alluvial sediments and the diachronous nature of the boundaries,

37

even within Pakistan (Barry et al., 1982; Willis, 1993; Zaleha, 1997). Consequently, the correlation is based mainly on magnetic polarity patterns, and to a lesser extent on lithological units (Johnson et al., 1982). The long normal magneto-polarity zone (C5n.2n or Chron 9) is a strong tool for correlation with the Potwar Basin of Pakistan, and where it appears in the Nagri Formation (Barry et al., 1982). The same polarity (C5n.2n) zone was also used to correlate between the Nepalese Siwalik sections (Tokuoka et al., 1986; Gautam and Rosler, 1999; Ojha et al., 2009). This long normal polarity episode appears in the upper half of the upper member of the Chisapani Formation (Gautam and Fujiwara, 2000). The lower and middle members and the lower half of the upper member of the Chisapani Formation are thus correlated with the Chinji Formation. Similarly, the Baka Formation is correlated with the Dhok Pathan and Tatrot Formations. The appearance of conglomerates in the Kuine and Panikhola Gaun Formations are correlated with the Pinjor and Boulder Conglomerate (Upper Siwaliks) Formations, respectively (Fig. 4.9).

The correlation with the Potwar Basin shows that the appearance of thick coarse- to very coarse-grained sandstones in the Middle Siwalik (Nagri Formation) at about 11.0 Ma records the increasing river size and discharge over that in the lower Chinji Formation (Willis, 1993; Zaleha, 1997). Similar thick, coarse-grained "salt and pepper sandstones" are observed in the Nepalese Siwaliks (Middle Siwaliks) at about 9-10 Ma. These sediments were derived from the Higher Himalaya, as indicated by petrographic analysis (Tokuoka et al., 1986; Zaleha, 1997; Kumar et al., 2003; Szulc et al., 2006). The changes in fluvial architecture and sediment grain size are due either to uplift of the source area or increase in rainfall, which increase the size of the catchment
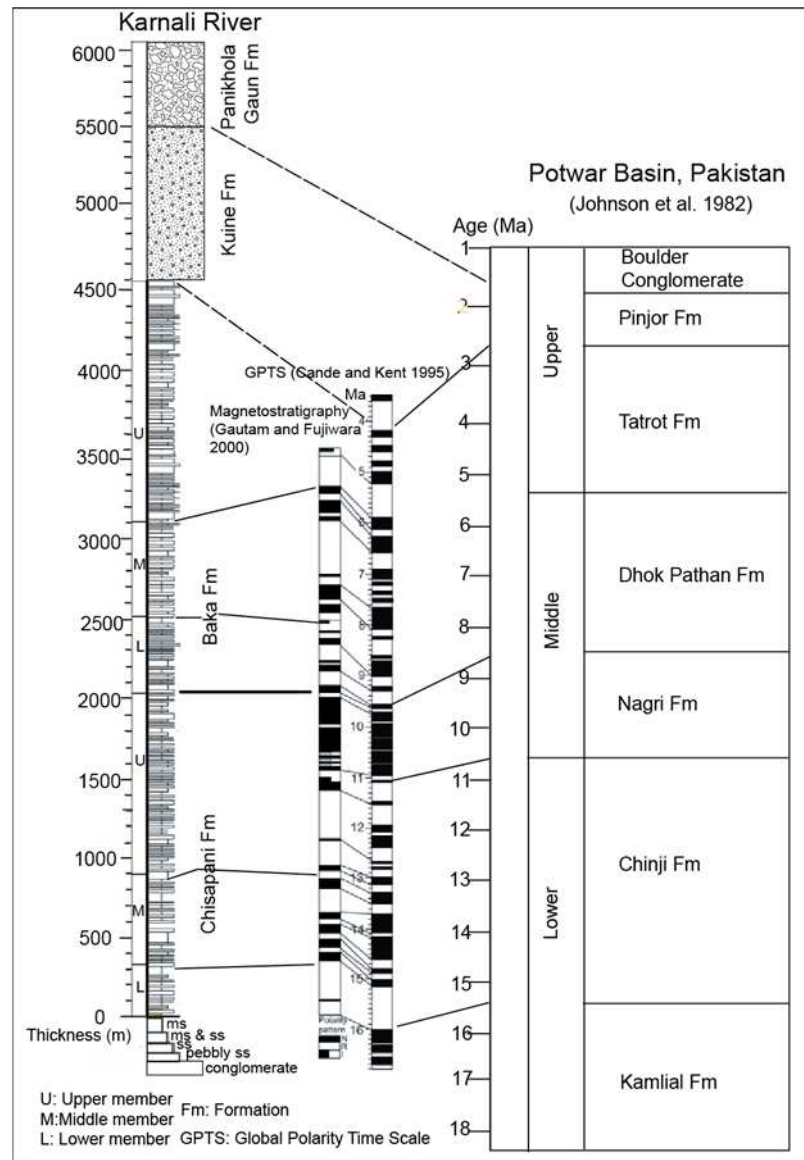
Fig. 4.9: Magnetostratigraphy and lithostratigraphy divisions of the Siwalik Group along the Karnali River section (modified from Gautam and Fujiwara, 2000) and its correlation with the Potwar Basin, Pakistan (Johnson et al. 1982). The dashed lines indicate the tentative correlation of the Kuine and Panikhola Gaun Formations (undated).

basin or discharge of the river, respectively (Damanti, 1993; Horton and DeCelles, 001).The Middle Siwalik sediments were therefore deposited by a large river system, comparable to large modern rivers such as the Koshi and Ganga River deposits (Willis, 1993; Zaleha, 1997). The diachronous evolution of such large drainage systems may thus be helpful to understand the stratigraphic depositional pattern in the Siwalik foreland basin in relation to the tectonic, climate and paleo-drainage system in the Himalaya region during the Middle Miocene to Early Pleistocene.

Chapter 5

FLUVIAL FACIES

5.1 Introduction

The Siwalik Group has been studied by several researchers to understand the fluvial depositional systems in several sections in Pakistan, India as well as those in Nepal (Willis, 1993; Khan et al., 1997; Zaleha, 1997; Kumar et al., 2003; 2004; Tokuoka et al. 1986, 1990, 1994; Hisatomi and Tanaka, 1994; Nakayama and Ulak, 1999; Ulak and Nakayama, 2001). These studies reconstructed the meandering and braided river systems and revealed that order of appearance of the fluvial systems consistence among the Siwalik sections but timing is differs. The parameters which affect these changes in fluvial systems are alluvial process (autocyclic) as well as allocyclic process, such as climate and tectonics of the hinterland (Willis, 1993; Zaleha, 1997).

The Siwalik Group along the Karnali River area of Nepal Himalaya has been the locus of a variety of studies (Gautam and Fujiwara, 2000; Huyghe et al., 2001; Szulc et al. 2006; Van der Beek et. al., 2006; Bernet et al., 2006). These studies focused on petrography, isotopes and age dating to understand the tectonics, exhumation as well as provenance of the sediments, which make the area more suitable to study about the paleoclimate and associated changes in fluvial depositional system. Huyghe et al. (2005) studied the depositional facies in broad scale and interpreted the similar order of fluvial systems with other area, which were mainly controlled by the climate and tectonics. However, their interpretation was limited by a lack of precise detail facies analysis at meter-scale. Although, there have been many studies regarding to

41

petrography, isotopes and age dating, however, no detail depositional facies information at meter-scale along the Karnali River section.

In this study, the main target is to describe the detail depositional facies and to reappraise the fluvial facies classification of Huyghe et al. (2005) from the Karnali River area and finally we compare the reconstructed fluvial systems with previous studies elsewhere in the Siwaliks, to reconstruct the changes in tectonics and climate.

5.2 Methods

The facies were identified based on lithofacies, bounding surfaces, internal sedimentary structures, textures, together with the paleocurrent directions. Paleocurrent directions were measured by measuring the inclination of cross-stratifications, ripples, and flute casts along with flow axis from parting lineation.

5.3 Depositional facies

Twelve sedimentary facies were identified from the all four formations. The lithofacies codes of Miall (1996) were used in this study (Table 5.1, Figs. 5.1, 5.2).

5.3.1 Mudstone facies

The mudstone facies comprises the facies Fl, Fm, and P (Fig. 5.1 A, B, C). Fl facies mainly grey in colour and contains parallel lamination. The thickness of this facies ranges from 0.5–1m. The Fm facies is generally massive, with some desiccation cracks, rain drop imprints, bioturbation and nodules or concretions. Individual bed ranges in thickness from 0.5 to 2 m. The Paleosols (P) facies mainly reddish brown to

greenish brown and contains nodules and concretions, roots, burrows and slickenside. Pedogenic carbonate is usually nodular but also present in forms of pedotubule. The thickness of the beds ranges from 3 to 5 m.

Fig. 5.1: Outcrop photographs of the lithofacies. A) Laminated mudstone (Fl). B) Massive mudstone with some roots (Fm). C) Reddish-brown paleosols (P). D) Coarse-grained trough cross-stratified sandstone (St). E) Planar cross-laminated sandstone (Sp). F) Parallel laminated sandstone (Sh).

Facies code	Symbol	Facies characteristics	Sedimentary structures	Interpretation
Gmm		Disorganized, matrix-supported, cobble, pebbles and boulder conglomerate interbedded with lenses of sandstone and mudstone.	Structureless or weak grading	Debris-flow deposits (Johnson, 1970; Miall, 1978, 1996).
Gt		Well imbricated, clast-supported conglomerates interbedded with lenses of sandstone and mudstone. Thickness: 5 to 30 m.	Trough/planar cross stratifications	Transverse bar and channel fill deposits. 3-D migrating dune (Miall, 1996; Bridge, 2003).
Gh		Clast-supported, imbricated horizontal bedded conglomerates. Thickness: up to 5 m.	Horizontal bedding, normal grading	Longitudinal bedforms, lag deposits or sieve deposits (Miall 1996; Einsele, 2000).
St		Fine to coarse-grained sandstones. Sand and mud clasts scattered on the surfaces, occasionally pebbly.	Trough cross-straitifications, solitary or grouped cross strata. Large size: 0.6 to 1 m, small size: 0.1 to 0.4 m. Inclination of strata: 12° to 33°	Transverse bar, migration of 3-D dune or megaripples in the lower flow regime (Collinson, 1996; Miall, 1996; Eriksson et al., 1998).
Sp		Fine- to coarse-grained sandstone, mud and sand clasts. Thickness: up to 1 m.	Planar cross-straitifications, with some horizontal lamination and ripples. Set size: up to 1 m. Inclination of strata: 10°-34°	Migration of straight crested 2-D dune or megaripples in the lower flow regime (Ashley, 1990; Miall, 1996; Hjellbakk, 1997; Collinson, 1996).
Sh		Very fine- to coarse-grained sandstone, occasionally sand and mud clasts scattred on the surface. Sheet type.	Horizontal lamination with some ripples and convolute laminations inclination occur (~5°)	Deposited by upper plane bed from current in the upper flow regime condition (Olsen, 1988; Miall, 1985, 1996; Bridge 2006; Fielding 2006).
Sr		Very fine to fine-grained, nodules, concreted and bioturbed sandstone. Bed thickness: 0.5 to 4 m.	Mainly current ripple and climbing ripples, wave and ladder ripples Ripple height: 3 to 5 cm	2-D migrating dune in a unidirectional current under lower flow condition by traction and suspension process (Kirk, 1983; Ashely, 1990; Bristow, 1993; Miall, 1996; Collinson, 1996).
Sm		Fine- to medium-grained, greenish grey sandstones with sparse silty lenses, mudclasts, burrows, nodules and concretions. Thickness: 0.5 to 4 m.	Massive or faint laminations	Rapid deposition by suspension or sediment gravity flow or syn-sedimentary deformation through liquifaction or fluidization caused by high sedimentation rate (Todd, 1989; Maizels, 1993; Miall, 1996; Owen, 1996).
Sc		Fine- to coarse-grained sandstones. Sand and mud clasts scattered on the surfaces.	wavy laminations and convolute laminations	Deformation by differential loading (Miall, 1996; Collinson, 1996)
Fl		Silty, sandy mudstones with some cracks, interbedded with very fine sandstone, sheet type, thickness: 0.5 to 3 m.	Well developed parallel laminations. Occasionally wavy structures	Accumated from suspension deposits in abandonment channels or overbank area during flood Stage (Miall, 1996; Hjellbakk, 1997; Uba et al., 2005)
Fm		Variagated, reddish brown to grey mudstones, usually massive with desiccations cracks, bioturbation, nodules and concretions. Thickness: 0.5 to 3 m.	Usually massive or faint laminations	Suspension deposits in the overbank area (Miall, 1996; Thomos et al., 2002; Bridge 2006)
P		Pedogenic features, calcrete, reddish brown to grey colour, nodules and concretions. Thickness: 3 to 5 m.	Massive, peodgenic features, pedotubules	Suspension settling in floodplain and chemical precipittaion i.e. mature paleosols (Miall, 1996; Thomos et al., 2002; Singh et al., 2011).

Table 5.1: Description and interpretation of the depositional facies (after Miall, 1996).

5.3.2 Sandstone facies

The sandstone facies St consists of medium- to coarse-grained, moderately to poorly-sorted trough cross-stratified sandstones (Fig. 5.1 D). The largest troughs are 0.6 m thick and 1.8 m wide, some small types are also evident (0.1 m thick to 0.4 m wide).
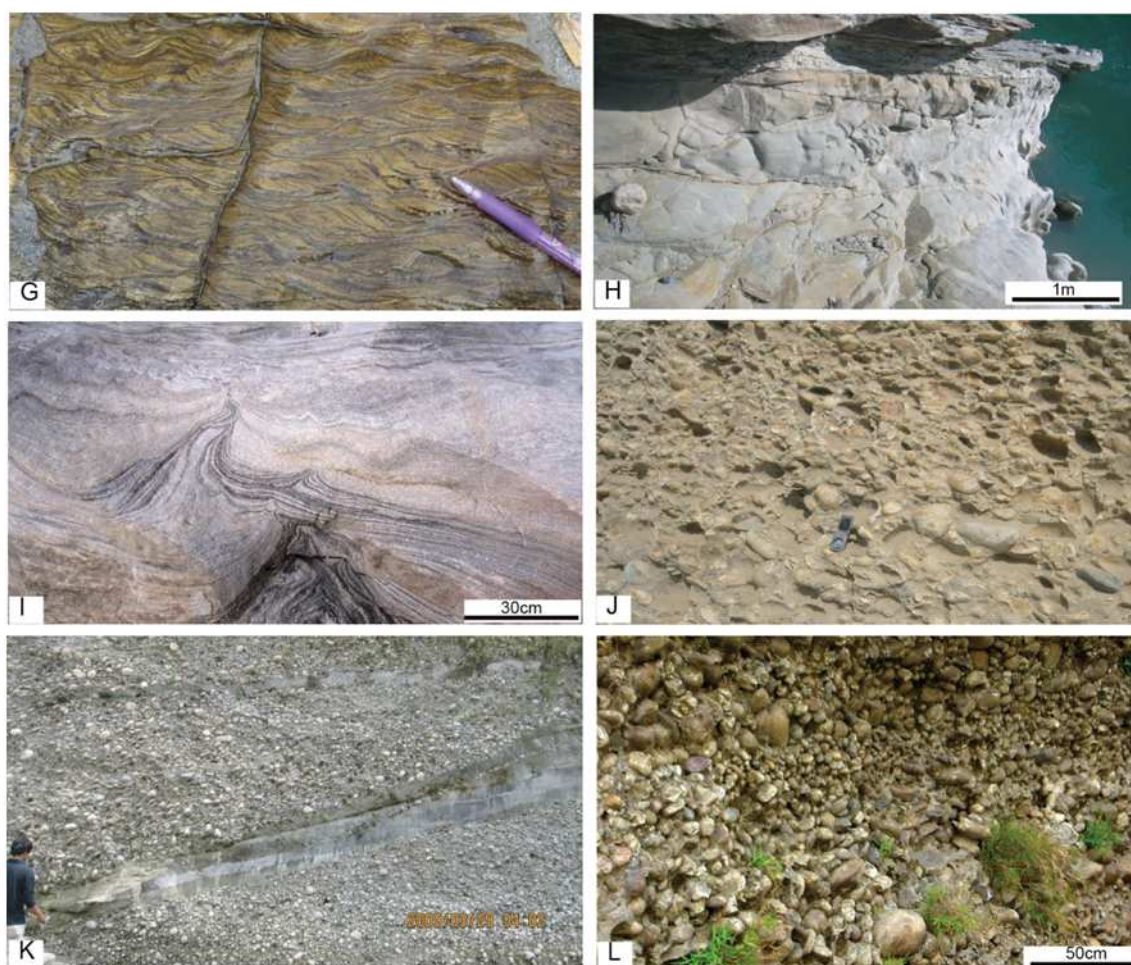
Fig. 5.2: Outcrop photographs of the lithofacies. A) Rippled laminated sandstone (Sr). B) Massive sandstone (Sm). C) Convolute laminated sandstone (Sc). D) Matrix-supported, poorly-sorted boulder conglomerate (Gmm). E) Clast-supported, well-sorted conglomerate (Gt) F) Normally-graded pebble to cobble conglomerate (Gh).

The facies Sp consist of fine- to coarse-grained, planar cross-stratified sandstones (Fig. 5.1 E). The thickness of the individual set is up to 1 m. Thickness of planar cross-strata typically decreases with decreasing grain size. The Sh facies is represented by very fine- to coarse-grained, parallel laminated sandstones (Fig. 5.1 F). Parallel laminations are slightly inclined in some cases (~5°). Facies Sr consists of very fine- to fine-grained sandstones with current and climbing ripples. (Fig. 5.2 G). Thickness of the facies ranges from 0.5 to 4 m. In some cases, ladder ripples also found in fine-grained sandstones. Facies Sm is composed of greenish grey to grey, fine- to medium-grained sandstones (Fig. 5.2 H). This sandstone facies contains abundant nodules, concretions and bioturbation. Thickness of this facies ranges from 0.5 m to 4 m. The facies Sc is generally found in the medium- to coarse-grained sandstones (Fig. 5.2 I).

5.3.3 Conglomerate facies

Conglomerate facies consists of stratified, poorly-sorted, matrix-supported boulder conglomerates (Gmm). The matrix of conglomerate is generally poorly-sorted sand. The length of clasts (a-axis) is up to 0.2 to 0.3 m. Gmm conglomerate beds range from 4 to 20 m (Fig. 5.2 J). The other facies includes well-sorted, imbricated, clast-supported trough or planar cross-stratified conglomerates (Gt), horizontal-stratified, normally-graded conglomerates (Gh) (Fig. 5.2 K, L). The thickness of the Gt bed sets ranges from 5 to 30 m. The shape of the pebbles is generally elliptical to tabular. The long axis of the pebbles reaches up to 8 cm. Gh facies is generally well-sorted, normally-graded conglomerates and its thickness is up to 5 m.

5.4 Facies associations

Six facies associations have been recognized on the basis of individual facies, architectural elements and bed geometry. Although Huyghe et al. (2005) analyzed facies association, we refined its classification based on bed by bed description.

5.4.1 Meandering river facies association

5.4.1.1 Facies association (FA1)

5.4.1.1.1 Description

The FA1 facies association is dominated by the mudstone facies Fm, Fl, and P along with subordinate sandstone facies Sr, St, Sp and Sh (Fig. 5.3). This association corresponds to the KFA1 facies association of Huyghe et al. (2005). This facies association is found in the lower member and lower half of the middle member of the Chisapani Formation. The FA1 consists of piles of fining-upward sediment successions. The thicknesses of the individual successions range from 1 to 5 m in the lower member, and reaches up to 12 m in the middle member. The bases of the successions are flat, or are represented by shallow irregular depressions up to 0.5 m relief. From the base to the top, the succession consists of facies St, Sp, Sh, and Sr, grading into facies Fm, Fl and P. Facies Sh appeared on the base of the some successions (Fig. 5.3 A). The successions show well developed lateral accretion patterns at the basal part of the succession (Fig. 5.4A). Paleocurrent directions are highly dispersed and range from southeast to northwest (azimuth, 162º to 308º) (Fig. 5.3 locs. C, D). The lateral accretion direction is also highly variable and directed northwest in average.
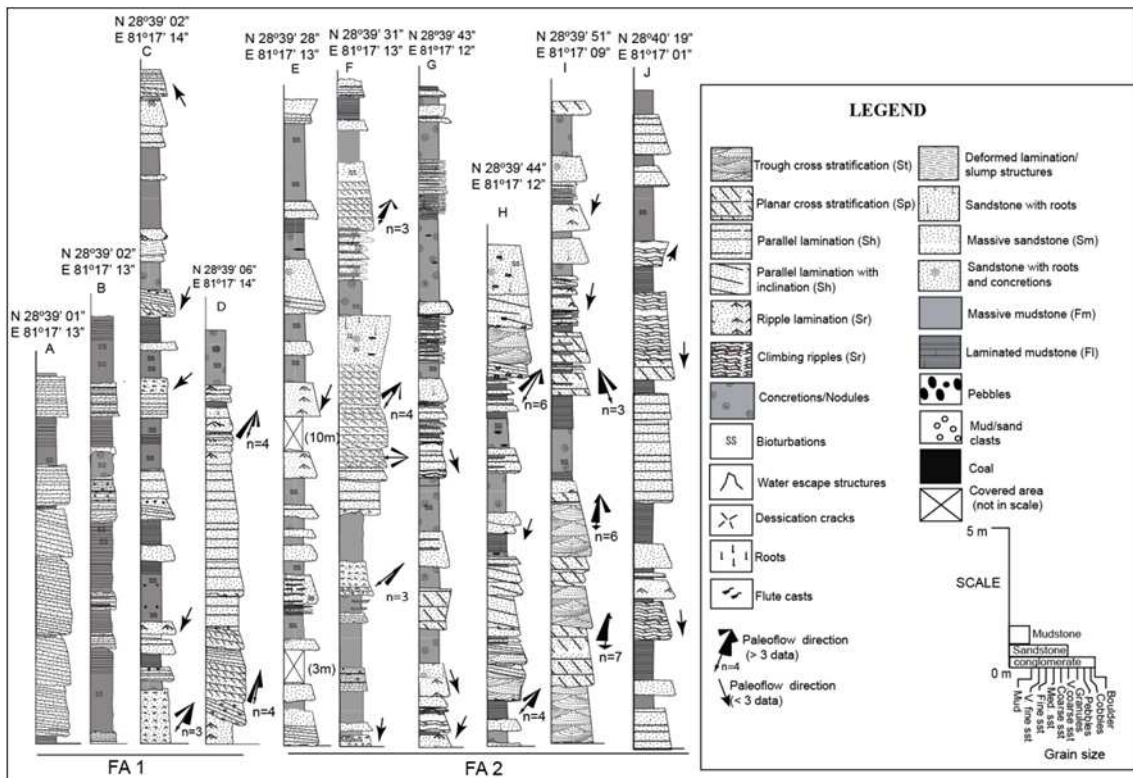
Fig. 5.3: Detailed representative columnar sections of facies associations FA1 and FA2, showing vertical relationship of the facies. Letters A, B, C… J (with latitude and longitude) at the top of each column indicates the location of the sections.

The mudstone beds (Fl) overlies the individual successions and have sheet-like pattern and show vertical accretion in the lower half of this facies association (Fig. 5.4 B). The reddish brown facies (red mudstone, P) is well developed in the upper half of this facies association (Fig. 5.4 C, D). Facies Sp and Sr beds are interbedded with mudstone intervals (Fl, Fm) in some locations and pinch out laterally over 10 to 50 m in wide outcrops. The lower half of this facies association is dominated by mudstone facies and grading sandier upward.
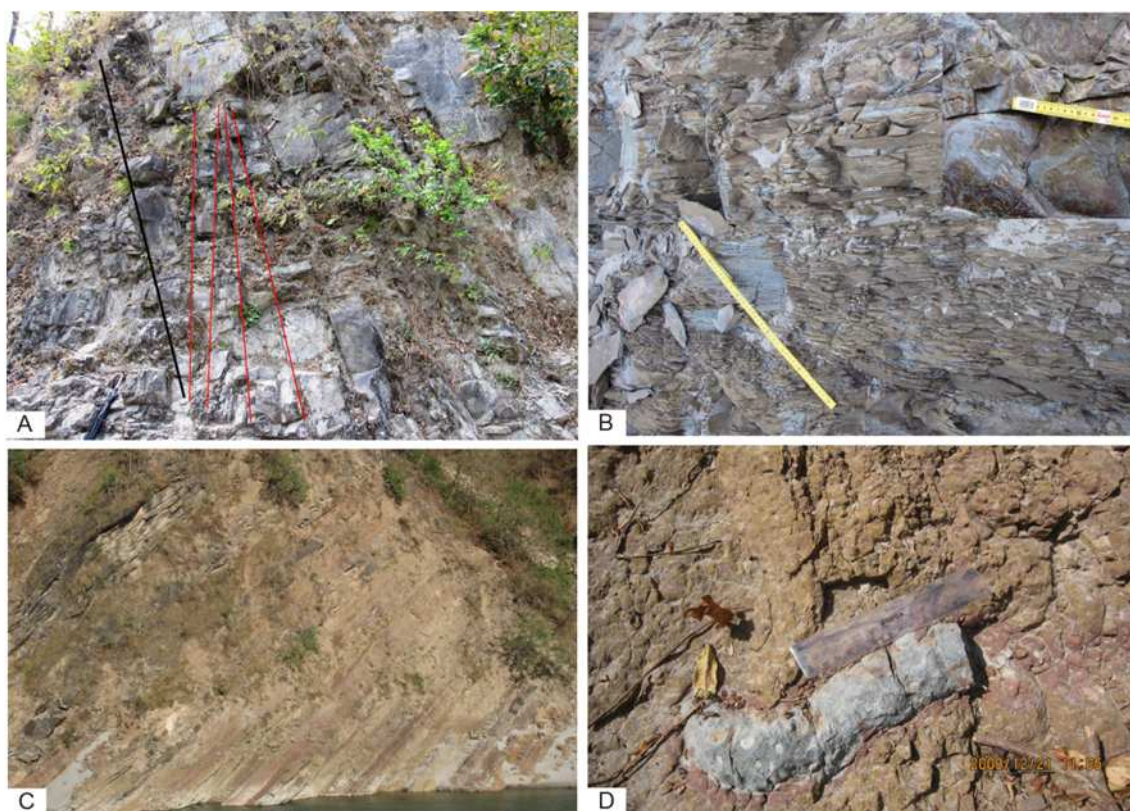
Fig. 5.4: Outcrop photographs of the facies association FA1. A) Typical example of the lateral accretion pattern. The black line indicates the bedding plane and red lines indicate the traces of the accretion units in sandstone. The hammer is 30 cm long. B) Laminated grey mudstones with roots traces and bioturbation, interpreted as flood plain deposits. The scale is 50 cm long. C) Typical outcrops of the red mudstone in the upper part of the FA 1. The outcrop is 10 m high. D) Detail of red soil beds containing nodules, concretions and bioturbation indicative of drier climate. The scale is 15 cm long.

5.4.1.1.2 Interpretation

The fining-upward sediment successions with lateral accretion pattern are typical characteristics of point bar deposits of the meandering river (Miall, 1996; Peakall et al., 2007). The highly dispersed paleocurrent and lateral accretion directions suggest that the channels are highly sinuous. The lenticular shape of interbedded planar cross-stratified sandstones (facies Sp) in the mudstone beds (Fl) interpreted as crevasse splay deposits (cf.Olsen, 1986; Miall, 1996). Mudstone facies, Fm and P, are interpreted

as flood plain deposits. The alternation of thin sheet mudstones and sandstones with ripples laminations are the evidence of deposited from suspension under calm water conditions (Hjellbakk, 1997). The predominance of reddish-brown soils (P) indicates seasonal dry and wet climatic conditions (Retallack, 1991; Khadkikar et al., 1999). The sandier-upward trend may represent the shift of depositional environment from distal to proximal setting with increased in sediment accumulation rates. The point bar deposits with abundant fine-grained facies (mud-dominated) are consistent with the characteristics of the fine-grained meandering river system (Miall, 1996; Nakayama and Ulak, 1999).

5.4.1.2 Facies association (FA2)

5.4.1.2.1 Description

Facies association FA2 is dominated by the sandstone facies St, Sp, Sr, Sh with subordinate facies Fl, Fm and P. This facies association appeared in the uppermost part of the middle and the upper members of the Chisapani Formation, and contains piles of fining-upward successions (Fig. 5.3). The bases of these successions are represented by an erosion surfaces and the basal parts of the successions contain intraformational mud clasts. From the base to top, the successions consist of facies St, Sp, Sh and Sr, grading into muddy facies Fm and Fl. Thickness of the individual fining-upward successions ranges from 1 to 15 m. The sandstone parts of these successions show well-developed lateral accretion patterns (Figs. 5.3 locs. H, I, and 5.5 A). The paleocurrent directions are dispersed from the southeast to the southwest (azimuth, 142° to 249°) (Fig. 5.3). The mudstone facies (Fl, Fm, and P) are thinly-bedded, greenish grey to grey in colour and intercalated with thinly laminated, rippled or climbing rippled sandstones and show

sheet-like geometry as a whole (Fig. 5.5 B, C).
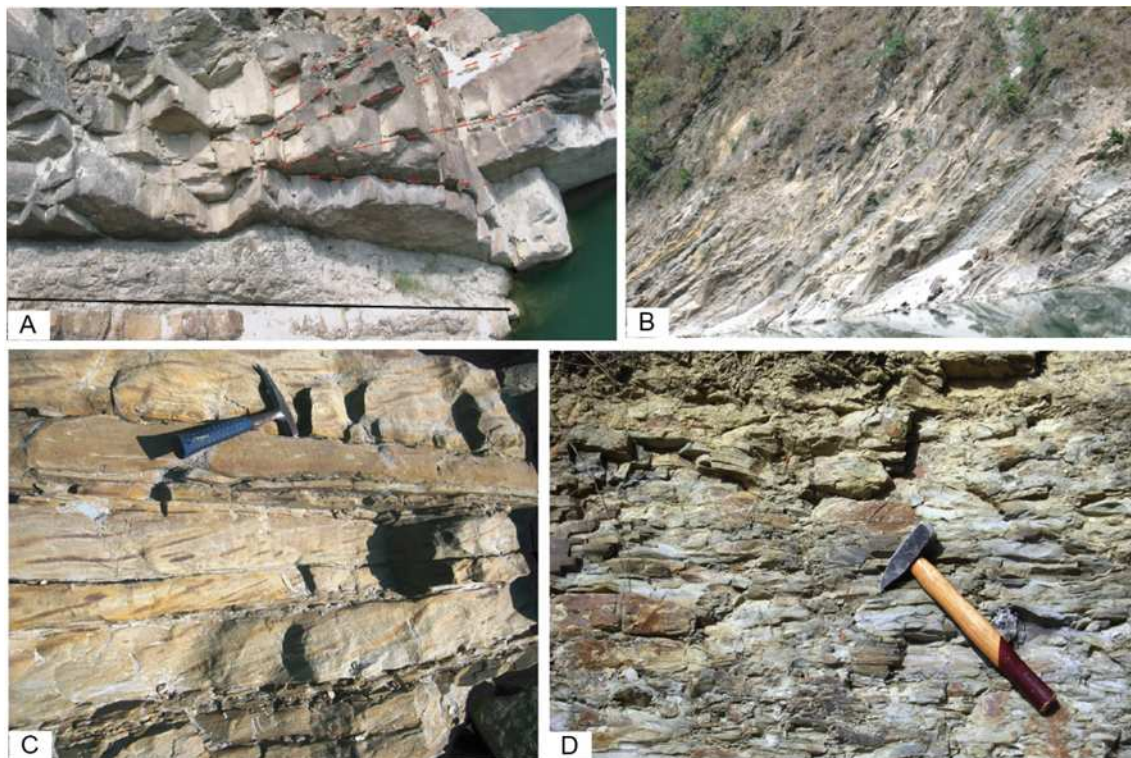
Fig. 5.5: Outcrop photographs of facies association FA 2. A) Typical example of the lateral accretion pattern. The outcrop is 10 m thick. The black line indicates the bedding plane, and red dot lines indicate the traces of the accretion units in sandstone. B) Alternations of thin sandstone (Fl) and mudstone (Fl) with sheet type geometry, interpreted as flood plain deposits. The outcrop is 20 m high. C) Alternation of climbing ripples and parallel laminated sandstones representing flood-flow deposits. 30 cm hammer for scale D) Detail of grey laminated soil beds indicating water logged conditions. 30 cm hammer for scale.
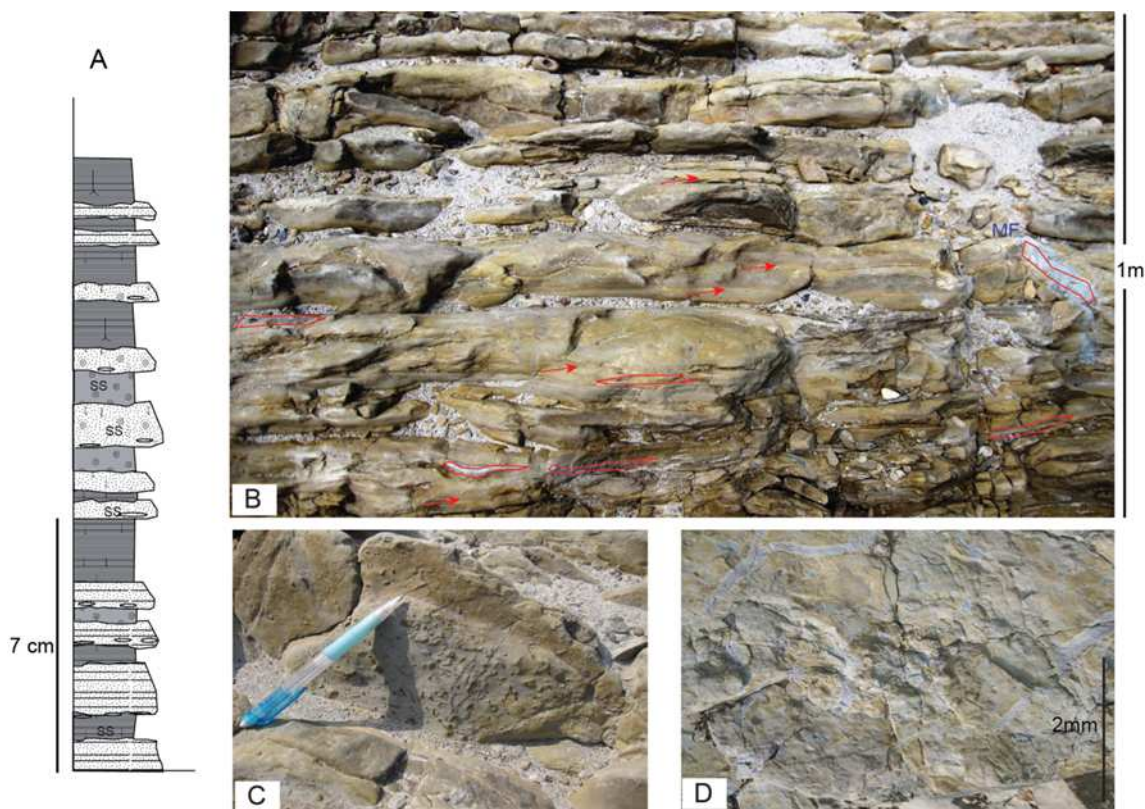
Fig. 5.6: Outcrop photographs of the playa lake facies in facies association FA2. A) Simplified columnar section composed of laminated mudstone beds with roots and bioturbation, mud flake layers, and laminated or massive very fine-grained sandstone beds, suggesting repeated drying and inundation of a playa lake. Legend as in Fig. 4. B) The bed at outcrop. Arrows indicate the laminated mudstone, dark color indicates the very fine grained sandstone and red ellipses indicate mud flake layer. C) Roots traces in the laminated mudstone beds. 15 cm pen for scale D) Desiccation cracks developed in the mudstone beds.

Total thickness of these thin-bedded sheet sandstones are up to 2 m. The frequencies of these sheet type beds tend to increase toward the upper member of the Chisapani Formation. This set is similar to the sheet-splay deposits reported in the other Siwalik sections (Hisatomi and Tanaka, 1994). This facies association contains alternations of laminated mudstone layer (Fl), mud flake layer and thin very fine-grained sandstone layer (Sh) or (Sm) (Fig. 5.5 D). The Fl layers are 2-10 cm and partly disrupted by desiccation cracks and foot prints (Fig. 5.6 A, B, C, D). The mud flakes are 2-5 mm in

diameter. The sandstone layers (Sh) or (Sm) are up to 20 cm thick. The overall thickness of these alternations is up to 1.5 m (Fig. 5.6).

5.4.1.2.2 Interpretation

The characteristics of the sandstones show that the channels features are similar to the facies association (FA1). The dispersal pattern of the paleocurrent suggests that the channel was slightly sinuous. Alternations of sheet-like thin sandstones (Sh, Sr) and mudstone beds (Fl) are interpreted as a flood plain deposits (Hisatomi and Tanaka, 1994; Miall, 1996, Nakayama and Ulak, 1999). Repeated occurrence of thin layers of sandstone (Sh and Sr) beds within facies Fl and Fm are formed by increased frequency of the floods (cf. Nakayama and Ulak, 1999). The paleosols facies indicate the highly seasonal climate with increased rainfall (Retallack, 1991; Tanaka, 1997). Alternation of thin laminated mudstone layer, mud flakes layer and fine-grained massive sandstone layer are interpreted as repetition of dry-up and inundation of the playa or ephemeral lake (Bordy and Catuneanu, 2001; Hampton and Horton, 2007; Bourquin et al., 2009; Sakai et al., 2010). The repeated occurrence of such laterally accreted channel sandstones with abundant sheet-type flood plain facies, and playa lake facies indicates the FA2 facies association was deposited by the flood-flow dominated meandering river system in seasonal climate. This facies association are corresponds to the KFA2 of Huyghe et al. (2005)'classification, but the lower and upper limits of this FA are differs.

5.4.2 Braided river facies association

5.4.2.1 Facies association (FA3)

5.4.2.1.1 Description

The facies association (FA3) is predominated by the sandstone facies St, Sp, Sh, Sr, Sc and Sm, and Fl and Fm facies as minor components (Fig. 5.7). This association is belongs to the KFA4 facies association of Huyghe et al. (2005). This facies association appeared in the lower and middle members of the Baka Formation. The facies association contains several sets of sandstone successions and each set contains fining-upward successions (Figs. 5.7, 5.8 A). The fining-upward succession contains facies St covers the erosional surface, which is followed by facies Sp, Sh, Sr and Sm in
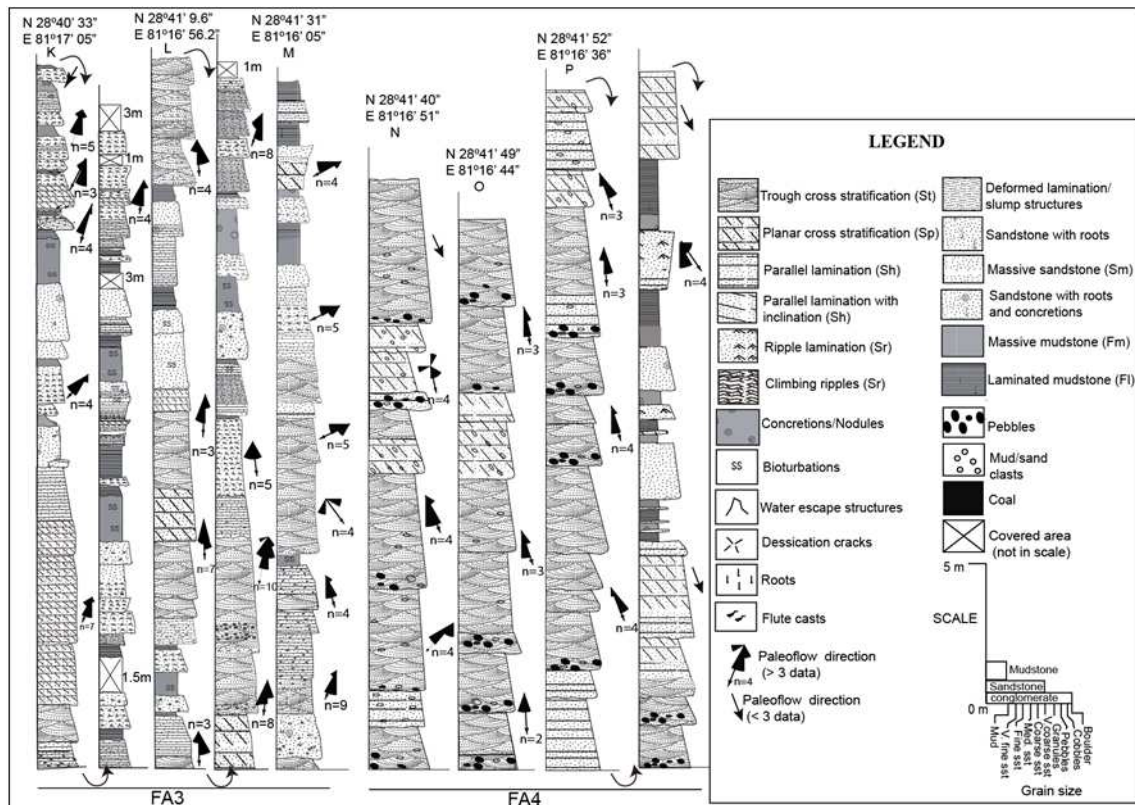
Fig. 5.7: Detailed representative columnar sections of facies associations FA3 and FA4. Letters K, L, M… P (with latitude and longitude) at the top of each column indicates the location of the sections.

ascending order, grades into the muddy facies Fm and Fl. The thickness of the individual fining-upward succession reaches up to 20 m. The compound cross-strata are
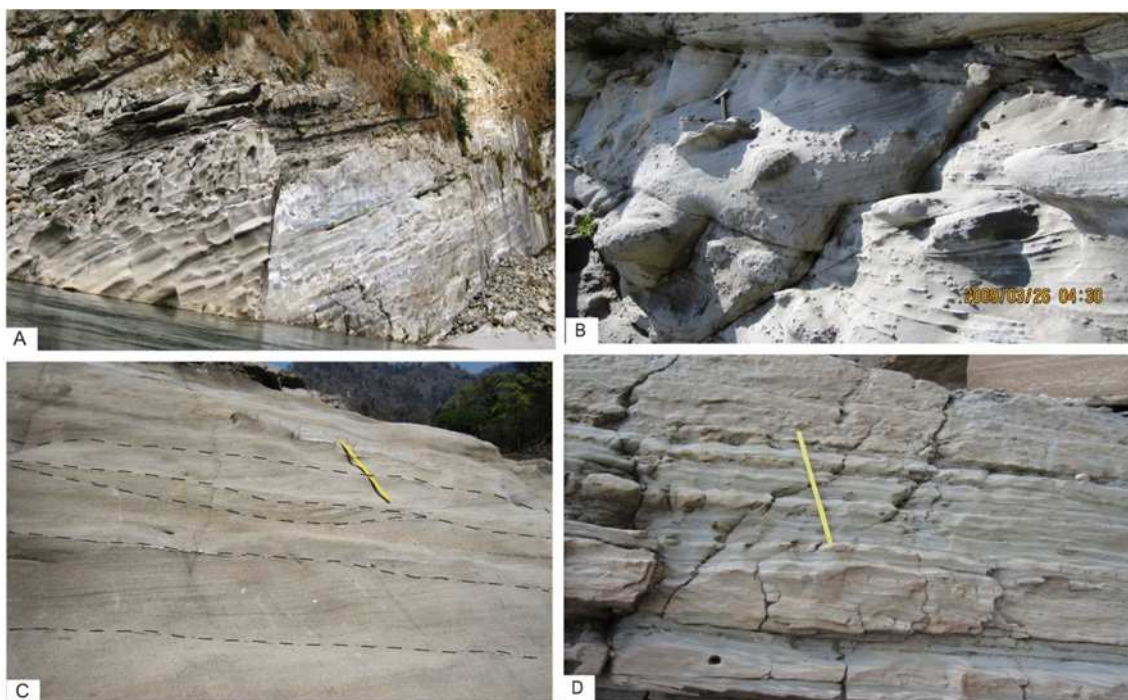
Fig. 5.8: Outcrop photographs of facies association FA 3. A) Coarse-grained, amalgamated, sheet sandstones of the braided river deposits. The outcrop is 10 m high. B) Trough cross-bedded sandstone indicating downstream accretion. 30 cm hammer for scale C) Large scale trough cross-stratification with several bounding surfaces showing migration of braided bars. The scale is 75 cm. D) Parallel lamination and rippled sandstones interpreted as overbank deposits on a flood plain. The scale is 50 cm long.

evident from the outcrops (sets of large scale inclined strata, Bridge, 2003) (Figs. 5.7, 5.8 B) and occupy at the lower and middle parts of the fining-upward successions. These inclined strata are commonly discontinuous. The large scale strata commonly composed of small scale sets of St and Sp or Sr and shows fining-upward grained size trend (1-4 m). These cross stratifications are commonly discordant. The first and second order surfaces of Miall (1985) separate these sets (Fig. 5.8 B, C). The paleocurrent directions are predominantly towards the southwest (mean azimuth 193°) (Fig 5.7). The dip directions of these set boundaries are similar to that of cross stratification i.e. toward southeast to southwest. In some cases, coarsening-upward successions are also evident.

These sandstones contain facies Sh, Sp at the base and massive facies Sm with bioturbation and concretions at the top and shows coarsening-upward trend or little variation of grain size. Thickness of these sandstones beds is up to 7 m. This type facies are intermittently associated with the lower part of FA2 facies association (Fig. 5.3, loc. F). The greenish-grey sandstone facies, Sm and mudstone facies Fm or Fl capped the upper part of the fining upward successions (Fig. 5.7 locs L, M). The individual sandstone successions are separated by the alternation of sheet type fine- to medium-grained sandstone facies Sr and Sh and mudstone facies Fl and Fm (Fig. 5.8, D). The thicknesses of these facies range from 0.2 to 2 m.

5.4.2.1.2 Interpretation

The large inclined cross-stratification with compound sets of facies St, Sp within individual fining-upward successions are interpreted as downstream accretion (Smith, 1972; Allen, 1983; Bristow, 1993; Miall, 1996; Bridge, 2003; Lunt et al., 2004). Unimodal, low paleocurrent dispersions and dominance of downstream accretion pattern suggest the braided channel deposits (Allen, 1983). Thick fining-upward successions correspond to channels depth, which reached up to 20 m. Discontinuous of these strata may be associated with occurrence of side bars or transitions from lower to upper bars deposits (Bridge and Tye, 2000; Bridge, 2006). Discordances in cross strata may have formed by shift in channel position by laterally and may be related to formation of mid channel bar (Bridge, 2006). The fining-upward trend of sets of St and Sp or Sr facies within the large inclined strata represent episodic discharge fluctuation (Godin, 1991; Bridge and Tye, 2000). Coarsening-upward successions also present if upstream part of braided bar (Bridge, 2006) or ephemeral braided stream facies is only

preserved (Bhattacharya and Morad, 1993). The Sm facies in the upper part of the succession is formed by rapid sediment deposition from mass flow process, triggered by falling water level after flooding (Maizels, 1993; Martin and Turner, 1998). The muddy facies (Fm and Fl) overlying the individual fining-upward successions suggests deposition by waning flood on sub aerially exposed bar top (Miall, 1996). The alternation of sheet type fine-grained, thinly bedded sandstone facies Sr, Sh and Fl, Fm represent the abandoned channel or flood plain deposits. This facies association corresponds to deep sandy braided river system also described in the other Siwalik successions (Nakayama and Ulak, 1999).

5.4.2.2 Facies association (FA4)

5.4.2.2.1 Description

This facies association is dominated by pebbly, coarse- to very coarse-grained, sandstones (facies St, Sp, Sh and Sr) with facies Fl and Fm as a minor component (Fig. 5.7). This facies association is found in the upper member of the Baka Formation. This facies association is corresponds to the KFA5 and KFA6 facies association of Huyghe et al. (2005). The geometry of the individual sandstone successions is sheet type. Each succession is marked by basal erosional surface that laterally well continues and show faint fining-upward trend (Fig.5.7). The thickness of the individual fining-upward succession is up to 7 m. Individual sheet boundaries also contain frequent erosion
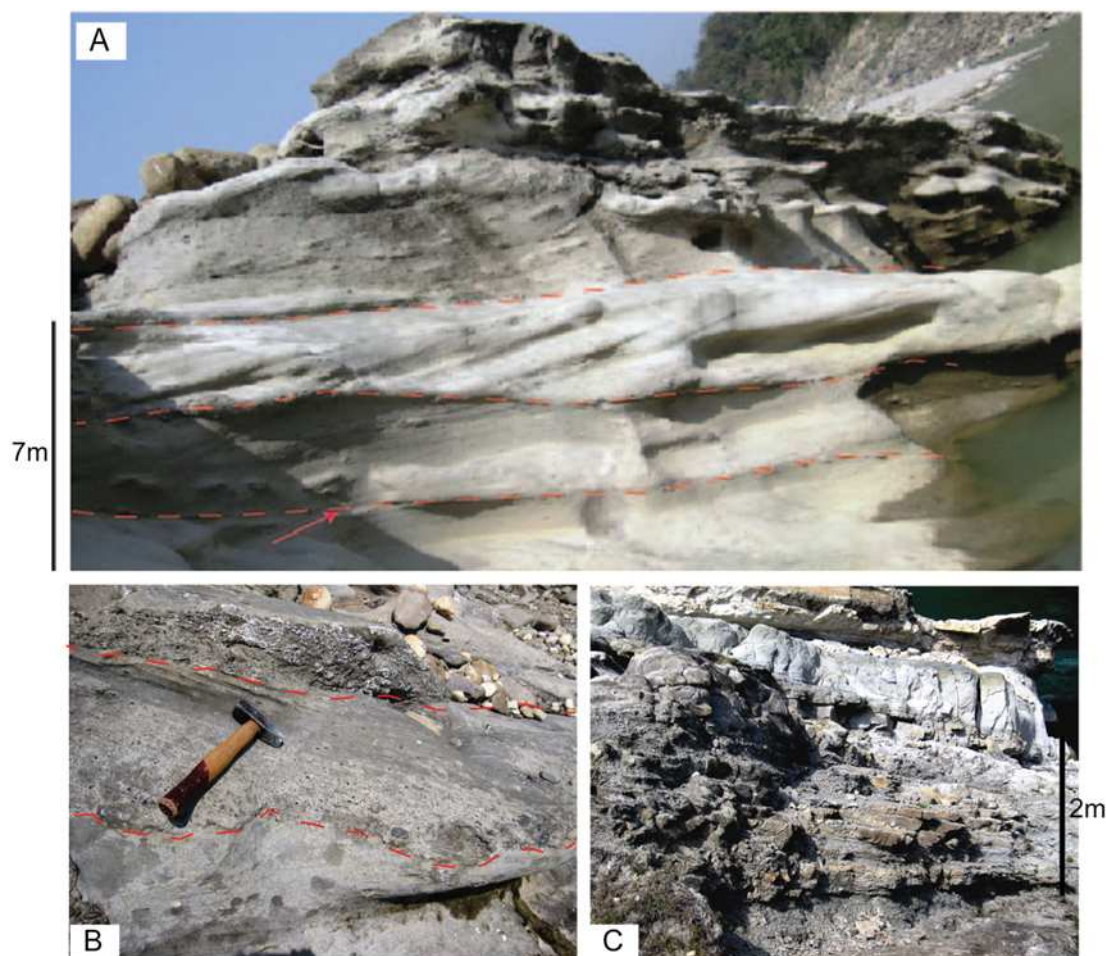
Fig. 5.9: Outcrop photographs of the facies association FA4. A) Very coarse-grained sheet sandstone showing trough and planar cross stratifications (Sp, St). The arrow indicates the erosional surface. Total thickness of the outcrop is 15 m. B) Erosional surfaces with pebbles representing shallow river channel. Hammer is 30 cm long C) Alternations of sandstone and mudstone in the flood plain.

surfaces with several mud/sand clasts (Fig. 5.9 A). Facies Sp and Sh are appeared in the

basal part of the successions and these facies beds show concave-up geometry (Fig. 5.7,

locs. N, O, P). The facies St beds with abundant pebbles and sand/mud clast cover the

erosional base of the successions in some locations (Fig. 5.9 A, B). The paleocurrent

directions are dominantly towards the southeast (Fig. 5.7, locs. N, O, P). The proportion

of mudstone facies Fl and Fm is very less as compared to sandstone facies and occupies

the upper most part of the successions (Fig. 5.9 C). Thickness of the mudstone facies

ranges from 0.5 to 2 m.

5.4.2.2.2 Interpretation

The faint-fining upward succession with facies St, Sp facies, frequent erosional surfaces containing abundant sand/mud clasts indicate the periodic reworked of fine-grained sediments due to laterally migration of bars in the channels (Kumar and Nanda, 1989; Miall, 1977). The laterally continuous sand sheet dominated by large scale, facies Sp and St reflect the migration of dune in high energy condition. The unimodal paleoflow direction and less proportion of facies Fm and Fl, suggest the bedforms were generated during the migration of compound bar of the relatively shallow channels of braided river (Smith, 1972; Miall, 1978, 1996; Roe and Hermansen, 1993). The thicknesses of the individual fining-upward successions, suggest the channel was shallower than that of the FA3 facies association. The abundant pebbles indicate the depositional site is much closer to the proximal part of the hinterland. This facies association is interpreted as shallow sandy braided river system (Miall, 1996; Nakayama and Ulak, 1999).

5.4.2.3 Facies association (FA5)

5.4.2.3.1 Description

This facies association is dominated by gravel facies Gt and Gh (Fig. 5.10 A, B, C). The sandy and muddy facies St, Sp and Fm occur as minor components. This facies association is corresponds to the KFA7 facies association of Huyghe et al. (2005). This

Fig. 5.10: Outcrop photographs of the facies association FA5. A) Trough cross-bedded conglomerate in a large outcrop. Outcrop is 15 m high. B) Clast-supported, cobble to pebble conglomerate (Gt) with a lens of sandstone (St). The outcrop is 5 m high. C) Close-up of imbricated pebbles.

facies association is found in the Kuine Formation. The Gt beds are generally gently inclined, and individual beds are overlain by facies St, and Sp at top (Fig. 5.10 A, B). Each inclined bed has an undulatory base and top, and their thickness varies from 1 to 2 m. Instead of Gt, the facies Gh appears in some locations.   The facies St, Sr and Fm are in lenticular shape and their thickness reaches up to 1 m. (Fig. 5.10 B).

5.4.2.3.2 Interpretation

Facies Gt and Gh contain imbricated gravels suggesting the high energy river system equivalent to gravel-laden braided streams (Maizel, 1989; Brierley et al, 1993; Bridge, 2006). The gravels were generally transported as bedload and were deposited under waning flow by progressively accretion of smaller clasts, in channels as lag

deposits and on longitudinal bars of gravelly braided river (Collinson, 1986; Rust 1984; Miall, 1990; Bridge, 2006). The variation in bed thickness is related to the periodic growth, migration of bar and their subsequent erosion (Pandita et al., 2011). The facies St and Sp suggests the winnowing of the fine sediments during the waning stage of flow toward the bar margin (Miall, 1996). This facies association is interpreted as gravelly braided river system (Miall, 1996; Nakayama and Ulak, 1999).

5.4.2.4 Facies association (FA6)

5.4.2.4.1 Description

This facies association is dominated by facies Gmm. Facies Gt, St or Sp or Fm also occur as minor components (Fig 5.11). This facies association is found in the Panikhola Gaun Formation. This facies association has not been classified by Huyghe et al. (2005). Facies Gmm is characterized by massive, generally poorly-sorted, matrix-supported conglomerate beds with disorganized grains fabric (Fig. 5.11 A). Thickness of the massive bed sets ranges from 4 to 20 m. Clast-supported conglomerate beds (Gt) are locally interbedded between the matrix-supported Gmm facies (Fig 5.11 B). The boundary between Gmm and Gt is slightly undulatory or flat. At some places, facies St, Sp or Fm are appeared as lens between facies Gmm beds.

5.4.2.4.2 Interpretation

The poorly-sorted Gmm beds, absence of stratification suggest that this facies was deposited from debris-flows (e.g. Johnson, 1970; Blair and McPherson, 1998; Miall, 1985, 1996). The clast-supported facies Gt beds and lenticular facies St, Sp or Fm beds are interpreted as stream-flow deposits, truncating the debris-flow deposits (Hartley,

1993). This facies association is corresponds to the debris-flow dominated braided river system in the other Siwalik sections (Nakayama and Ulak, 1999).

Fig. 5.11: Outcrop photographs of the facies association FA6. A) Matrix-supported, poorly sorted conglomerate (Gmm) with almost no erosional surface with underlying sandstones (St), typical of debris flow deposits. The compass is 15 cm long. B) Alternation of lens shaped sandstone and clast-supported conglomerate (Gt) interpreted as stream flow deposits. Outcrop is 3 m high.

Chapter 6

PETROGRAPHY AND PROVENANCE

6.1 Introduction

Sandstone compositions are influenced by the composition of the source rocks, the nature of the sedimentary processes operating, and the types of dispersal paths that link the source and the depositional basin (Dickinson and Suczek 1979). The provenance of sediments includes all aspects of the source area, including the source rocks present, climate, relief, and hydrodynamics of the depositional environment (Pettijohn et al. 1987, Johnsson 1993). Tectonic setting is also regarded as a major controlling factor for the variations in composition of sedimentary rocks (Ingersoll and Suczek 1979, Dickinson 1985, Johnsson 1993).

The minerals occurring in sedimentary rocks are generally used as guides for the identification of provenance and tectonic setting of an area. The most commonly used approach in provenance studies is to consider sandstone composition in the context of a tectonic framework. Standard methods for sandstone provenance analysis use modal analysis of detrital framework components (Dickinson and Suczek 1979, Dickinson 1985). Such methods have been used to determine the provenance of the fluvial succession of the Siwalik Group, which is an important repository recording the provenance and tectonic history of the Himalaya (Critelli and Ingersoll 1994).

The present study targets the Siwalik Group along the Karnali River area of Nepal Himalaya (Fig. 1.1). A variety of studies in this geologic section have focused on isotopes and age dating, to understand the regional tectonics, exhumation, and the provenance of the sediments (Gautam and Fujiwara 2000, Huyghe et al. 2001, 2005,

Szulc et al. 2006, Van der Beek et. al. 2006, Bernet et al. 2006). Despite these isotopic and chronological studies, no detailed petrographic information is yet available for the Karnali River section. The aim of our present study is to describe the petrography of Siwalik sandstones from the Karnali River section in detail, and determine their provenance. We also examine the factors controlling the variations in sediment composition, based on multivariate statistical analysis.

6.2 METHODS

6.2.1 Point count method

Forty-eight sandstone samples from Karnali River Siwalik Group were selected for petrographic analysis. Of these, 26 samples were from the Chisapani Formation, and 22 from the Baka Formation (Table 6.1). Point counting was carried out to identify individual grain or crystals larger than 0.0625 mm, using the Gazzi-Dickinson method (Zuffa 1985). A total of 500 grains were counted for each thin section, using a Swift point counter. The framework constituents were counted with grid spacing designed to fully cover each slide, at horizontal spacing of 0.2 mm. The detrital modes were recalculated to 100% as the sum of quartz (Q), feldspar (F) and lithic fragments (L) (Table 2). These recalculated parameters were plotted on QFL triangular diagrams for classification (Pettijohn 1975, Folk 1980) and determination of provenance (Dickinson et al. 1983).

6.2.2 Statistical framework

Once all the point counts were completed, compositions were recalculated to 100% for the multivariate statistics, with respect to quartz, feldspar and lithic grains, as

Fmtn	mbr	Sample no.	GPS location	Grain size	Lithofacies	Bedding type
Baka Formation	Upper member	G-5	N28°41'59"/ E81°16'30"	coarse (salt & pepper)	trough cross strat., pebbly	thick
		G-3	N28°41'58"/ E81°16'31"	coarse (salt & pepper)	trough cross strat., pebbly	thick
		G-2	N28°41'55"/ E81°16'31"	coarse	trough cross strat., pebbly	thick
		BK-23	N28°41'52"/ E81°16'36"	v. coarse (salt & pepper)	trough cross strat., pebbly	thick
		G-1	N28°41'49"/ E81°16'44"	v. coarse (salt & pepper)	trough cross strat., pebbly	thick
	Middle member	BK-14	N28°41'40"/ E81°16'51"	fine	planar cross stratification	thick
		BK-13	N28°41'33"/ E81°16'51"	coarse (salt & pepper)	trough cross stratification	thick
		F-1	N28°41'31"/ E81°16'51"	coarse (salt & pepper)	trough cross stratification	thick
		E-1	N28°41'31"/ E81°16'51"	coarse (salt & pepper)	trough cross stratification	thick
		D-9	N28°41'25"/ E81°16'50"	coarse (salt & pepper)	trough cross stratification	thick
		D-7	N28°41'10"/ E81°16'56"	fine	planar cross stratification	thick
		BK-11	N28°41'10"/ E81°16'56"	coarse (salt & pepper)	trough cross stratification	thick
		BK-9	N28°41'03"/ E81°16'57"	coarse (salt & pepper)	ripple lamination	thin
		D-6	N28°41'03"/ E81°16'57"	coarse (salt & pepper)	trough cross stratification	thick
		BK-7	N28°40'56"/ E81°17'02"	coarse (salt & pepper)	trough cross stratification	thick
	Lower member	D-5	N28°40'51"/ E81°17'02"	coarse	trough cross stratification	thick
		BK-5	N28°40'49"/ E81°17'03"	fine	massive, concretion	thin
		BK-4	N28°40'45"/ E81°17'03"	coarse (salt & pepper)	trough cross stratification	thick
		D-3	N28°40'43"/ E81°17'03"	coarse (salt & pepper)	trough cross stratification	thick
		D-2	N28°40'36"/ E81°17'04"	coarse (salt & pepper)	trough cross stratification	thick
		BK-2	N28°40'36"/ E81°17'04"	medium	parallel lamination	thin
		D-1	N28°40'33"/ E81°17'05"	medium (salt & pepper)	trough cross stratification	thick
Chisapani Formation	Upper member	C-24	N28°40'21"/ E81°17'02"	medium	parallel lamination	thick
		C-22	N28°40'19"/ E81°17'01"	very fine	parallel lamination	thin
		C-21	N28°40'09"/ E81°17'02"	medium	planar cross stratification	thick
		C-20	N28°40'01"/ E81°17'07"	coarse	planar cross stratification	thick
		B-36	N28°40'01"/ E81°17'07"	coarse	planar cross stratification	thick
		B-35	N28°40'01"/ E81°17'07"	coarse (salt & pepper)	trough cross stratification	thick
		B-17	N28°39'53"/ E81°17'09"	medium	trough cross stratification	thick
		C-15	N28°39'51"/ E81°17'09"	fine	ripple lamination	thin
		B-14	N28°39'51"/ E81°17'09"	coarse	trough cross stratification	thick
		B-8	N28°39'48"/ E81°17'11"	fine	planar cross stratification	thick
		B-6	N28°39'47"/ E81°17'12"	medium	planar cross stratification	thick
		C-12	N28°39'47"/ E81°17'12"	very fine	climbing ripple lamination	thin
		KS-9	N28°39'44"/ E81°17'12"	coarse	trough cross stratification	thick
		KS-8	N28°39'34"/ E81°17'14"	fine	planar cross stratification	thin
		KS-7	N28°39'21"/ E81°17'13"	v. coarse (salt & pepper)	trough cross stratification	thick
	Middle member	KS-6	N28°39'26"/ E81°17'13"	medium	planar cross stratification	thick
		KS-5	N28°39'25"/ E81°17'13"	fine	massive concreted sst	thin
		KS-4	N28°39'21"/ E81°17'14"	fine	planar cross stratification	thin
		C-5	N28°39'21"/ E81°17'14"	fine	ripple lamination	thin
	Lower member	A-39l	N28°39'11"/ E81°17'15"	fine	planar cross stratification	thick
		KS-3	N28°39'11"/ E81°17'15"	fine	trough cross stratification	thick
		KS-2	N28°39'07"/ E81°17'14"	fine	planar cross stratification	thick
		C-3	N28°39'07"/ E81°17'14"	very fine	parallel lamination	thin
		R-1	N28°39'06"/ E81°17'14"	fine	planar cross stratification	thin
		A-3	N28°39'01"/ E81°17'12"	fine	planar cross stratification	thick
		KS-1	N28°39'01"/ E81°17'12"	medium	planar cross stratification	thick

Table 6.1 List of samples with GPS locations, grain size, lithofacies, and bedding type. Shaded samples are thin bedded facies sandstones.

well as muscovite, biotite, carbonate and cement. Data were also grouped by formation and grain size /facies (thick- and thin-bedded sandstones) to analyze other factors affecting the composition of the sediments (Table 6.1).

Univariate statistics (arithmetic mean and standard deviation) are widely used in provenance analysis (Ingersoll 1978, Howard 1994). However, both parameters are semi-quantitative, because they assume a normal distribution of each component and independence of the components from each other (Allen and Johnson 2010). These assumptions are not valid in ternary diagrams (Weltje 2002). Recent work by Weltje (2002), Ohta and Arai (2007) and Ingersoll and Eastmond (2007) used several multivariate statistical methods to evaluate sandstone compositions. These methods included Principal Component Analysis (PCA), multivariate means, and confidence regions.

PCA is a technique that combines numerous variables into several independent latent variables that underline the multivariate data. PCA can be viewed as a search for the orthogonal coordinates that explain the greatest amount of variation within the data. In undertaking the PCA and expressing the results graphically on ternary diagrams, we followed the approaches described by Weltje (2002), Von Eynatten et al. (2003), and Buccianti and Esposito (2004). These methods are based on the statistical analytical technique for compositional data described by Aitchison (1986). In brief the following sequence of operations was carried out, using CoDaPack 2 software (Thio-Henestrosa and Comas 2011).

1. The petrographic compositional data, whose natural sample space is a simplex, were mapped into Euclidean real sample space using log-ratio transformation (e.g. clr,

alr).

2. Following the log-ratio transformation, the first and second principal components were extracted in the usual way via PCA, using biplots.

3. The log-ratio coordinates were back-transformed to the two-dimensional simplex space ternary diagrams by inverse log-ratio transformation.

4. Within the ternary diagrams, we utilized Weltje's multivariate means and 90%, 95%, and 99% confidence ellipsoids. The boundaries of the multivariate confidence regions for population means were calculated to discriminate the factors controlling the compositions of the sediments.

6.3 RESULTS

6.3.1 Petrography of the individual formations

6.3.1.1 Chisapani Formation

Of the 26 samples analyzed for the Chisapani Formation, seven were taken from the lower member, four from the middle member, and 15 from the upper member (Tables 6.1, 6.2). The Chisapani Formation sandstones are matrix-poor, moderately to well-sorted, and individual grains are sub-rounded to rounded. Quartz grains are mainly monocrystalline, but some polycrystalline grains are present (Fig. 6.1 A, B). Quartz is the dominant mineral in this formation, ranging from 33% (B-6) to 59.8% (KS-7). Feldspar contents are low, ranging from only 0.8% to 4.0% (KS-1). The feldspars are mainly plagioclase and orthoclase (Fig. 6.1C). Average feldspar content is approximately equal in all three members. Lithic grain contents vary widely, from 4.8% (C-3) to 37.2% (B-17) (Table 6.2). The lithic grains are mainly sedimentary and metamorphic, although some plutonic clasts also occur. In all three members the

Chisapani Formation

Sample	Qtz	Feld	Lithic	Musc	Biot	Chl	CO3	Alt	Mat	Cem	Opq	Oth	Q	F	L	ln Q/F	ln Q/L
							Modal composition (%)							Recalculated QFL		logratio	
C-24	37.2	1.4	14.8	1.4	2.4	0.0	23.8	3.4	7.4	6.6	0.2	1.4	69.7	2.6	27.7	3.3	0.9
C-22	38.0	0.8	25.8	3.8	3.0	0.0	11.0	0.2	7.8	8.6	0.2	0.2	58.8	1.2	39.9	3.9	0.4
C-21	47.2	0.8	34.4	0.4	2.6	0.0	6.0	1.2	2.8	3.4	1.0	0.2	57.3	1.0	41.7	4.1	0.3
C-20	55.4	3.0	14.6	2.2	2.0	0.6	10.8	0.2	4.4	6.2	0.2	0.4	75.9	4.1	20.0	2.9	1.3
B-36	54.8	1.6	13.0	0.4	2.2	0.0	15.8	0.6	7.4	3.6	0.4	0.2	79.0	2.3	18.7	3.5	1.4
B-35	45.2	2.0	15.8	1.0	0.6	0.0	17.4	0.0	8.6	8.8	0.4	0.2	71.7	3.2	25.1	3.1	1.1
B-17	40.8	4.4	37.2	2.6	3.0	0.4	4.4	0.0	2.0	5.2	0.0	0.0	49.5	5.3	45.1	2.2	0.1
C-15	40.0	2.2	20.6	5.0	6.0	0.0	12.8	0.4	5.6	6.0	0.4	1.0	63.7	3.5	32.8	2.9	0.7
B-14	46.8	1.8	20.6	1.8	1.6	0.4	12.4	0.0	5.2	9.4	0.0	0.0	67.6	2.6	29.8	3.3	0.8
B-8	33.0	2.0	21.0	3.2	0.6	0.0	21.8	0.4	5.4	11.0	1.0	0.4	58.9	3.6	37.5	2.8	0.5
B-6	33.0	1.4	19.2	4.0	2.6	0.2	21.0	0.0	8.2	9.8	0.2	0.4	61.6	2.6	35.8	3.2	0.5
C-12	41.0	1.6	16.2	8.2	7.4	0.0	11.8	0.8	4.4	8.2	0.2	0.2	69.7	2.7	27.6	3.2	0.9
KS-9	45.6	2.0	15.6	5.6	4.2	0.0	11.2	0.0	5.6	7.2	0.8	2.2	72.2	3.2	24.7	3.1	1.1
KS-8	37.4	0.8	13.0	3.2	2.0	0.0	20.0	0.6	11.0	11.4	0.2	0.4	73.0	1.6	25.4	3.8	1.1
KS-7	59.8	1.8	22.8	1.8	0.8	0.0	1.2	0.4	4.6	5.6	1.4	0.0	70.9	2.1	27.0	3.5	1.0
KS-6	46.8	4.2	20.6	2.0	1.2	0.4	10.8	0.6	5.4	7.0	0.4	0.0	65.4	5.9	28.8	2.4	0.8
KS-5	45.8	1.8	24.2	1.4	0.2	0.0	7.8	0.0	8.6	9.8	0.4	0.6	63.8	2.5	33.7	3.2	0.6
KS-4	48.8	2.0	19.4	3.0	0.4	0.0	3.8	0.2	9.0	13.0	0.2	0.2	69.5	2.8	27.6	3.2	0.9
C-5	50.6	1.2	29.8	1.4	1.2	0.2	4.6	0.8	5.6	3.8	0.6	0.2	62.0	1.5	36.5	3.7	0.5
A-39l	49.2	2.2	20.2	2.8	2.2	0.0	6.2	0.2	9.0	7.4	0.0	0.6	68.7	3.1	28.2	3.1	0.9
KS-3	51.2	2.2	15.2	3.4	2.4	0.1	11.0	0.6	5.4	7.0	1.2	0.4	74.6	3.2	22.2	3.1	1.2
KS-2	56.0	1.6	22.2	1.2	0.6	0.6	3.6	1.6	3.4	8.2	0.0	1.0	70.2	2.0	27.8	3.6	0.9
C-3	36.4	1.0	4.8	3.0	0.2	0.0	10.4	0.0	8.0	35.0	0.6	0.6	86.3	2.4	11.4	3.6	2.0
R-1	36.0	1.2	22.2	0.4	0.4	0.2	17.0	0.4	10.2	12.0	0.6	0.6	60.6	2.0	37.4	3.4	0.5
A-3	54.6	1.0	19.6	1.2	0.6	0.0	7.2	0.0	6.0	9.2	0.2	0.4	72.6	1.3	26.1	4.0	1.0
KS-1	55.4	4.0	18.4	1.0	0.4	1.0	5.6	1.6	3.8	7.4	0.2	1.2	71.2	5.1	23.7	2.6	1.1
Mean	*45.6*	*1.9*	*20.0*	*2.5*	*2.0*	*0.2*	*11.1*	*0.5*	*6.3*	*8.9*	*0.4*	*0.5*	*67.9*	*2.8*	*29.3*	*3.2*	*0.8*
Max	*59.8*	*4.4*	*37.2*	*8.2*	*7.4*	*1.0*	*23.8*	*3.4*	*11.0*	*35.0*	*1.4*	*2.2*	*86.3*	*5.9*	*45.1*	*2.7*	*0.6*
Min	*33.0*	*0.8*	*4.8*	*0.4*	*0.2*	*0.0*	*1.2*	*0.0*	*2.0*	*3.4*	*0.0*	*0.0*	*49.5*	*1.0*	*11.4*	*3.9*	*1.5*
S.D	*7.8*	*1.0*	*6.7*	*1.8*	*1.8*	*0.3*	*6.2*	*0.7*	*2.3*	*5.9*	*0.4*	*0.5*	*7.7*	*1.2*	*7.6*	*1.8*	*0.0*

Baka Formation

Sample	Qtz	Feld	Lithic	Musc	Biot	Chl	CO3	Alt	Mat	Cem	Opq	Oth	Q	F	L	ln Q/F	ln Q/L
							Modal composition (%)							Recalculated QFL		logratio	
G-5	41.0	4.2	21.8	4.4	1.8	0.2	14.6	0.0	4.4	7.2	0.0	0.4	61.2	6.3	32.5	2.3	0.6
G-3	40.0	3.2	20.6	4.6	3.0	0.2	12.0	0.0	9.0	6.6	0.2	0.6	62.7	5.0	32.3	2.5	0.7
G-2	39.8	3.4	20.2	2.4	6.6	0.4	12.4	0.0	7.2	7.4	0.0	0.2	62.8	5.4	31.9	2.5	0.7
BK-23	37.0	1.0	19.8	6.0	12.2	0.2	8.8	1.0	5.6	7.2	0.2	1.0	64.0	1.7	34.3	3.6	0.6
G-1	46.0	3.8	19.8	4.8	3.4	0.2	6.8	2.0	4.6	8.4	0.0	0.2	66.1	5.5	28.5	2.5	0.8
BK-14	49.0	2.8	16.4	2.2	5.4	0.4	7.2	1.8	7.6	6.4	0.2	0.6	71.9	4.1	24.1	2.9	1.1
BK-13	47.0	2.0	14.2	4.8	10.8	3.4	3.2	1.4	3.8	8.4	0.2	0.8	74.4	3.2	22.5	3.2	1.2
F-1	41.8	5.0	25.8	4.2	2.6	0.4	12.0	0.0	3.6	4.4	0.0	0.2	57.6	6.9	35.5	2.1	0.5
E-1	36.8	6.2	16.0	3.2	5.2	0.4	21.8	0.0	4.4	5.2	0.0	0.8	62.4	10.5	27.1	1.8	0.8
D-9	42.6	3.6	25.4	6.2	4.6	0.0	5.2	0.8	3.4	7.6	0.0	0.6	59.5	5.0	35.5	2.5	0.5
D-7	41.8	6.2	15.8	0.6	5.8	1.6	17.0	0.0	5.2	6.0	0.0	0.0	65.5	9.7	24.8	1.9	1.0
BK-11	41.8	2.2	17.0	5.6	6.0	1.6	11.0	1.2	7.0	6.4	0.2	0.0	68.5	3.6	27.9	2.9	0.9
BK-9	23.4	0.2	4.4	12.0	16.2	1.8	22.2	0.4	6.2	12.6	0.2	0.4	83.6	0.7	15.7	4.8	1.7
D-6	48.6	4.6	22.0	1.4	2.2	0.0	10.4	0.0	6.0	4.6	0.2	0.0	64.6	6.1	29.3	2.4	0.8
BK-7	60.0	2.2	12.6	0.6	2.2	0.0	8.6	0.6	8.2	4.2	0.0	0.8	80.2	2.9	16.8	3.3	1.6
D-5	42.6	5.6	15.8	0.6	1.4	0.2	17.4	0.0	6.8	8.8	0.4	0.0	66.6	8.8	24.7	2.0	1.0
BK-5	28.2	1.0	6.6	3.6	5.8	0.0	25.2	1.4	14.8	12.4	0.0	1.0	78.8	2.8	18.4	3.3	1.5
BK-4	52.0	5.0	16.4	2.6	1.2	0.0	11.2	0.4	6.6	4.6	0.0	0.0	70.8	6.8	22.3	2.3	1.2
D-3	56.2	3.8	16.6	3.0	2.6	0.4	6.6	0.0	5.0	5.0	0.2	0.6	73.4	5.0	21.7	2.7	1.2
D-2	43.0	4.4	18.6	3.8	3.2	0.0	11.8	0.0	5.4	8.8	0.4	0.8	65.2	6.7	28.2	2.3	0.8
BK-2	41.8	1.2	14.8	13.2	9.8	0.6	11.4	0.4	2.6	4.6	0.0	0.4	72.3	2.1	25.6	3.6	1.0
D-1	50.0	2.2	20.2	1.2	2.4	0.2	12.4	0.0	4.8	6.2	0.2	0.2	69.1	3.0	27.9	3.1	0.9
Mean	*43.2*	*3.4*	*17.3*	*4.1*	*5.2*	*0.6*	*12.2*	*0.5*	*6.0*	*7.0*	*0.1*	*0.4*	*68.2*	*5.1*	*26.7*	*2.7*	*1.0*
Max	*60.0*	*6.2*	*25.8*	*13.2*	*16.2*	*3.4*	*25.2*	*2.0*	*14.8*	*12.6*	*0.4*	*1.0*	*83.6*	*10.5*	*35.5*	*4.8*	*1.7*
Min	*23.4*	*0.2*	*4.4*	*0.6*	*1.2*	*0.0*	*3.2*	*0.0*	*2.6*	*4.2*	*0.0*	*0.0*	*57.6*	*0.7*	*15.7*	*1.8*	*0.5*
S.D	*8.1*	*1.7*	*5.1*	*3.2*	*3.9*	*0.8*	*5.6*	*0.7*	*2.6*	*2.3*	*0.1*	*0.3*	*6.8*	*2.5*	*5.7*	*0.7*	*0.3*

Table 6.2: Recalculated modal point count data (%) and calculated Q/F and Q/L logratios for the Chisapani and Baka Formations.
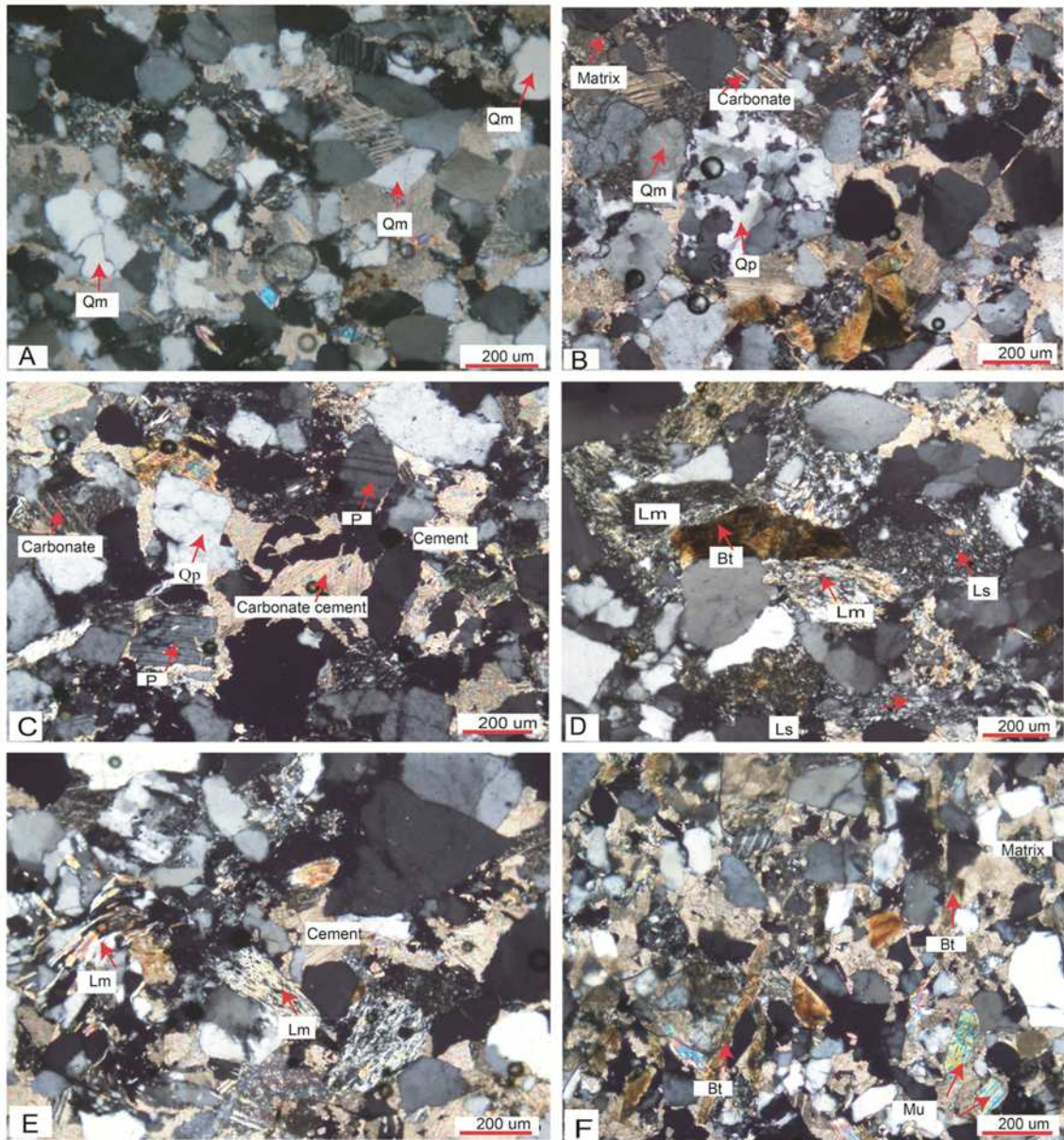
Fig. 6.1: Photomicrographs of sandstones from the Chisapani and Baka Formations A) Monocrystalline quartz (Qm) B) Polycrystalline quartz (Qp) C) Plagioclase feldspar and carbonates D) Sedimentary (Ls and metamorphic lithic grains (Lm) E) Metamorphic lithic grains (Quartz-mica schist) F) Mica grains, variegated colour indicates muscovite (Mu and dark brown colour indicates biotite (Bt).

metamorphic lithics are dominantly quartz-mica schists and phyllites. Muscovite and

biotite (mica) occur as accessory minerals in the Chisapani Formation. The amount of

mica present ranges from 0.4% to 8.2% for muscovite, and 0.2% to 7.4% for biotite. The percentage of mica increases toward the upper member. Carbonate is other important constituent in the Chisapani Formation, occurring as intraclasts, and cement (Fig 6.1 A, C). Carbonate contents range from 1.2% (KS-7) to 23.8% (C-24), and increase toward the upper member. Mica and carbonates are the only components to show noticeable stratigraphic change at some intervals within this formation (Table 6.2).

6.3.1.2 Baka Formation

The Baka Formation is represented by 22 sandstones, with seven from the lower member, ten from the middle member, and five from the upper member (Tables 6.1, 6.2). The sandstones are matrix-poor and are moderately to well sorted, and contain angular to sub-rounded framework grains. Quartz is again the dominant mineral, with contents ranging from 23.4% (BK-9) to 60.0% (BK-7). Feldspar grains consist of plagioclase, orthoclase and microcline, and form up to 6.2% of the mode (D-7, E-1). Lithics are mainly metamorphic rock fragments such as mica schists, foliated quartz, and phyllite (Fig. 6.1 D, E, F). The proportions of biotite and muscovite range from 1.2% (BK-4) to 6.2% (BK-9) and 0.6 % (BK-7) to 12% (BK-9) respectively, and contents increase toward the upper member (Table 6.2), reaching maximums of 12.2% (biotite) and 6.0% (muscovite) in sample BK-23 (Table 6.2, Fig. 6.1F). Carbonate contents contain range from 3.2% (BK-13) to 25.2% (BK-5), but no clear stratigraphic change is evident. Heavy minerals, opaque minerals and chlorite occur in minor amounts (Table 6.2). Feldspar and Mica contents show the same changes in some intervals in this formation.

6.3.2 Classification of the sandstones

According to this classification scheme of Pettijohn (1975), most samples are
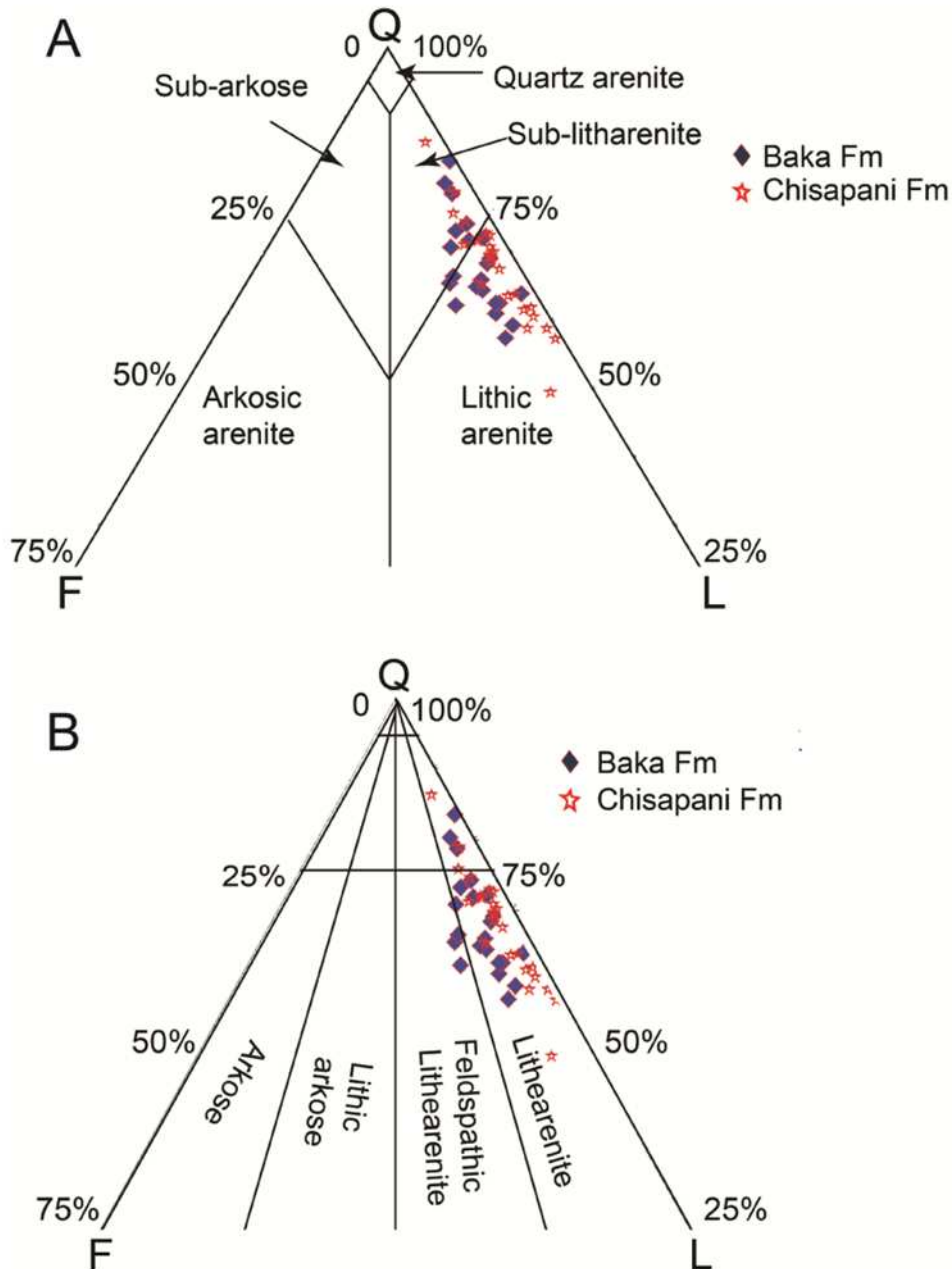
Fig. 6.2: Classification of Karnali River Siwalik sandstones A) QFL diagram based on Pettijohn (1975), showing sublitharenite to lithic arenite sandstones. B) QFL diagram of Folk (1980) showing litharenite to feldspathic litharenite sandstones.

lithic arenites, and the remainder sub-litharenites (Fig. 6.2A). Using the Folk (1980) diagram, slightly higher feldspar content in a few Baka Formation sandstones leads to their classification as feldspathic litharenites, while the majorities are litharenites (Fig. 6.2 B). However, there is no significant contrast in the compositions of these two formations, and high quartz/feldspar ratio is maintained throughout the succession.

6.3.3 Comparison with the other Siwalik sections

The QFL characteristics of the Karnali River samples were also compared with those from other Siwalik sections in the Surai Khola, Arun-Tinau Khola, Hetauda, and Muskar Khola districts (Dhital et al. 1995, Tokuoka et al. 1986, Tamrakar et al. 2003, Chirouze et al. 2012) (Fig. 6.2C).
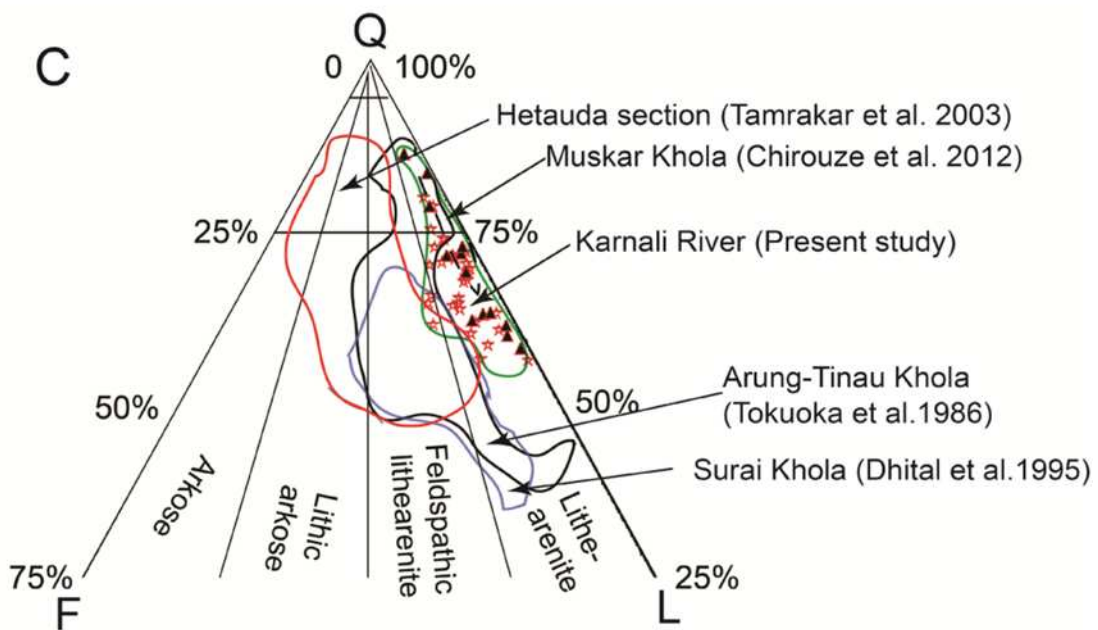
C) Comparison with sandstones from different sections of the Siwalik Group, Nepal.

This shows that QFL compositions are similar among these areas, except for lower feldspar content in the Karnali section. Surai Khola and Arung Khola sandstones have the highest feldspar and lithic fragment contents, and are classified as litharenites and feldspathic litharenites. Similarly, Hetauda section sandstones have indicates that higher feldspar and quartz contents, and are classified as lithic arenites through to arkosic arenites. The Muskar Khola samples contain the least feldspar. The overall recalculated QFL composition of the Chisapani Formation is $Q_{68}F_3L_{29}$, and that of the Baka Formation $Q_{68}F_5L_{27}$ (Tables 2). These results are comparable with previous studies from the Surai Khola and Bakiya Khola sections, which are characterized by quartzolithic compositions of $Q_{57}F_4L_{39}$ and $Q_{59}F_6L_{35}$ respectively (Critelli and Ingersoll 1994).

6.2 Comparison with the surrounding area

Based on the QFL scheme of Dickinson et al. (1983), Karnali River sandstones plot in the recycled orogen field (Fig. 6.3A), consistent with previous results from the Surai Khola and Bakiya Khola sections (Critelli and Ingersoll 1994). The Arung-Tinau Khola and Hetauda-Bakiya Khola sections have the highest feldspar and lithic grain contents among all Siwalik sections. These compositional variations are probably due to contributions from Lesser Himalayan granitoids such as the Agra Granite and the Palung Granite in west-central and eastern Nepal. The recycled orogen provenance of the Karnali samples is also consistent with that for Siwalik sandstones from the Potwar Plateau (Fig. 6.3B). The only significant different is the higher feldspar content in the Potwar Plateau relative to the Siwalik Group in Nepal. This compositional variation in the Potwar Siwalik sediments may be related to contributions of detritus derived from volcanic sources in their hinterland (Critelli and Ingersoll 1994).
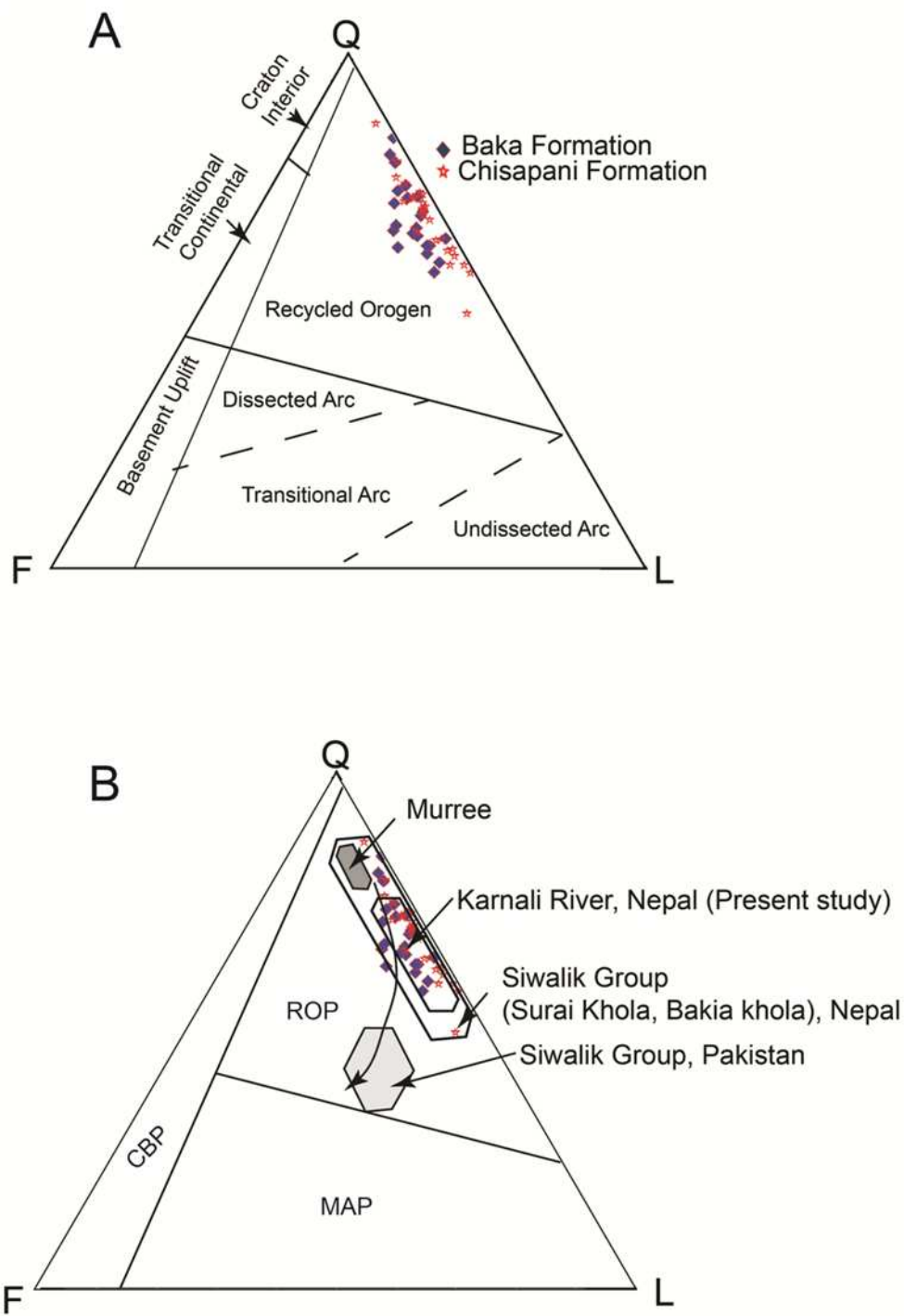
Fig. 6.3: QFL provenance plot (Dickinson, et al. 1983) for the Karnali sandstones. A) QFL plot for the Siwalik Group along the Karnali River section, indicating derivation from a recycled orogen source. B) QFL plot showing regional comparison in the Himalaya foreland basin (modified from Critelli and Ingersoll 1994).

74

6.4 Analysis of controlling factors using multivariate statistics

6.4.1 Principal Component Analysis (PCA) and Weltje's confidence regions

PCA loadings of clr-transformed data are presented in Table 6.3. The first principal component (PC1) shows a positive correlation with clr-transformed quartz, feldspar, lithics, carbonate and cement components, and negative correlation with muscovite and biotite. The second principal component (PC2) is positively correlated with muscovite, carbonates and cements, and negatively correlated with quartz, feldspar, and lithics components. PC1 and PC2 capture 46% and 24% of the total variability, respectively. Collectively 70% of the total variability is explained by these two components, with a smaller amount (17%) being accounted for the third principal component (PC3).

	PC1	PC2	PC3	PC4	PC5	PC6
Quartz	0.247	-0.055	0.067	-0.364	0.188	-0.788
Feldspar	0.369	-0.500	0.156	0.630	0.198	0.101
Lithics	0.282	-0.207	0.171	-0.482	-0.569	0.386
Muscovite	-0.415	0.406	0.586	0.298	-0.267	-0.129
Biotite	-0.716	-0.440	-0.220	-0.192	0.228	0.112
Carbonate	0.045	0.281	-0.741	0.285	-0.365	-0.107
Cement	0.188	0.516	-0.018	-0.175	0.588	0.424
Varience explained (%)	45.76	22.62	17.27	8.92	3.96	1.47
Cum.Prop.Exp.	0.458	0.684	0.857	0.946	0.985	1.000

Table 6.3: Results of Principal Component Analysis (PCA) for the Chisapani and Baka Formations

PC1 and PC2 are illustrated as a biplot (Gabriel, 1971; Aitchison and Greenacre, 2002) in Fig. 6.4. Samples from the Chisapani Formation plot randomly on the biplot. PC1 is positively correlated with quartz, feldspar, and lithic fragments. Carbonate is also positively correlated, but plots in a near-perpendicular direction to PC1. Muscovite and biotite are negatively correlated in PC1. Similarly, carbonate muscovite and cement are positively correlated in PC2, with all other components negatively correlated. Samples

from the Baka Formation also plot randomly, although a few samples tend to be concentrated near the quartz and feldspar components. The carbonate is mainly originated from the Lesser Himalayan sources and feldspar, muscovite and biotite are indicators of the Higher Himalayan source. These components of data suggest that PC1 probably related to the mixed sources from the Lesser and Higher Himalayas, and PC2 is correlated with the Higher Himalaya (Fig. 6.4). The data for both formations are strongly influenced by both PC1 and PC2, probably due to mixed sediments from the Lesser and Higher Himalayas.

The PCA biplot confirms that there is a strong relationship between quartz, feldspar and lithic grains in both the Chisapani and Baka Formations (Fig. 6.4). To more clearly discriminate between these components, we have used another multivariate
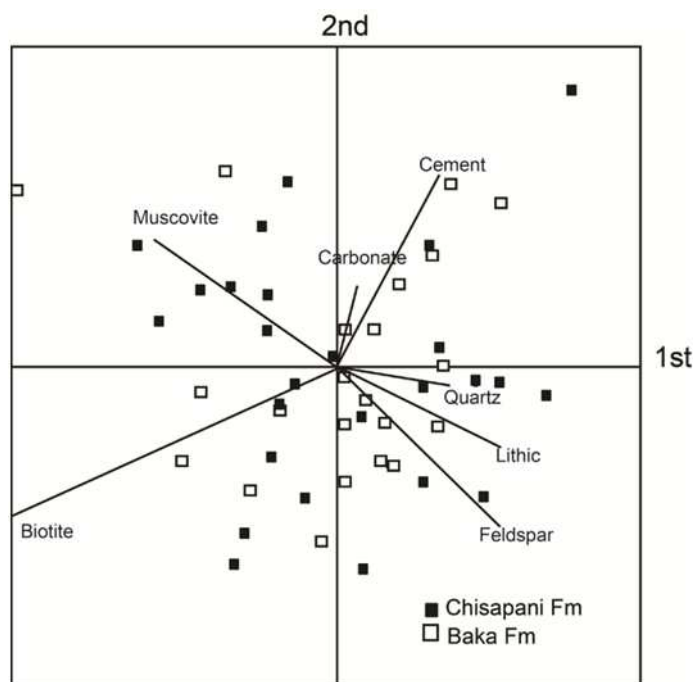
Fig. 6.4: Principal Component Analysis (PCA) biplot of the clr-transformed data from Table 2. Scattered data indicates little variation in sediment composition between the fomations (see text for details).
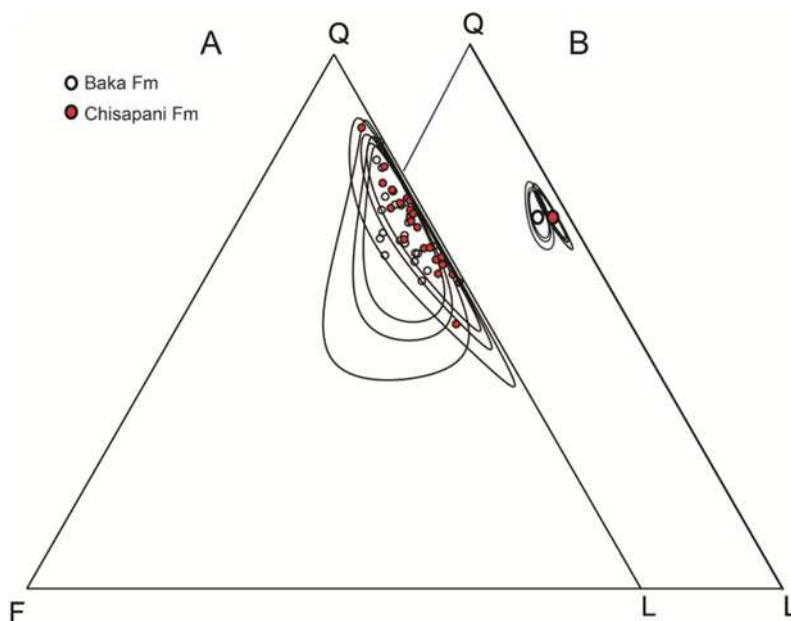
Fig. 6.5: Multivariate ellipsoids (Weltje 2002) for the Chisapani and Baka Formations. Confidence regions are 90%, 95% and 99%. A) Predictive regions of the data points. B) Confidence regions of the population mean. See text for details.

statistical method adopted by Weltje (2002). This method is formalized by use of the multivariate additive logistics normal distribution (Aitchison 1986). Stattegger and Mortan (1992), Prins and Weltje (1999) and Garzanti et al. (2000) have also used ternary confidence regions for petrographic data, based on this model. The purpose of these confidence regions were given by Weltje (2002) as:

- Confidence regions of the entire population can be used to predict the range of variation in observations;

- Confidence regions of the population mean are useful for deciding if samples differ significantly from each other.

The multivariate confidence regions of the Chisapani and Baka Formations are shown in Figure 6.5. Most of the data falls within the 90% confidence regions of both formations. The mutual clustering of the Chisapani and Baka Formations data and the

nearly total overlap of their confidence regions indicates general lack of significant compositional variation between the formations, and that the sediments mixed (Weltje 2002). This suggests the sediments in each formation were simultaneously derived from both the lesser Himalaya and Higher Himalaya. Slight change in the composition of the Baka Formation and subtle shift of the data towards the 95% and 99% confidence regions likely reflects some contribution from a different source area (i.e. Higher Himalaya), or some local influence such as hydraulic sorting during transportation (Weltje, 2002, Allen and Johnson, 2010) (Fig 6.5B).

6.4.2 Grain size and facies control on sediments (thick vs. thin-bedded sandstones)

Thick-bedded sandstones in the Karnali section consist mainly of trough to planar cross-stratified, medium to coarse-grained sandstones, with bed thicknesses ranging from 4.0 to 10.0 m. These thick-bedded sandstones are interpreted as channel deposits. The thin-bedded (shaded part) sandstones sampled here are mainly very fine to medium-grained, and cross-stratified to rippled (Table 6.1). Bed thicknesses range from 0.5 to 2.0 m, and the beds are interpreted as being either flood plain or crevasse splay deposits (Sigdel et al., 2011).

We have also applied the multivariate statistics method here to test for contrast between grain size/facies groups, based on the compositions of the thinly and thickly bedded sandstones (Table 6.1). The biplot from the PCA analysis shows random distribution in all coordinate planes (Fig. 6.6). The Weltje triangular confidence 90%, 95% and 99% regions for the two facies also overlap each other, indicating the sediments are well mixed, and no specific control is exercised by the principal components (Fig. 6.7). The slightly different locations of the population means of the

confidence regions suggest changes in the source area, or minor influence by the facies/grain size of the sediments.
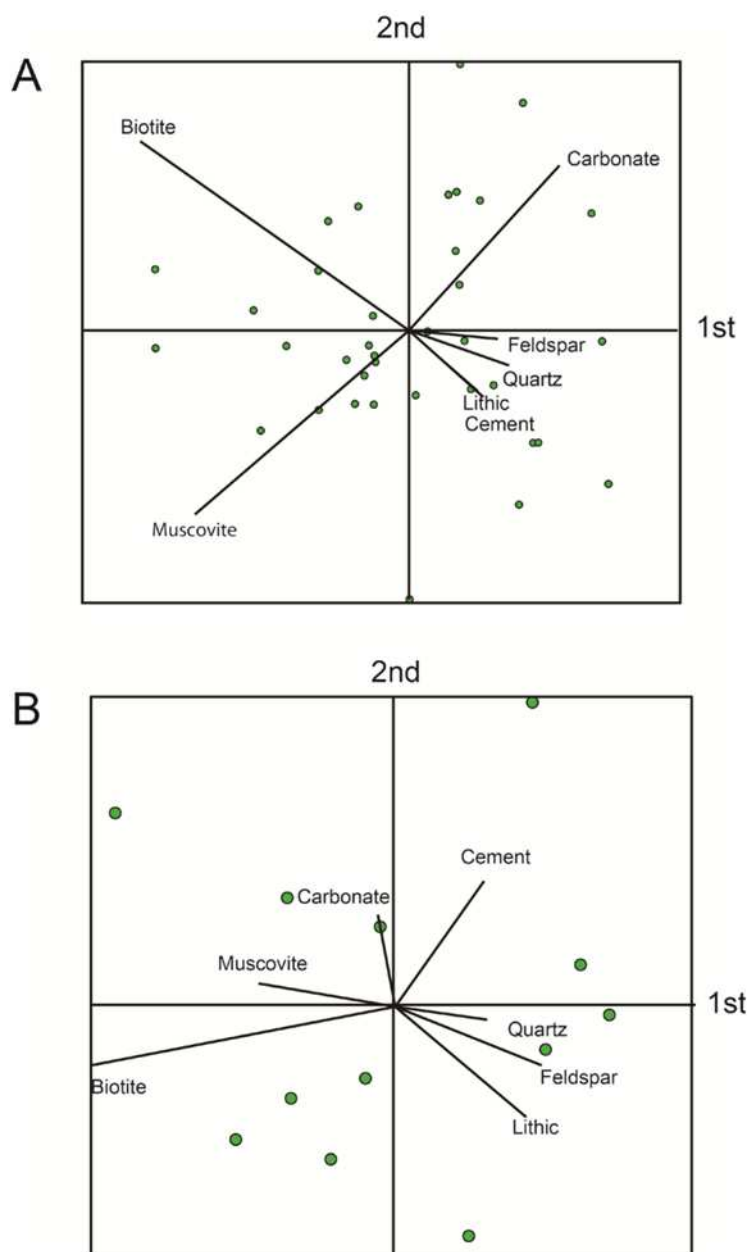
Fig. 6.6: Principal Component Analysis (PCA) biplot of clr-transformed data by grain size. Data are grouped on the basis of facies and grain size. (A) thick-bedded; (B) thinly-bedded. See text for details.
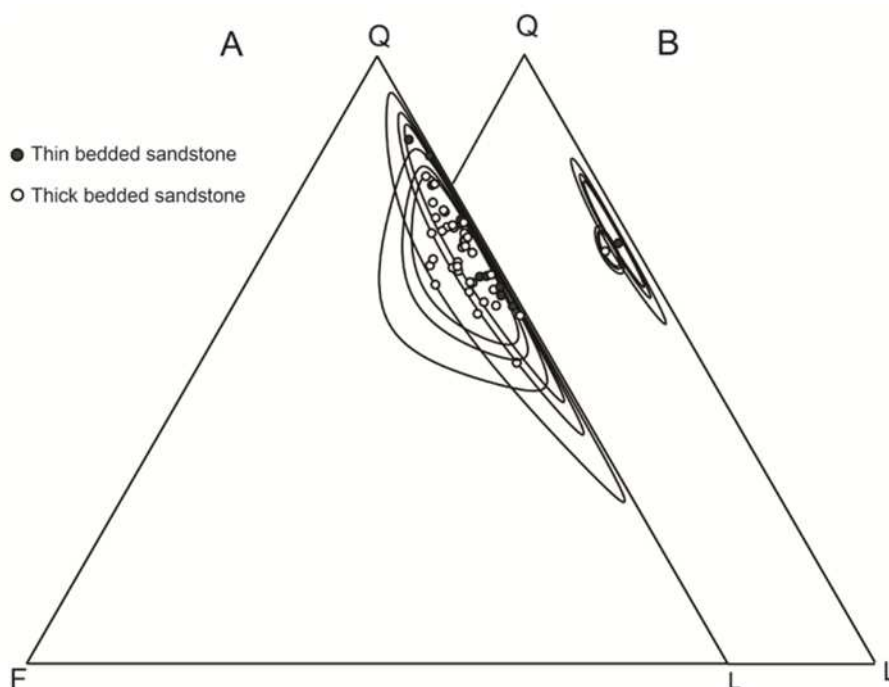
Fig. 6.7: Multivariate ellipsoids (Weltje 2002) of the thick and thinly-bedded sandstones Confidence regions are 90%, 95% and 99%. A) Predictive regions of the data points. B) Confidence regions of the population mean. See text for details.

6.4.3 Climatic-physiographic control on sediments

A general petrographic measure of the weathering trends of sandstone may be defined in term of the log-ratios of principal framework elements (*cf* Aitchison, 1986), for example as log (Q/F) or log (Q/L), where Q = quartz, F = feldspar and L = lithic fragments (Weltje 1994). The log-ratios for individual samples are listed in Tables 6.2. For many types of sand, values of both log-ratios are expected to correlate with weathering intensity, because quartz is more resistant to weathering than feldspar and lithic fragments. The combination of these log-ratios in a single diagram permits the distinction of parent rock type, weathering history, and paleotopography (Weltje et al., 1998) (Fig. 6.8). Based on this diagram, all except two of the Karnali samples fall in the field of weathering index 1 (Fig. 9). The Chisapani Formation samples mainly fall near

the boundary between weathering index 0 and 1, towards metamorphic and sedimentary

parentage. Samples from the Baka Formation plot nearer the boundary between
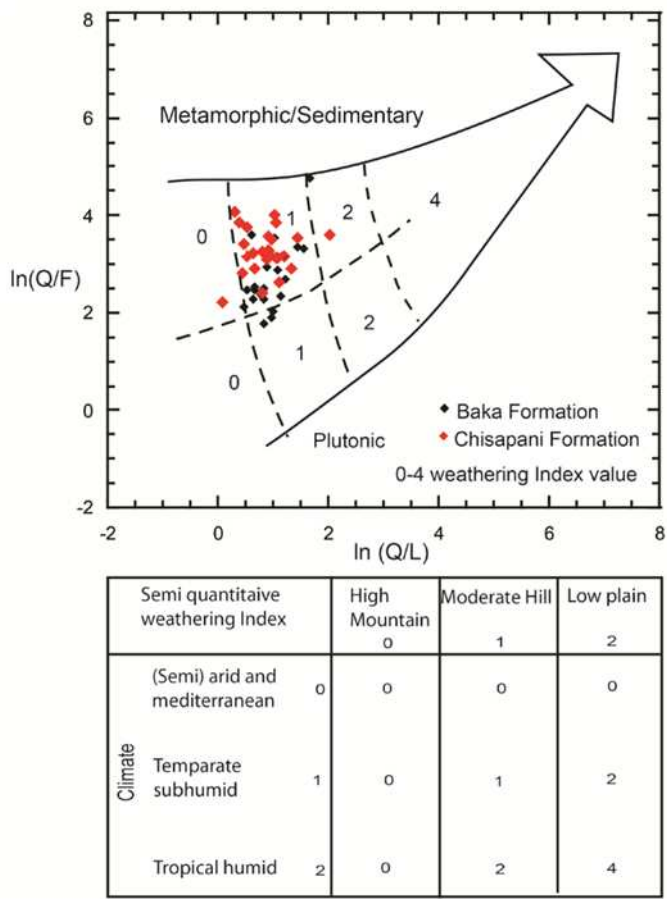
Fig. 6.8: Log-ratio plot after Weltje (1994). Q – Quartz; F – Feldspar; L – Lithic fragments. Fields 0-4 refer to the semi-quantitative weathering indices defined on the basis of relief and climate, as indicated in the table.

metamorphic/sedimentary and plutonic parentage. These indices indicate that the

sediments were mainly derived from high mountains (Higher Himalaya) and moderate

hills (Lesser Himalaya), and the influence of climate on the sediment compositions was

very small (0-1) (Fig. 6.8).

Chapter 7

DISCUSSIONS

7.1 Lithostratigraphy

7.1.1 Ages of the Lower - Middle and Middle - Upper Siwalik boundaries

Previous lithostratigraphic and magnetostratigraphic studies of sections from the Hetauda-Bakiya Khola area (Harrison et al., 1993; Sah et al., 1994), Arung Khola-Tinau Khola (Tokuoka et al., 1986, 1990; Gautam and Appel, 1994), Surai Khola (Corvinus and Nanda, 1994; Dhital et al., 1995; Appel and Rosler, 1994) and our new lithostratigraphic and magnetostratigraphic work by Gautam and Fujiwara, (2000) in the Karnali River permit regional correlation in the Siwalik Group across Nepal Himalaya. Basically, the stratigraphy of these areas differs. The traditional tripartite (Lower, Middle and Upper Siwaliks) stratigraphic boundaries are used here to discuss the stratigraphic patterns and their age. Several previous studies have already indicated that there are discrepancies in the ages of these boundaries between locations (Tables 7.1).

The Lower–Middle Siwalik boundary is defined as the top of the Rapti Formation in the Hetauda-Bakiya Khola area (ca. 9.5 Ma), the top of the Arung Khola Formation in the Arung Khola–Tinau Khola area (ca. 8.5 Ma), and the top of the Chor Khola Formation in the Surai Khola (ca. 8.3 Ma). The top of the Chisapani Formation in the Karnali River section is dated around 9.6 Ma, only slightly older than the age in the Hetauda–Bakiya Khola area (Table 7.1).

The Lower and Middle Siwalik boundary is defined based on the grain-size and increasing thickness of sandstone beds, together with the appearance of distinctive "salt

Age (Ma)	Karnali River (Present Study)		Surai Khola (Dhital et al. 1995)		Arung Khola-Tinau Khola (Tokuoka et al. 1986, 1990)		Hetauda-Bakiya Khola (Sah et al. 1994), (Nakayama and Ulak 1999)	
							Churia Mai Fm	
1	Panikhola Gaun Fm		Dhan Khola Fm		Deorali Fm		Churia Khola Fm	
2					Chitwan Fm			
3	Kuine Fm		Dobata Fm		Upper mbr			
4	Baka Fm	Upper mbr	Surai Khola Fm	Upper mbr	Binai Khola Fm	Middle mbr	Amlekhganj Fm	Upper mbr
5								
6				Middle mbr				
7		Middle mbr		Lower mbr				
8				Shivgarhi mbr		Lower mbr		Middle mbr
9		Lower mbr	Chor Khola Fm					Lower mbr
10	Chisapani Fm	Upper mbr		Jungali Khola mbr	Arung Khola Fm	Upper mbr	Rapti Fm	Upper mbr
11								Middle mbr
12				Bankas Fm		Middle mbr		Lower mbr
13								
14		Middle mbr				Lower mbr		
15		Lower mbr						

Table 7.1: Lithostratigraphic classification of the Siwalik Group in the Nepal Himalaya and its correlation. The bold lines indicate that the boundaries between the Lower-Middle and Middle-Upper Siwaliks. Black part indicates the no deposition. Fm: Formation, mbr: member

and pepper sandstone". These sandstone beds contain more mica grains than underlying sandstone intervals, suggestive of derivation from the Higher Himalayan Belt. The fining-upward successions that characterize these sandstones may represent channel fill deposits (Miall, 1996). The thickening trend of such succession implies that river size increased through time. In the present day Himalayan river systems, the channels become deeper downstream from the upstream braided region to the downstream

meandering region; bed-thickness also increases in the same direction, hence recording increased water discharge and sediment supply through time (Zaleha, 1997).

The appearance of the "salt and pepper" sandstones indicate not only that the drainage basins of the river systems had reached the Higher Himalayan belt, but also that they had deeply incised the Higher Himalayan rocks. The earlier appearance of such sandstones in the Karnali River section indicates that its drainage basin spread into the Higher Himalayas earlier than in other areas. The appearance of such sandstones also coincides with the increase in uplift rate of the Himalaya in western Nepal at about 12-9 Ma (DeCelles et al., 1998, Robinson et al., 2001, Huyghe et al., 2005). Therefore, the timing of the Lower – Middle Siwalik boundary in the Karnali River section is consistent with the timing of the uplift.

The Middle and Upper Siwalik boundaries also show variations in ages. In the Hetauda-Bakiya Khola area it is dated at around 3.0 Ma, compared to ~2.5 Ma in the Arung Khola – Tinau Khola and ~4.0 Ma in the Surai Khola. Although the specific age of the boundary has not yet been obtained in the Karnali River section, it is expected to be around 3.9 Ma, based on calculated sedimentation rate (Gautam and Fujiwara, 2000). Corvinus and Nanda (1994) and Dhital et al. (1995) reported that the Dobata Formation, which forms the lower part of the Upper Siwaliks in the Surai Khola; Nakayama and Ulak (1999), considered that it had an anastomosed river origin. In contrast, in other areas the Upper Siwaliks is represented by a conglomeratic facies (alluvial fan deposits). The onset of "normal" Upper Siwalik deposition around the Surai Khola area should thus be recognized as the base of the first conglomeratic deposits in the Dhan Khola Formation (around 2.3Ma).

The Middle – Upper Siwaliks boundary is marked by a change from sandy to

gravelly facies (Nakayama and Ulak, 1999). These facies are closely related to the progradation of alluvial fans; these were developed by the southward-flowing transverse drainage pattern created by the activity of thrusts (DeCelles et al., 1988; Heller and Poala, 1992; Kumar et al., 2003). This thrust activity is manifested by the trapping of coarse detritus sediment in the proximity of the thrust front, and transportation of finer-grained material toward distal environments (Heller and Paola 1992). The progradation rate of alluvial fans along the vicinity of the MFT is consistent with the diachronous boundaries between the Middle and Upper Siwaliks (Burbank, 1992; Brozovic and Burbank, 2000). In the modern environment, activity of thrust splays in the footwall of the Main Frontal Thrust (MFT) has caused large-scale progradation of alluvial fans (gravel fans near the foot of the Siwalik Hills) toward the present Indo-Gangatic plain (Pati et al., 2011). However, the Surai Khola section experienced a different environmental change, marked by the appearance of anastomosed river deposits. This clearly suggests that the environment of the Surai Khola area changed temporarily to become an inter-alluvial fan region. Because the distribution of coarse-grained river deposits is limited to the places where the rivers crossed the Himalayan Frontal Thrusts at their time of deposition, the diachrony of this boundary should be expected to be larger than that of the Lower and Middle Siwaliks. Based on comparison with the Siwalik deposits in the Nepal Himalaya, the Siwalik Group sediments along the Karnali River were deposited from rivers with larger drainage systems than in other areas. In large river systems, local climate (i.e. local precipitation) has minimal effect on the fluvial channel style, which can change only by regional or basin-wide precipitation. Previous paleoclimatolotical studies from the Siwalik Group of Nepal Himalayas have less focused on the paleodrainage systems into account. The

Karnali River section is thus a sedimentary succession which is suitable for the analysis of paleoclimate related to the uplift of the Himalayas in the future.

7.2 Fluvial Facies

7.2.1 Fluvial systems and their comparison with previous work

Our facies analysis and paleocurrent data show that Siwalik Group sediments along the Karnali River section were deposited from a highly sinuous fine-grained meandering river system (15.8-13.5 Ma), a flood-flow dominated meandering river system with intermittent appearance of a sandy braided river system (13.5-9.6 Ma), a deep and shallow sandy braided river system (9.6-3.9 Ma), and gravelly braided (~3.9-~2.0 Ma) to debris-flow dominated braided river systems, in ascending order (Fig. 7.1). This reconstruction differs slightly from the earlier interpretation by Huyghe et al. (2005). The major differences lie in the timing of appearance and characteristics of the flood-flow dominated meandering system, and that the anastomosed river system was not identified in our study.

We estimate the timing of the appearance of the flood-flow deposits at around 13.5 Ma, some 0.4 Ma earlier than that suggested by Huyghe et al. (2005). The reason for the discrepancy in this facies association boundary is unsure, because Huyghe et al. (2005) did not describe the boundary. We believe the boundary we have defined is appropriate, as: i) the appearance of flood-flow dominated system is interpreted to have been associated with an increase in water discharge. Soil colour also changed from reddish-brown to grey or pale greenish-grey, suggesting increased water logging conditions (Retallack, 1991), and ii) playa deposits were identified from FA2, which
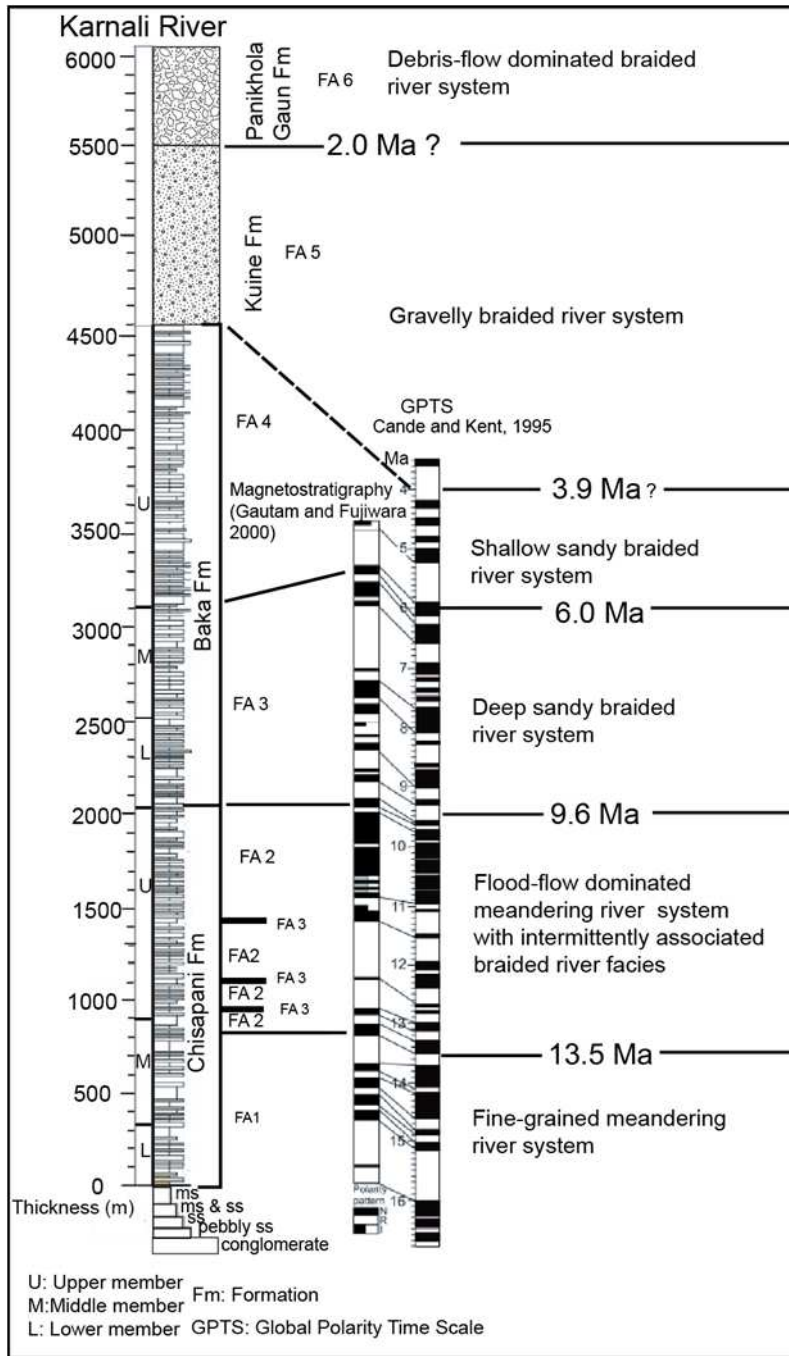
Fig. 7.1: Classification of the fluvial system in the study area based on the magnetostratigraphic time frame (modified from Gautam and Fujiwara, 2000).

also suggests more frequent water supply with higher seasonality than in the FA1 phase. Furthermore, we recognized a shallow sandy braided river facies in the interval from which Huyghe et al. (2005) identified an anastomosed river system. This sandy braided river facies is characterized by laterally continuous sheet sandstones dominated by large scale facies Sp and St and unimodal paleoflow direction, which indicates the frequent shifting of shallow channels of braided river (Smith, 1972; Miall, 1996), and hence we reinterpret the anastomosed river system of Huyghe et al. (2005) as a braided river system.

7.2.2 Significance of the change from a fine-grained meandering system to a flood-flow dominated meandering system around 13.5 Ma

The change from fine-grained meandering river deposits with red soils (FA1) to the flood flow-dominated meandering river deposits with greenish-grey to yellowish-brown soils (FA2) indicates increased water discharge in the river channel after 13.5 Ma. This increased water discharge arose from increased precipitation related to climate change (Nakayama and Ulak, 1999). However, this facies changes is diachronous in Siwalik sections, occurring at around 10.5 Ma, 10.0 Ma and 9.5 Ma in the Bakiya Khola, Tinau Khola, and Surai Khola areas, respectively (Nakayama and Ulak, 1999; Ulak and Nakayama, 2001) (Table 7.2). Although Huyghe et al. (2005) inferred that larger river catchment size contributed to the earlier appearance of this facies in the Karnali River than in other areas, they provided no specific discussion on the size of the river catchment, or how it affected the fluvial depositional system.

River catchment size may be a possible cause of the diachronous facies change, as Huyghe et al. (2005) inferred. Rivers with small catchments size could be strongly

affected by orographic precipitation associated with local uplift, as small increases in precipitation can change the channel characteristics. In contrast, if catchments are large, river characteristics (especially width and depth) should respond only to regional precipitation changes, because water supply from their larger area suppresses the effect of local increase or decrease of precipitation on discharge and river channel characteristics. Presence of large catchment systems in the past has been identified by analysis of river channel deposits and provenance. Such studies in the Tinau Khola section have shown that the sediments were deposited by a larger river system in the past i.e. the paleo-Kaligandaki River (Tokuoka et al., 1986; Hisatomi and Tanaka, 1994; Nakayama and Ulak, 1999; Ulak and Nakayama 2001; Szulc et al., 2006). Petrographic and isotopic analyses from the Karnali section also indicate the earlier supply of detritus from both the Higher and Lesser Himalaya (DeCelles et al., 1998; Robinson et al., 2001; Szulc et al., 2006), suggesting the sediments were supplied from a large catchment system, probably the paleo-Karnali River.

The reason why the flood-flow dominated river system developed earlier in the Karnali River section than in the central and eastern parts of the Nepal Siwaliks remains unclear, however. As noted above, the Karnali River section contains sediments that were deposited mainly from a large catchment system. The Karnali section thus provides a record of regional climate, and hence the increase in water discharge around 13.5 Ma can be interpreted to have been due to intensification of the Indian Summer Monsoon. Earlier uplift in the western part of the Nepal Himalaya may also have caused higher orographic rainfall in this region.

Ojha et al. (2000) reported the magnetostratigraphy of the Khutia Khola section, which is located about 50 km west of the Karnali River (Fig. 1.1), and showed that the

age of base of the Middle Siwaliks was about 11.05 Ma which is 1.5 Ma earlier than the

Karnali River section.

Age (Ma)	Karnali River *Present study*	Surai Khola *Nakayama and Ulak (1999)*	Arun - Tinau Khola *Ulak and Nakayama (2001)*	Hetauda- Bakiya Khola *Nakayama and Ulak (1999)*
1	Debris-flow dominated braided river system	Debris-flow dominated braided river system	Debris-flow dominated braided river system	Debris-flow dominated braided river system
2	~2.0 Ma	—1.0 Ma—	—1.0 Ma—	—1.0 Ma—
3	Gravelly braided river system	Gravelly braided river system	Gravelly braided river system	Gravelly braided river system
		—2.5 Ma—	—2.5 Ma—	—3.0 Ma—
3		Anastomosed river system	Shallow sandy braided river system	
4	~3.9 Ma	—4.0 Ma—		
5	Shallow sandy braided river system	Shallow sandy braided river system		Shallow sandy braided river system
		Deep sandy braided river system	Deep sandy braided river system	
6	6.0 Ma	—6.5 Ma—		
7				
8	Deep sandy braided river system	Flood-flow dominated meandering river system	—8.2 Ma—	Deep sandy braided river system
				—9.0 Ma—
9			Flood-flow dominated meandering river system	Flood-flow dominated meandering river system
9.6 Ma	9.6 Ma	9.5 Ma		
10			—10.0 Ma—	—10.5 Ma—
11	Flood-flow dominated meandering river system	Fine-grained meandering river system	Fine-grained meandering river system	Fine-grained meandering river system
12				
13	—13.5 Ma—			
14				
15	Fine-grained meandering river system			
16				

Table 7.2: Comparison of the fluvial systems in different sections of the Siwalik Group of the Nepal Himalaya.

According to their lithological description, muddy facies predominate in the Lower

Siwaliks in Khutia Khola. Consequently, it is probable that the Khutia Khola succession

was deposited from smaller river systems than was the case in the Karnali River section.

In general, the Middle Siwaliks are the deposits of braided streams, and they contain

detrital grains (salt and pepper) derived from the Higher Himalayas. Although it is

difficult to discuss the timing of the alluvial fan development in the Siwalik successions

associated with the Himalayan Uplift without three dimensional distributions of the

alluvial fan facies (cf. Burbank, 1992), the earlier appearance of the alluvial fan facies (Middle Siwaliks) in the Khutia Khola section together with supply of detritus from the Higher Himalayas implies that early uplift of that source may have promoted erosion, even in small river systems in the western Nepal Himalaya. Therefore, the early uplift of the western part of Nepal Himalaya may have caused change in the climatic pattern (monsoonal precipitation) earlier than in the central and eastern parts. The early uplift is contemporaneous with increased exhumation rate of the Higher Himalaya (Szulc et al., 2006) and higher sedimentation rate (Gautam and Fujiwara, 2000) recorded in the Karnali section. Several other studies have identified diachronous uplift and exhumation of the Nepal Himalaya, with earlier uplift and exhumation in the western part (Arita and Ganzawa, 1997; Szulc et al., 2006; Bernet et al., 2006; Chirouze et al., 2012). As discussed above, the climate change at 13.5 Ma is a response to early uplift of the western Nepal Himalaya. Integrated study of uplift of the western Himalaya at that time and related climate change is lacking to date. However, Liu et al. (2009) showed that extension of drier areas in western China and restriction of humid areas to southern China during the late middle Miocene (13.5 Ma) may reflect the early uplift of the western Himalaya. This uplift blocked deep penetration of wind jet streams originating from the Indian Ocean to the Tibetan Plateau, creating a rain shadow zone in western China (drier area) and wet and humid climate in the frontal Himalaya, and associated intensification of the Indian Summer Monsoon.

7.3 Provenance

The multivariate statistical analysis (PCA biplots and Weltje's confidence

interval of geometric means and ellipsoids) enables direct comparison between the datasets to evaluate if minute differences in composition can be detected. These analyses found slight variation in sediment composition between the Chisapani and Baka Formations. These contrasts are mainly linked to the source area and tectonics, rather than being controlled by the facies, grain size, or climate.

7.3.1 Regional controlling factors (source lithology and tectonic setting)

All Karnali Siwalik sandstones fall well within the recycled orogen provenance field on the QFL provenance diagram of Dickinson et al. (1983), indicating that bulk compositions do not vary significantly within the section (Fig 6.3A). The sandstones are characteristically rich in quartz and lithic grains, and poor in feldspar. Within such recycled orogens, clastic detritus is dominantly derived from sedimentary and metamorphic rocks exposed and eroded by orogenic uplift of fold belts and thrust sheets (Dickinson and Suczek 1979, Dickinson 1985).

The sandstones of the Karnali River section are characterized by an assemblage of monocrystalline and polycrystalline quartz, feldspar, carbonates, mica schist lithics, muscovite and biotite. These detrital grains were derived mainly from sedimentary and low- to high-grade metamorphic sources. The abundant monocrystalline quartz grains are of plutonic origin (Young, 1976), probably from the Dadeldhura granite (Szulc et al. 2006, Bernet et al. 2006).

Temporal changes in petrographic modes in the Karnali section indicate that the proportion of carbonates increased after 13.0 Ma (Fig. 7.2). These were probably derived from the Lesser Himalaya. This result is consistent with an increase in $^{87}Sr/^{86}Sr$ ratio from 12.0 Ma onwards (Szulc et al., 2006). Huyghe et al. (2001, 2005) also

reported more negative εNd isotopes values from the Karnali section after 13.0 with peak around 10.0 Ma (Fig. 7.2). Similarly, the proportions of feldspar and mica grains (Higher Himalayan source) decrease in the interval from 12.0-9.0 Ma. The combination of these results suggests that between 12.0-9.0 Ma the Karnali Siwalik sediments were mainly derived from the Lesser Himalayan zone, probably due to the development of the Lesser Himalayan duplex. Similarly, DeCelles et al. (1998) and Robinson et al. (2001) documented strongly negative εNd isotopes values from other Siwalik sections (Khutia Khola, Surai Khola) at about 12.0-9.0 Ma, perhaps reflecting deeper erosion of both granitoids and high-grade metamorphic rocks in that unit. This result is alsoconsistent with increased proportions of heavy minerals (Szulc et al., 2006) and the shift to positive εNd isotope values (Huyghe et al., 2001, 2005) in that interval (Fig. 7.2). Decrease in feldspar and mica content after 6.0 Ma, together with somewhat higher carbonate content, indicates increased supply of the Lesser Himalayan-derived sediments, as also supported by shift to more negative εNd isotopes values (Huyghe et al., 2001,2005). However, heavy mineral assemblages (Szulc et al., 2006) and significant mica contents indicate that sediments also continued to be supplied from the Higher Himalaya after 6.0 Ma (Fig. 7.2).

By combining our petrographic results with previous isotopic and age data, we can constrain provenance of the Karnali River Siwalik succession.
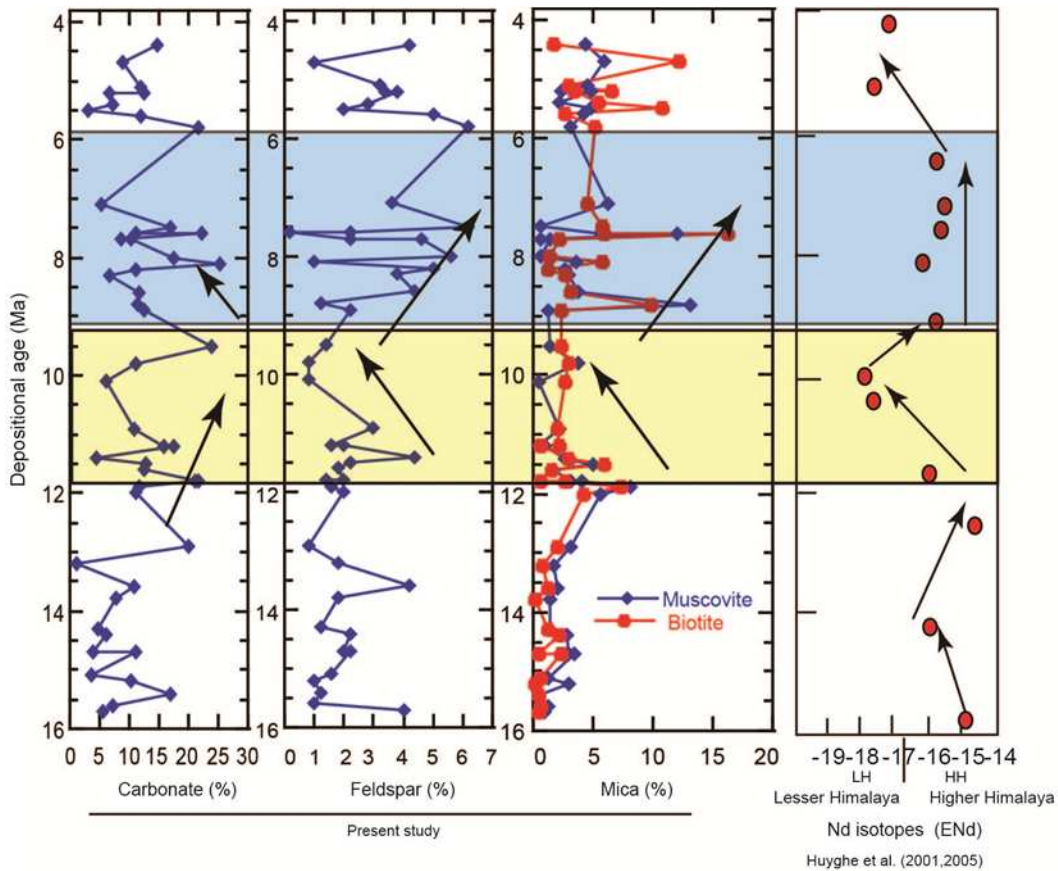
Fig. 7.2: Vertical variations of carbonate, feldspar, and mica content in Karnali River sandstones with depositional age, and comparison with εNd isotopes values from Huyghe et al. (2001, 2005).

Our data confirms that the sediments were mainly derived from the Higher Himalaya and Lesser Himalaya, throughout the period of deposition. The Higher Himalaya was a major source terrain even in the early stage (16.0 Ma) of deposition of the Siwalik Group, with increased sediment supply from the Lesser Himalaya after 13.0 Ma, concurrent with continued supply from the Higher Himalaya. It seems that the Higher Himalaya has maintained a high elevation at least since the Miocene, and that the Lesser Himalaya may have undergone uplift (Lesser Himalayan Duplex) after 13.0 Ma, as shown by the petrographic analysis in this study. However, appearance of 'salt and pepper' sandstones (increase in feldspar and mica grains) in the Middle Siwalik

after 9.6 Ma indicates dominant supply from the Higher Himalayan source. This is comparable with results from the Surai Khola, Tinau Khola and Bakiya Khola sections, albeit with some time variation (8.5 to 9.5 Ma). Our petrographic results together with mica age (Szulc et al., 2006) and fission track (Bernet et al., 2006) data from all Siwalik sections suggest lateral continuity in tectonic uplift of the Himalaya, but an earlier beginning in far western Nepal.

7.4 Himalayan tectonics, paleoclimate and Siwalik sedimentation

The sedimentation history of the Siwalik Group along the Karnali River area started in the middle Miocene (16 Ma) with appearance of fine-grained meandering river system (FA1) (Lower and Middle members of the Chisapani Formation). During this time period, the Main Central Thrust (MCT) as well as Dadeldhura Thrust (DT) and Ramgarh Thrust (RT) were active (Prakash et al., 1980; Szulc et al., 2006, Bernet et al., 2006). The Higher Himalaya ranges were the major source of the Siwalik sediment and the Lesser Himalaya had low relief and its southern boundary was marked by RT. During that time, the height of the Himalaya may have not been sufficient to block the wind from the Indian Ocean and, hence no significant and frequent rainfall occurred in this region. The less rainfall with dominant dry period may have caused the high evaporation and chemical weathering on the flood plain as indicated by the red paleosols containing abundant nodules and concretions (Fig. 7.3).
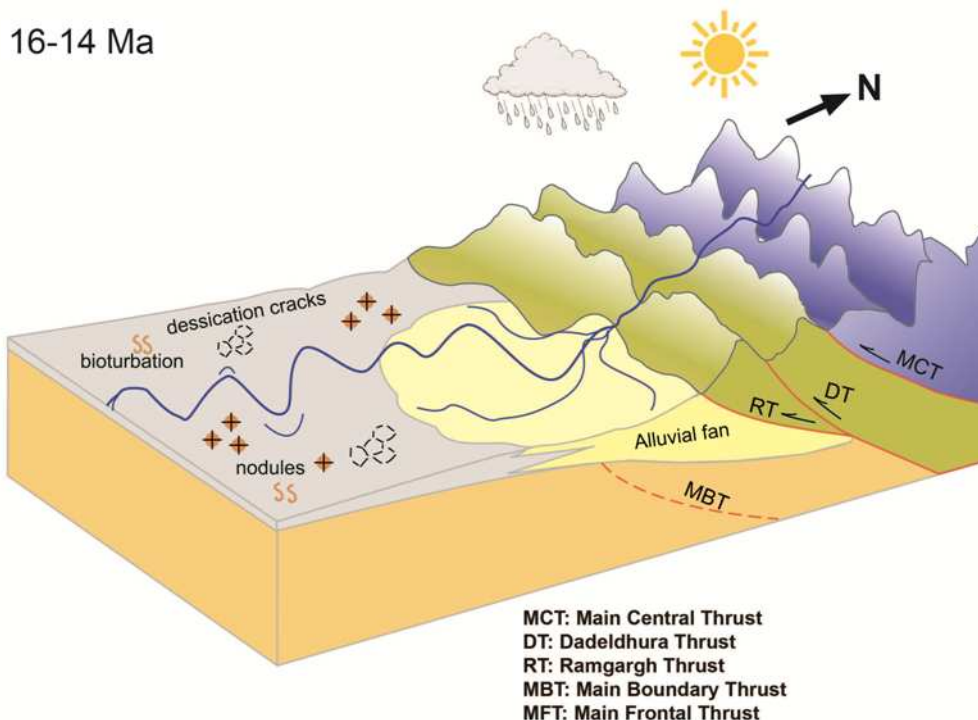
Fig. 7.3: Schematic depositional model for the FA1 facies association in relation to tectonic, climate and provenance of the western Nepal Himalayan. Note: Height of the Higher Himalaya and Lesser Himalaya was fear and no significant rainfall occurred. Wet and dry seasons prevailed with high evaporation represented by the abundant nodules and concretions in the flood plain i.e drier condition dominant.

After the 13.5 Ma, in the upper member of the Chisapani Formation, the sedimentation pattern was changed with increase in flood discharge in the river channel (flood-flow dominated meandering river system, FA2).The increased flood discharge was due to increased precipitation in the catchment of the river and the change in climate from drier to wetter condition in high seasonality. The flood-plain deposits of this fluvial system clearly reflect this phenomenon (see 5.4.1.2). The increase in precipitation was resulted by the orographic precipitation due to the uplift of the Higher

Himalaya and Lesser Himalaya. The Higher Himalaya was uplifted by continuous under-thrusting along the MCT and activity of RT and MBT led the uplift of the Lesser Himalayan rock (Lesser Himalayan Duplex) as additional significant sources of detritus (Huyghe et al., 2005). The height of Higher Himalaya may have blocked the moistures from the Indian Ocean having been resulted the orographic precipitation in the catchment of the paleo-Karnali River which was dominantly extended in the Lesser Himalaya as of present scenario (Fig.7.4)
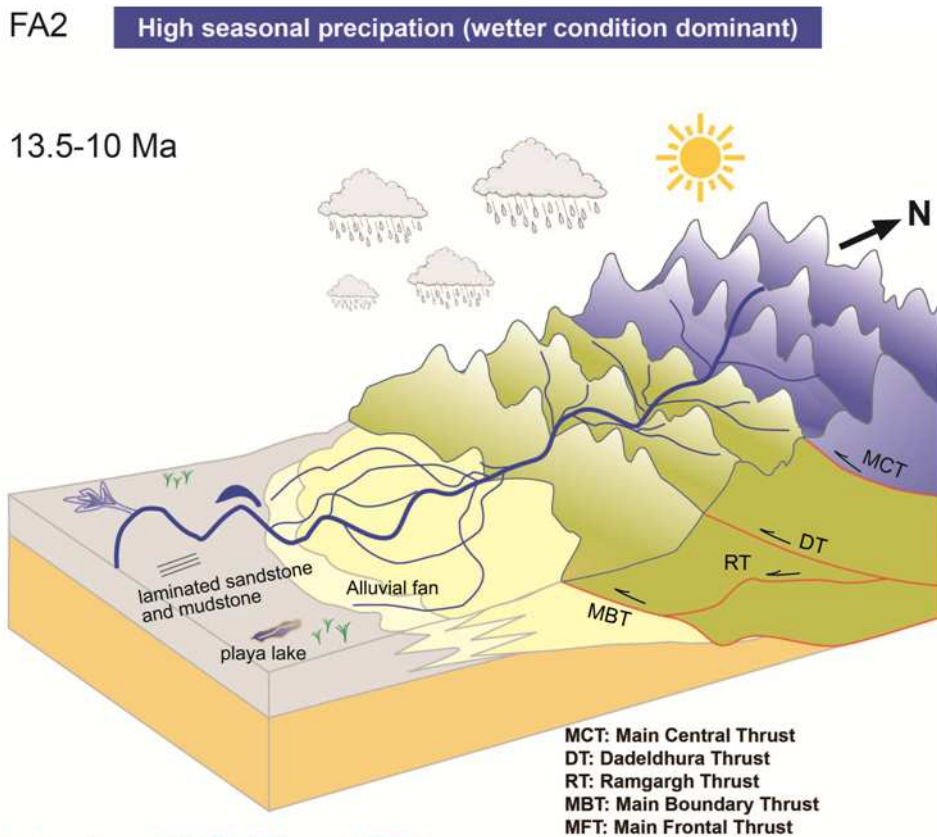
Fig. 7.4: Schematic depositional model for the FA2 facies association in relation to tectonic, climate and provenance of the western Nepal Himalaya. Note: Height of the Higher Himalaya was significantly increased which may have caused the high orographic precipitation and the Lesser Himalaya also uplifted which caused the increase in Lesser Himalayan sediments during the deposition. Due to high seasonal rainfall, increase in flood discharge in the river channels i.e wetter condition dominant.

97
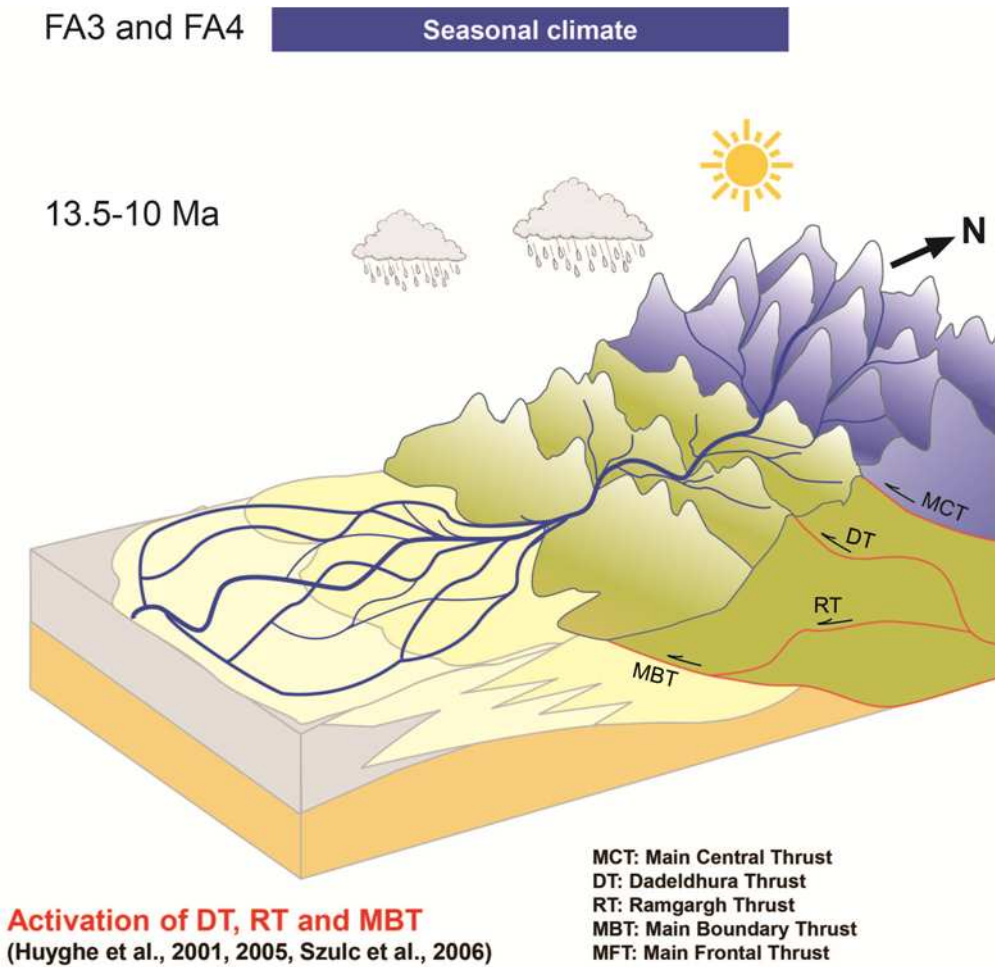
Fig. 7.5: Schematic depositional model for the FA3-FA4 facies associations in relation to tectonic, climate and provenance of the western Nepal Himalaya. Note: deep incision of the Higher Himalaya or close to the Higher Himalaya (Dadeldhura Granite) by paleo-Karnali River may have supplied the coarse 'salt and pepper' sandstones. Seasonal climate was prevailed.

The fluvial facies at around 9.6 Ma shows change from meandering river (fine-grained facies) to braided river facies (coarse salt and pepper) sandstones (FA3-FA4). Although it is difficult to discuss the timing and causes of the alluvial fan development (Middle Siwalik) in the Siwalik successions associated with the Himalayan Uplift without three dimensional distributions of the alluvial fan facies (cf. Burbank, 1992), the basinal subsidence, source area uplift, basinal topography, and size
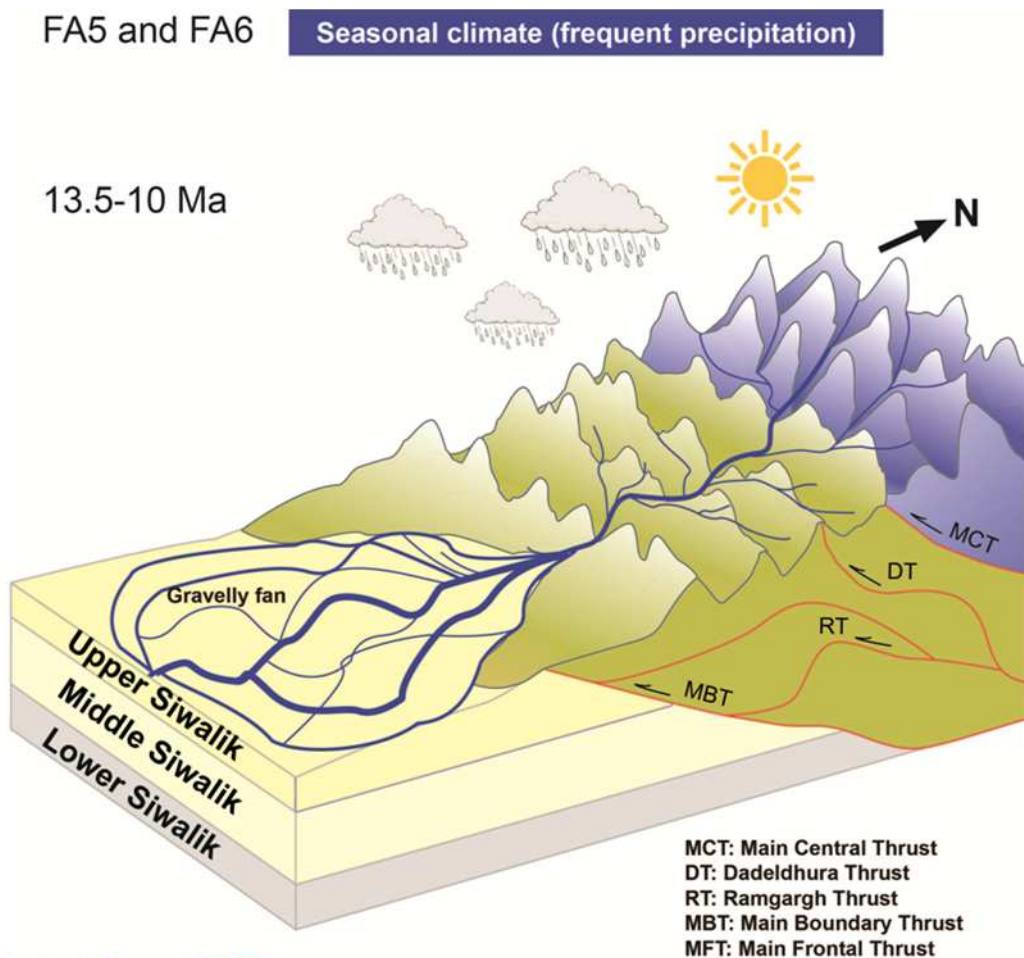
Fig. 7.6: Schematic depositional model for the FA5-FA6 facies associations in relation to tectonic, climate and provenance of the western Nepal Himalaya. Note: Activity of the MBT may have caused further uplift of the Lesser Himalaya which shortens the distance between hinterland and depositional basin and progradation of the large alluvial fan (gravelly braided river). Seasonal climate was prevailed with increase in precipitation than before.

of catchment may have played role on changing this sedimentary facies (Kumar et al., 2003). However, it is clear from mineralogical evidence (salt and pepper sandstones) that the Higher Himalaya and close to the Higher Himalaya (Dadeldhura Granite) were uplifted by the activities of Dadeldhura Thrust (DT) (Huyghe et al., 2005; Szulc et al., 2006). This process may have caused high relief and high incision of the Higher

Himalaya, which resulted the increased supply of metamorphic detritus (muscovite and biotite) till 6.0 Ma (Fig. 7.5). Apart from tectonic controls on basin fill, climate has exerted an influence on the facies change which is related to precipitation (Kumar et al., 2003). Grey to greenish and brown-coloured paleosols with calcareous nodules suggests humid warm climate and the plot on the Weltje's (1998) diagram also indicates the climate was temperate humid climate (Fig. 6.9).

After *ca*.5 Ma, the vast and abrupt increase in supply of the conglomerates over the sandstone could be either due to the continuous collision of plates or changes into the energy conditions. This collision may have caused further activation of Main Boundary Thrust (MBT) (DeCelles et al., 1998; Szulc et al., 2006). The activities of MBT may have caused further uplift of the Lesser Himalayan rocks, and shortening distance between depositional basin and hinterland. These activities trapped the coarse detritus in the proximity of thrust front and finally progradation of the alluvial fan dominated by the gravelly braided river systems (FA5-FA6). The dominant clast type is quartzite of the Lesser and Higher Himalayan rocks with subrounded to rounded clasts indicates the high concentration of sediment load and long distance transport respectively. This reflects high water content in the catchment area to mobilize coarse material for long distance downstream transport. High water discharge will be available by increased rainfall (Fig. 7.6). The increase in rainfall in this time (< 6 Ma) may have due to the full phase of Monsoonal precipitation as mentioned by the previous researchers (Quade et al., 1995, Nakayama and Ulak, 1999).

Chapter 8

CONCLUSIONS

Based on the studies on lithostratigraphy, depositional facies and petrography, the following conclusions have been drawn:

1. The stratigraphy of an almost complete succession of the Siwalik Group was studied in the Karnali River section. The Siwalik Group in this section consists of the Chisapani, Baka, Kuine, and Panikhola Gaun Formations, in ascending order, all newly defined in this study.

2. The Chisapani Formation is equivalent to the Lower Siwalik, and is dominated by mudstone. It is here subdivided into lower, middle, and upper members. The Baka Formation corresponds to the Middle Siwalik, and is characterized by "salt and pepper" sandstone. The Baka Formation is also subdivided into lower, middle, and upper members. The Kuine and Panikhola Gaun Formations together correspond to the Upper Siwaliks. The Kuine Formation is characterized by well-sorted and imbricated pebble to cobble conglomerates, whereas the overlying Panikhola Gaun Formation consists of poorly-sorted, matrix-supported boulder conglomerates.

3. The correlation with the stratigraphy of the Surai Khola, Tinau Khola, and Hetauda Bakiya Khola sections confirms that the boundary between the Lower and Middle Siwaliks is diachronous, as previously reported, over an age range of ~1 Myr. The top of the Chisapani Formation (Lower-Middle Siwalik boundary) is dated at about 9.6 Ma, slightly older than the age of equivalent horizons in the other sections. The earlier appearance of sediments originating from the Higher Himalaya can be recognized in the Karnali drainage basin, which cut back into the Higher Himalayas

101

earlier than in other areas. Similarly, the boundary between the Middle and Upper Siwaliks is also highly diachronous, with ages of 3.9 Ma (Karnali River) and 4.0 Ma (Surai Khola), and 2.5 Ma (Tinau Khola) and 3.0 Ma (Hetauda-Bakiya Khola).

4. These boundaries are strongly linked to the progradation of alluvial fans, and hence could be related to the propagation of major southern thrust systems (MBT and MFT) in the Himalaya.

5. Twelve depositional facies and six facies associations were identified in the Siwalik Group along the Karnali River section, based on detailed and refined facies analysis.

6. The individual facies associations represent a fine-grained meandering river system (FA1) flood-flow dominated meandering river system with intermittently appeared braided river facies (FA2), deep and shallow sandy braided river systems (FA3 and FA4, respectively), followed by a gravelly braided river system (FA5) and a debris flow-dominated braided river system (FA6), in ascending order.

7. Huyghe et al. (2005) proposed the flood-flow dominated meandering system (their KFA2) and sandy flood-flow dominated meandering system (their KFA3) in the upper part of middle and upper members of the Chisapani Formation, and an anastomosed river system (KFA6), in the upper member of Baka Formation, However these deposits are here reinterpreted as a flood-flow dominated meandering system with intermittent appearance of a braided river system (FA2). A shallow sandy braided river system (FA4) was identified in the upper member of Baka Formation, rather than the anastomosed river system proposed by Huyghe et al. (2005).

8. The reconstructed fluvial systems show that major changes in the fluvial systems occurred at around 13.5 Ma and 9.6 Ma. The change from a fine-grained meandering

system to a flood-flow dominated meandering system at 13.5 Ma, is 0.4 Ma earlier than proposed by Huyghe et al. (2005), and 3-4 Ma earlier than in other Siwalik sections.

9. This change arose from increased flood in river channels from increased water discharge, due to intensification of the Indian Summer Monsoon. Similarly, appearance of the braided river alluvial fan facies (Middle Siwaliks) at 9.6 Ma in the Karnali River and at 11.05 Ma in the Khutia Khola sections suggest early progradation of alluvial fans in the western Nepal Himalaya.

10. The early uplift and erosion of the Higher Himalaya in western Nepal may thus have played a significant role in changing climate, as well as changing the fluvial depositional systems.

11. Multivariate statistics identify the slight variations in sediments composition between the Chisapani and Baka Formations. These variations are mainly linked to the source area and tectonics, rather than to the facies, grain size and climate.

12. QFL diagrams show that all sediments were having a recycled orogen provenance. The detrital modes of the Siwalik Group along the Karnali River sandstones were mainly derived from sedimentary rocks as well as metamorphic source terrain.

13. The results of these detrital modes together with previous studies suggest that most of the sediments were derived from the Higher Himalaya, even at an early stage of deposition with simultaneous contribution from the Lesser Himalaya.

14. A small change in sediment composition from the Chisapani to Baka Formations was related to source area change from the Lesser Himalaya to Higher Himalaya. This was probably due to upliftment of the Higher Himalaya by collision, which might cause deep incision and erosion of the Higher Himalayan metamorphic rocks.

Acknowledgements

permission to export samples.

I would like to express my thanks to all the staff of the Department of Geoscience, Shimane University for their assistance and support in numerous ways. I also acknowledge Assoc. Prof. B. P. Roser, Shimane University for his critical reading and helpful comments on the manuscript preparation. I would also like to give special thanks to Prof. Y. Sawada, for his guidance and tips in the point counting and study of petrographic thin sections. I thank all of my Japanese as well as international colleagues in Shimane University for their help in numerous ways.

I would like to thank Dr. D. Adhikari, Dr. S. Bhandari, and Mr. S. Adhikari for their unquestioning support during my stay in Japan.

Last but not least I am deeply grateful to my parents, my wife Sirjana, to my lovely son Samik and my sister and brother for this achievement. Their loving support and endless patience and constant encouragement made this research to happen.

Ashok Sigdel

Matsue-Shi, Japan

July 2013

References

Aitchison, J., 1986.The Statistical Analysis of Compositional Data. Chapman & Hall, London, 416 p.

Aitchison, J., Greenacre, M., 2002. Biplots of compositional data. Journal of Royal Statistical Society: Series. C, Applied. Statistics, v. 51, pp. 375–392.

Allen, J.L., Johnson C.L, 2010. Facies control on sandstone composition (and influence of statistical methods on interpretations) in the John Henry Member, Straight Cliffs Formation, Southern Utah, USA. Sedimentary Geology, v. 230, pp. 60-75.

Allen, J.R.L., 1983. Studies in fluviatile sedimentation: bars, bar complexes and sandstone sheets (low-sinuosity braided streams) in the Brownstones (L. Devonian), Welsh Borders. Sedimentary Geology, v. 33, pp. 237–293.

Amatya, K.M. and Jnawali, B.M., 1994. Geological map of Nepal (Scale 1:1000, 000). Department of Mines and Geology (DMG), Kathmandu, Nepal.

Appel, E., Rosler, W., and Cornivus, G. 1991. Magnetostratigraphy of the Miocene-Pleistocene Surai Khola, Siwaliks in west Nepal. Geophysical Journal of International, v. 105, pp. 423-426.

Appel, E. and Rosler, W., 1994. Magnetic polarity stratigraphy of the Neogene Surai Khola section (Siwalik, SW Nepal). Himalayan Geology, v. 15, pp. 63-68.

Arita, K., Ganzawa, Y., 1997. Thrust tectonics and uplift of the Nepal Himalaya revealed from fission-track ages. Journal of Geography, v.106, pp. 156–167.

Auden, J.B., 1935. Traverses in the Himalaya. Record of Geological Survey of India, v. 69, pp. 123-167.

Barry, J.C., Lindsay, Jacob E.H. and L.L., 1982. A biostratigraphy zonation of the

Middle and Upper Siwaliks of the Potwar Plateau of northern Pakistan. Palaeogeography, Palaeoclimatolology, Palaeoecology, v. 37, pp. 95-130.

Barry, J.C., Johnson, N.M., Raza, S.M. and Jacob, L.L., 1985. Neogene mammalian faunal change in southern Asia: Correlations with climatic, tectonic, and eustatic events. Geology, v.13, pp. 637-640.

Bernet, M., Van der Beek, P., Pik, R., Huyghe, P., Mugnier, J.L., Labrin, E., and Szulc, A.G. 2006. Miocene to recent exhumation of central Himalaya determined from combined detrital zircon fission-track and U/Pb analysis of Siwalik sediments, western Nepal. Basin Research, v. 18, pp. 393-412.

Bhattacharya, A., Morad, S., 1993. Proterozoic braided ephemeral fluvial deposits: an example from the Dhandraul Sandstone Formation of the Kaimur Group, Son Valley, central India. Sedimentary Geology, v. 84, pp.101–114.

Blair, T. C., McPherson, J.G., 1998. Recent debris-flow processes and resultant form and facies of the Dolomite alluvial fan, Owens Valley, California. Journal of Sedimentary Research, v. 68, pp. 800–818.

Bordy, E.M., Catuneanu, O., 2001. Sedimentology of the upper Karoo fluvial strata in the Tuli Basin, South Africa. Journal of African Earth Science, v. 33, pp. 605–629.

Bourquin, S., Guillocheau, F., Pe´ron, S., 2009. Braided rivers within an arid alluvial plain (example from the Lower Triassic, western German Basin): recognition criteria and expression of stratigraphic cycles. Sedimentology, v. 56, pp. 2235–2264.

Bordet, P. 1955. La teconique de 1' Himalaya de 1'Arun et de la region de 1'Everest (Nepal oriental). Comptes rendus des séances de 1'Academie des Sciences Paris Serie D, v. 240, pp. 212-214.

Bordet, P., Colchen, M., Le Fort, P. 1972. Some features of the geology of the Annapurna range Nepal Himalaya. Himalayan Geology, v. 2, pp. 537-563.

Bridge, J.S., Tye, R.S., 2000. Interpreting the dimensions of ancient fluvial channel bars, channels, and channel belts from wireline logs and cores. American Association of Petroleum Geologists Bulletin, v. 84, pp. 1205–1228.

Bridge, J.S., 2003. Rivers and Flood plain, Backwell Scientific, Oxford, 504 p.

Bridge, J.S., 2006. Fluvial facies models: recent developments. In: Posamentier, H., Walker, R.G. (Eds.), Facies Models Revisited. SEPM (Society for Sedimentary Geology) Special Publication, v. 84, pp. 85–170.

Brierley, G.J., Liu, K., Crook, K.A.W., 1993. Sedimentology of coarse-grained alluvial fans in the Markham Valley, Papua New Guinea. Sedimentary Geology, v.86, pp.297–323.

Bristow, C.S., 1993. Sedimentology of the Rough Rock: a Carboniferous braided river sheet sandstone in northern England, *in* Best, J.L., and Bristow, C.S., eds., Braided Rivers: Geological Society of London, Special Publication, v. 75, pp. 291–304.

Brozovic, N. and Burbank, D.W., 2000. Dynamic fluvial systems and gravel progradation in the Himalayan foreland. Geological Society of America Bulletin, v. 112, pp. 394–412.

Buccianti, A. and Esposito, P., 2004. Insights into Late Quaternary calcareous nannoplankton assemblages under the theory of statistical analysis for compositional data. Palaeogeography, Palaeoclimatology, Palaeoecology, v. 202, pp. 209–227.

Burbank, D.W. 1992. Cause of recent Himalayan uplift deduce from deposited pattern in the Ganga basin. Nature, v. 357, pp. 680–683.

Burbank, D.W., Beck, R.A. and Mulder, T., 1996. The Himalayan Foreland: Asian Tectonics. Cambridge University Press, pp. 149-188.

Burchfiel, B.C., Chen, Z., Hodges, K.V., Liu, Y., Royden, L.H., Deng, C., Xu, J. 1992. The south Tibetan Detachment System Himalayan orogen. Extension contemporaneous with and parallel to shortening in a collisional mountain belt. Geological Society of America, Special Paper, v. 269, pp. 41.

Cande, S.C. and Kent, D.V., 1995. Revised calibration of the geomagnetic polarity time scale for the late Cretaceous and Cenozoic. Journal of Geophysical Research, v. 100(B4), pp. 6093-6095.

Chen, Y., Courtillot, V., Cogne, J.P., Besse, J., Yang, Z., and Enkin, R. 1993. The configuration of the Asia prior to the collision of India: Cretaceous paleomagnetic constraints. Journal of Geophysical Research, v. 98, pp. 21927-21941.

Chirouze, F., Bernet, M., Huyghe, P., Erens V., Dupont-Nivet, G. and Senebier, F., 2012. Detrital thermochronology and sediment petrology of the middle Siwaliks along the Muksar Khola section in eastern Nepal. Journal of Asian Earth Science, v. 44, pp. 94-106.

Collinson, J.D., 1986. Alluvial Sediments, In: H.G. Reading (Ed.) Sedimentary Environments and Facies, 2nd Ed., Blackwell, Oxford, 20–62.

Copeland, P. and Harrison, T.M., 1990. Episodic uplift in the Himalaya revealed by $^{40}Ar/^{39}Ar$ analysis of detrital K-feldspar and muscovite, Bengal fan. Geology, v. 18, pp.354–357.

Corvinus, G. and Nanda, A.C., 1994. Stratigraphy and paleontology of the Siwalik Group of Surai Khola and Rato Khola in Nepal. N. Jb. Geol. Palaeont. Abh., v. 191, pp. 25-68.

Critelli S. and Ingersoll, R.V., 1994. Sandstone Petrography and Provenance of the Siwalik Group (northwestern Pakistan and western-southeastern Nepal). Journal of Sedimentary Research, v. A 64, pp. 815-823.

Damanti, J.F., 1993. Geomorphic and structural controls on facies patterns and sediment composition in a modern foreland basin. In: Alluvial Sedimentation (ed. by M. Marzo & C. PuigdefaÁbregas), Special Publication of International Association of Sedimentology, v. 17, pp. 221-233.

Department of Mines and Geology (DMG/HMGN), 1987, Geological Map of Far Western Nepal, 1:250,000.

Department of Mines and Geology (DMG/HMGN), 2003, Geological Map of Petroleum Exploration Block-2, Karnali, Far Western Nepal, 1:250,000

Dettman, D.L., Kohn, M.J., Quade, J., Ryerson, F.J., Ojha, T.P. and Hamidullah, S. 2001. Seasonal stable isotope evidence for a strong Asian monsoon throughout the past 10.7 m.y., Geology, v. 29, 31–34.

Dhital, M.R., Gajurel, A.P., Pathak, D., Paudel, L.P. and Kizaki, K. 1995. Geology and structure of the Siwaliks and Lesser Himalaya in the Surai Khola-Bardanda area, mid-western Nepal. Bulletin Department of Geology, Tribhuvan University, v. 4, pp. 1-70.

DeCelles, P.G., Gehrels, G.E., Quade, J., Ojha, T.P., Kapp, P.A. and Upreti, B. N., 1998. Neogene foreland basin deposits, erosional unroofing, and the kinematic history of the Himalayan fold-thrust belt, western Nepal. Geological Society of America Bulletin, v. 110, pp. 2-21.

Dickinson, W.R. and Suczek, C., 1979. Plate tectonics and sandstone compositions. American Association of Petroleum Geologists Bulletin, v. 63, pp. 2164– 2182.

Dickinson, W.R., Beard, L.S., Brakenridge, G.R., Erjavec, J.L., Ferguson, R.C., Inman, K.F., Knepp, R.A., Lindberg, F.A. and Ryberg, P.T., 1983, Provenance of North American Phanerozoic sandstone in relation to tectonic setting. Geological Society of America Bulletin, v. 94, pp. 222–235.

Dickinson, W.R. 1985, Interpreting detrital modes of greywacke and arkose. Journal of Sedimentary Petrology, v.40, pp. 695-707.

Fatmi, A.N., 1973, Lithostratigraphic units of the Kohart-Potwar Province, Indus Basin, Pakistan. Memorier of Geological Survey of Pakistan, v. 10, pp. 1-80.

Folk R. L., 1974. Petrology of Sedimentary Rocks, Austin Texas, Hemphill's, 182p.

Folk, R.L., 1980. Petrology of Sedimentary Rocks, Hamphills, Austin, 201p.

Gabriel, K.R., 1971. The biplot graphic display of matrices with application to principal component analysis. Biometrika, v. 58, pp. 453–467.

Gansser, A., 1964. Geology of the Himalayas. Interscience, London, 289 p.

Garver, J.I., Brandon, M.T., Roden-Tice, M.K., Kamp, P.J.J., 1999. Exhumation history of orogenic highlands determined by detrital fission track thermochronology. In: Ring, U. et al. (Eds.), Exhumation Processes: Normal faulting, Ductile Flow, and Erosion: Geological Society of London Special Publications, v. 154, pp. 283–304.

Garzanti, E., Ando´, S., and Scutella, M., 2000. Actualistic ophiolite provenance: the Cyprus case. Journal of Geology, v. 108, pp. 199– 218.

Gautam, P. and Appel, E., 1994. Magnetic polarity stratigraphy of the Siwalik Group sediments of the Tinau Khola section in west central Nepal revisited. Geophysics Journal of International, v. 117, pp. 223-234.

Gautam, P. and Fujiwara, Y., 2000. Magnetic polarity stratigraphy of Siwalik Group sediments of the Karnali River section in western Nepal. Geophysics Journal of

International, v. 142, pp. 812-824.

Glennie, K.W. and Ziegler, M.A., 1964. The Siwalik Formations of Nepal. International Geological Congress, 22, Delhi, v. 25, pp. 82-95.

Godin, P.D. 1991. Fining-upward cycles in the sandy braided-river deposits of the Westwater Canyon Member (Upper Jurassic), Morrison Formation, New Mexico. Sedimentary Geology, v. 70, 61–82.

Gupta, S.S., 1997. Study and documentation of vertebrate fossils from the Siwalik Group of Jammu Sub Himalayan foot hills. Records of Geological Survey of India, v. 129 (8), pp. 5-7.

Gupta, S.S. and Verma, B.C., 1988. Stratigraphy and vertebrate fauna of the Siwalik Jammu District Group, Mansar Uttarbani section, J & K. J. Palaeontological Society of India, v. 33, pp. 117-124.

Gupta, S.S., 2000. Lithostratigraphy and structure of the Siwalik succession and its relationship with the Murree succession around Ramnagar area, Udhampur district, Jammu and Kashmir. Himalayan Geology, v. 21, pp. 53-61.

Hagen, T., 1969. Report on the Geological Survey of Nepal: Preliminary Reconnaissance. Denkschr. Naturw. Ges. v. 86, 185 p.

Heim, A., Gansser, A. 1939. Central Himalaya: Geological observations of the Swiss expedition 1936. Mem. Soc. Helv. Sci. Nat. v.73 (1), pp. 1-245.

Hampton, B.A., Horton, B. K., 2007. Sheetflow fluvial processes in a rapidly subsiding basin, Altiplano plateau, Bolivia. Sedimentology, v. 54, pp. 1121–1147.

Harrison, T.M., Copeland, P., Hall, S.A., Quade, J., Burner, S., Ojha, T.P. and Kidd, W.S.F., 1993. Isotopic preservation of Himalayan/Tibetan uplift, denudation and climatic histories in two molasses deposits. Journal of Geology, v. 101,pp. 157-175.

Harrison, T.M., Grove, M., Lovera, O.M., Catlos, E.J. 1998. A model for the origin of Himalayan anatexis and inverted meta-morphism. Journal of Geophysical Research, v. 103, 27, pp. 017-27,032.

Hartley, A.J., 1993. Sedimentological response of an alluvial system to source area tectonism: the Seilao Member of the Late Cretaceous to Eocene Purilactis Fm. of Northern Chile. International Association of Sedimentologists Special Publication, v. 17, pp. 489–500.

Heller, P.L. and Paola, C., 1992. The large scale dynamics of grain-size variation in alluvial basins, 2: Application to syntectonic conglomerate. Basin Research, v. 4, pp. 91-102.

Hérail, G. and Mascle, G. 1980. Les Siwalik du Népal central: structure et géomorphologie d'un péimont en cours de déformation. Bulletin Association of Geography France, v. 471, pp. 259-267.

Hisatomi, K. and Tanaka, S. 1994. Climatic and environmental changes at 9.0 and 7.5 Ma in the Churia (Siwalik) Group, West Central Nepal. Himalayan Geology, v. 15, pp. 161–180.

Hjellbakk, A., 1997. Facies and fluvial architecture of a high-energy braided river: the Upper Proterozoic Seglodden Member, Baranger Peninsula, northern Norway. Sedimentary Geology, v. 114, pp. 131–161.

Hodges, K., 2000. Tectonics of the Himalaya and southern Tibet from two perspectives, Geological Society of America Bulletin, v. 112(3), pp. 324-350.

Howard, J.L., 1994. A note on the use of statistic in reporting detrital clastic compositions. Sedimentology, v. 41, pp. 747–753.

Horton, B. K. and DeCelles P. G., 2001, Modern and ancient fluvial megafans in the

foreland basin system of the central Andes, southern Bolivia: implications for drainage network evolution in fold-thrust belts. Basin Research, v. 13, pp. 43-63.

Hubbard, M.S., Harrison, T.M. 1989. ^{40}Ar/^{39}Ar age constraints on deformation and metamorphism in the Main Central Thrust zone and Tibetan Slab, Eastern Nepal Himalaya. Tectonics, v. 8, pp. 865-880.

Huyghe, P., Mugnier, J.L., Gajurel, A.P, and Decaillau, B., 2005. Tectonic and climatic control of the changes in the sedimentary record of the Karnali river section (Siwaliks of western Nepal). The Island Arc, v. 14, pp. 311-327.

Huyghe, P., Galy, A., Mugnier, J.L., France-Lanord, C., 2001. Propagation of the thrust system and erosion in the Lesser Himalaya: Geochemical and sedimentological evidence. Geology, v. 29, pp. 1007-1010.

Ingersoll, R.V., 1978. Petrofacies and petrologic evolution of the Late Cretaceous fore-arc basin, northern and central California. Journal of Geology, v. 86 (3), pp. 335–352.

Ingersoll, R. V. and Suczek C.A., 1979. Petrology and Provenance Neogene sand from Nicobar and Bengal fans. DSDP site 211 and 218. Journal of Sedimentary Petrology, v. 49, pp. 1217-1228.

Jackson, M., Bilham, R. 1994. Constraints on Himalayan deformation inferred from vertical velocity fields in Nepal and Tibet. Journal of Geophysical Research, 99 (B7), v. 13, pp.897-13,912.

Johnson, N.M., Opdyke, N.D., Johnson, G.D., Lindsay, E.H. and Tahirkheli, R.A.K., 1982. Magnetic polarity stratigraphy and age of the Siwalik group rocks of Potwar plateau, Pakistan. Palaeogeography, palaeoclimatology, Palaeoecology, v. 37, pp. 17-42.

Johnson, G. D., Opdyke, N.D., Tandon, S. K. and Nanda, A. C., 1983. The magnetic polarity stratigraphy of the Siwalik Group at Haritalyangar (India) and a new last appearance datum for *Ramapithecus* and *Sivapithecus* in Asia. Palaeogeography, Palaeoclimatology, Palaeoecology, v. 44, pp. 223-249.

Johnson, N.M., Stix, J., Tauxe, L., Cerveny, P.F. and Tahirkheli, R.A.K., 1985. Paleomagnetic chronology, fluvial processes and tectonic implication of the Siwalik deposits near Chinji village, Pakistan. Journal of Geology, v. 93, pp. 203-226.

Johnson, A. M., 1970. Physical Processes in Geology*:* San Francisco (Freeman, Cooper & Co.) 577p.

Johnsson, M.J. and Meade, R.H., 1990. Chemical weathering of fluvial sediments during alluvial storage: the macuapanim island point bar, Solimoes River, Brazil. Journal of Sedimentary Petrology, v. 60, pp. 827-842.

Johnsson, M.J, 1993, The system controlling the composition of clastic sediments. In : Processes Controlling the Composition of Clastic Sediments (Ed. by M.J Johnsson and A. Basu), Special Paper Geological Society of America., v. 284, pp. 1-19.

Khadkikar, A. S., Nathew, G., Malik, J.N., Gunda Rao, T.K., Chogaonkar, M.P., Merh, S.S., 1999. The influence of the South-west Indian Monsoon on continental deposition over past 130 kyr, Gujarat, western India. Terra Nova, v.11, pp. 273–277.

Khan, I.A., Bridge, J.S., Kappelman, J., Wilson, R., 1997. Evolution of Miocene fluvial environments, eastern Potwar Plateau, northern Pakistan. Sedimentology, v. 44, pp. 221–251.

Kumar, G. 1997. Geology of Arunachal Pradesh. Bangalore: Geological Society of India, 217 p.

Kumaravel, V., Sangode, S.J., Kumar, R. and Siva Siddaiah, N., 2005. Magnetic polarity stratigraphy of Plio–Pleistocene Pinjor Formation (type locality), Siwalik Group, NW Himalaya, India. Current Science, v. 88, pp. 1453-1461.

Kumar, R., Nanda, A.C., 1989. Sedimentology of the Middle Siwalik Subgroup of Mohand area, Dehara Dun valley, India. Geological Society of India, v. 34, pp. 597–616.

Kumar, R., Ghosh, S.K. Sangode, S.J., 2003. Mio–Pliocene sedimentation history in the northwestern part of the Himalayan foreland basin, India. Current Science, v. 84, pp. 1006–1013.

Kumar, R., Sangode, S.J., Ghosh, S.K., 2004. A multistorey sandstone complex in the Himalayan Foreland Basin, NW Himalaya, India. Journal of Asian Earth Sciences, v. 23, pp. 407–426.

Le Fort, P., 1975. Himalaya: the collided range: Present knowledge of the continental arc. American Journal of Science, v. 275A, pp. 1-44.

Lewis, G.E., 1937. A new Siwalik correlation. American Journal of Science, v. 33, pp. 191-204.

Liu, L., Eronen J.T., Fortelius M., 2009. Significant mid-latitude aridity in the middle Miocene of East Asia. Palaeogeography, Palaeoclimatology, Palaeoecology, v. 279, pp. 201–206.

Liu, G., Einsele, G. 1994. Sedimentary history of the Tethyan basin in the Tibetan Himalaya. Geologischen Rundschau, v. 83, pp. 32-61.

Lunt, I.A, Bridge, J.S., Tye, R.S. 2004. A quantitative, three dimensional depositional model of gravelly braided rivers. Sedimentology, v. 51, pp. 377–414.

Maizels, J.K., 1989. Sedimentology, paleoflow dynamics and flood history of

jökulhlaup deposits: paleohydrology of Holocene sediment sequences in southern Iceland sandur deposits. Journal of Sedimentary Petrology, v.59, pp. 204–223.

Maizels, J.K. 1993. Lithofacies variations within sandur deposits: the role of runoff regime, flow dynamics and sediment supply characteristics. Sedimentary Geology, v. 85, pp. 299–325.

McLennan, S.M., Hemming, S., McDaniel, D.K., Hanson, G.N., 1993. Geochemical approaches to sedimentation, provenance and tectonics. In: Johnsson, M.J., Basu, A. (Eds.), Processes Controlling the Composition of Clastic Sediments. Geological Society of America, Special Paper, v. 284, pp. 21–40.

Miall, A.D., 1977. A review of the braided river depositional environment. Earth Science Reviews, v. 13, pp. 1–62.

Miall, A.D., 1978. Lithofacies types and vertical profile models in braided river deposits: a summary. In: A.D. Miall (Editor), Fluvial Sedimentology. Canadian Society of Petroleum Geology Memoir, v. 5, pp.597–604.

Miall, A.D., 1985. Architectural-element analysis: a new method of facies analysis applied to fluvial deposits. Earth Science Review, v. 22, pp. 261–308.

Miall, A. D., 1990. Principles of Sedimentary Basin Analysis. Second Edition, Springer, 668p.

Miall, A.D., 1996. The Geology of Fluvial Deposits: Sedimentary Facies, Basin Analysis, and Petroleum Geology. Springer-Verlag, New York. 582p.

Mugnier, J.L., Delcaillau, B., Huyghe, P. and Leturmy, P., 1998. The break-back thrust splay of the Main Dun Thrust (Himalayas of western Nepal): evidence of an intermediate displacement scale between earthquake slip and finite geometry of thrust systems. Journal of Structural Geology, v. 20, pp. 857-864.

Mugnier, J.L., Leturmy, P., Mascle, G., Huygle, P., Chalaron, E., Vidal, G., Husson, L. and Delcaillau, B., 1999. The Siwalik of Western Nepal: I. geometry and kinematics. Journal Asian Earth Science, v. 17, pp. 629-642.

Najman, Y., K. Johnson, N. White, and G. Oliver, 2004. Evolution of the Himalayan foreland basin, NW India. Basin Research, v. 16, pp. 1-24.

Nakata, T., 1989. Active faults of the Himalaya of India and Nepal. Geological Society of America Special Paper, v. 232, pp. 243-264.

Nakayama, K. and Ulak, P.D., 1999. Evolution of fluvial style in the Siwalik Group in the foothills of the Nepal Himalaya. Sedimentary Geology, v. 125, pp. 205-224.

Ohta, T. and Arai, H., 2007. Statistical empirical index of chemical weathering in igneous rocks: A new tool for evaluating the degree of weathering. Chemical Geology, v. 240, pp. 280–297.

Ojha, T.P., Butler R.F., Quade, J., DeCelles, P.G., Richards, D. and Upreti, B.N., 2000. Magnetic polarity stratigraphy of the Neogene Siwalik Group at Khutia Khola, far western Nepal. Journal of Geological Society of America Bulletin, v. 112, pp. 424-434.

Ojha, T.P., Butler R.F., DeCelles, P.G. and Quade, J., 2009. Magnetic polarity stratigraphy of the Neogene foreland basin deposits of Nepal. Basin Research, v. 21, pp. 61-90.

Olsen, H., 1988. The architecture of a sandy braided-meandering river system: an example from the Lower Triassic Solling Formation (M.Buntsandstein) in W-Germany. Geologische Rundschau, v. 77, pp. 797–814.

Opdyke, N.D., Johnson, N.M., Johnson, G.D., Lindsay, E.H. and Tahirkheli, R.A.K.,

1982. Plaeomagnetism of the Middle Siwalik formations of Northern Pakistan and Rotation of the Salt Range Decollement and age of the Siwalik group rocks of Potwar plateau, Pakistan. Palaeogeography, Palaeoclimatology, Palaeoecology, v. 37, pp. 1-15.

Pandita, S.K., Bhat S.K., Kotwal S.S., 2011. Facies evaluation of Boulder Conglomerate Formation, Upper Siwalik, Jammu Himalaya. Himalayan Geology v. 32, pp. 63–69.

Pandey, M.R., Tandukar, R.P., Avouac, J.P., Lave, J., Massot, J.P. 1995. Interseismic strain accumulation on the Himalayan crustal ramp (Nepal). Geophysical Research Letter, v. 22, pp. 751-754.

Pati, P., Prakash B., Awasthi, A.K. and Acharya, V., 2011. olocene tectono-geomorphic evolution of parts of the Upper and Middle Gangetic plains, India. Geomorphology, v. 128, pp. 148-170.

Patriat, P., Achache, J., 1984. India-Eurasia collision chronology has implications for crustal shortening and driving mechanism of plates. Nature, v. 311, pp. 615–621.

Peakall, J., Philip, J., Best J.L., 2007. Meander-bend evolution, alluvial architecture, and the role of cohesion in sinuous river channels: A flume study. Journal of Sedimentary Research, v. 77, pp. 197–212.

Pettijohn, F.J., 1975. Sedimentary Rocks, 3rd ed. Harper & Tow, New York, 628 p.

Pettijohn, F.J., Potter, P.E. and Siever, R., 1987. Sand and sandstone, 2nd ed. Springer-Verlag, 533 p.

Parrish, R.R., and K.V. Hodges, 1996. Isotopic constraints on the age and provenance of the Lesser and Greater Himalayan sequences, Nepalese Himalaya, Geological Society of America Bulletin, v.108, pp.904-911,

Piligram, G.E., 1913. The correlation of the Siwaliks with mammal horizons of Europe. Records of Geological Survey of India, v. 43 (4), pp. 264-326.

Prakash, B., Sharma, R.P. and Roy, A.K., 1980. The Siwalik Group (molasse) sediments shed by collision of continental plates. Sedimentary Geology, v. 25, pp. 127-159.

Prins, M.A. and Weltje, G.J., 1999a. End-member modeling of siliciclastic grain-size distributions: the late Quaternary record of eolian and fluvial sediment supply to the Arabian Sea and its paleoclimatic significance. In: Harbaugh, J.W., Watney, L.,

Rankey, E.C., Slingerland, R., Goldstein, R.H., Franseen, E.K. (Eds.), Numerical Experiments in Stratigraphy: Recent Advances in Stratigraphic/Sedimentologic Computer Simulations. SEPM Special Publication, v. 62, pp. 91– 111.

Quade, J., Cerling, T.E., and Bowman, J.R. 1989. Development of Asian monsoon revealed by marked ecological shift during the latest Miocene in northern Pakistan. Nature, v. 342, pp. 163-166.

Quade J., Cater, J.M.L, Ojha, T.P., Adam J., and Harrison, T.M. 1995. Late Miocene environmental change in Nepal and the northern Indian subcontinent: Stable isotope evidence form paleosols, Geological Society of America Bulletin, v. 107, pp. 1381-1297.

Ranga Rao, A., Agarwal, R.P., Sharma, U.N., Bhalla, M.S. and Nanda, A.C., 1988. Magnetic polarity stratigraphy and vertebrate palaeontology of the Upper Siwalik Subgroup of Jammu Hills, India. Journal of Geological Society of India, v. 31 (4), pp. 361-385.

Raza, S. M., 1983. Taphonomy and paleoecology of Middle Miocene vertebrate assemblages, southern Potwar Plateau, Pakistan. Unpublished Ph.D. Dissertation,

Yale University, New Haven, Connecticut, 414 p.

Retallack, G.J., 1991. Miocene Paleosols and Ape Habitats of Pakistan and Kenya. Oxford University Press, New York Oxford. 346p.

Robinson, D.M., DeCelles, P. G., Patchett, P.J. and Garzione, C.N. 2001. The kinematic evolution of the Nepalese Himalaya interpreted from Nd isotopes. Earth and Planetary Science Letter, v. 192, pp. 507-521.

Robinson, D.M., DeCelles, P. G. and Copeland, P. 2006. Tectonic evolution of the Himalaya thrust belt in western Nepal: Implication for channel flow models. Geological Society of America Bulletin, v. 118, pp. 868-885.

Roe, S.L., Hermansen, M., 1993. Processes and products of large, Late Precambrian sandy rivers in northern Norway. International Association of Sedimentologists, Special Publication, v. 17, pp. 151–166.

Rosler, W.,Metzler, W. and Appel, E., 1997. Neogene magnetic polarity stratigraphy of some fluviatile Siwalik sections, Nepal. Geophysics Journal of International, v. 130, pp. 89-111.

Rowley, D.B., 1996. Age of initiation of collision between India and Asia: a review of stratigraphic data. Earth and Planetary Science Letters, v. 145, pp. 1–13.

Rust, B.R., Gibling, M.R., Legun, A.S., 1984. Coal Deposition in an anastomosing-fluvial system: the Pennsylvanian Cumberland Group south of Joggins, Nova Scotia, Canada. International Association of Sedimentologists Special Publication, v. 7, pp. 105–120.

Sah, R.B. Ulak, P.D., Gajurel, A.P. and Rimal, L.N., 1994. Lithostratigraphy of the Siwalik sediments of the Amlekhganj-Hetauda area, sub-Himalaya of Nepal. Himalayan Geology, v. 15, pp. 37-48.

Sakai, H. 1983. Geology of the Tansen Group of the Lesser Himalaya in Nepal. Memoirs of the Faculty of Science, Kyushu University Series D, Geology, v. 25, pp. 27-74.

Sakai, H. 1985. Geology of the Kali Gandaki Supergroup of the Lesser Himalayas in Nepal. Memoirs of the Faculty of Science Kyushu University Series D Geology, v.25, pp.337-397.

Sakai, T., Saneyoshi, M., Tanaka, S., Sawada, Y., Nakatsukasa, M., Mbua, E., Ishida, H., 2010. Climate shift recorded at around 10 Ma in Miocene succession of Samburu Hills, northen Kenya Rift, and its significance. Geological Society of London, Special Publication, v. 342, pp. 109–127.

Sangode, S.J., Kumar, R. and Ghosh, S.K., 1996. Magnetic polarity stratigraphy of the Siwalik sequence of Haripur area, NW Himalaya. Journal of Geological Society of India, v. 47, pp. 683-704.

Sanyal P., Bhattacharya S.K., Kumar R., Ghosh S.K and, Sangode S.J., 2004. Mio–Pliocene monsoonal record from Himalayan foreland basin (Indian Siwalik) and its relation to vegetational change. Palaeogeography, Palaeoclimatology, Palaeoecology, v. 205, pp. 23– 41.

Seeber, L., Armbruster, J.G. 1981. Great detachment earthquakes along the Himalayan arc and long-term furcating. Earthquake prediction. An International review Maurice Ewing Series 4. American Geological Union, pp. 259-277.

Shah, S.M.I., 1977. Stratigraphy of Pakistan. Published by the Director General, Geological Survey of Pakistan, Quetta, 175 p.

Sharma, C.K., 1977. Geology of Nepal. Educational Enterprises, Kathmandu, 164 p.

Sharma, M., Sharma, S., Shukla U. K., Singh, I. B., 2002. Sandstone body architecture

and stratigraphic trends in the Middle Siwalik Succession of the Jammu area, India. Journal of Asian Earth Sciences, v. 20, pp. 817–828.

Sigdel, A., Sakai T., Ulak, P.D., Gajurel A. P. and Upreti, B.N., 2011. Lithostratigraphy of the Siwalik Group, Karnali River section, far-west Nepal Himalaya. Journal of Nepal Geological Society, v. 43 (Spec. Issue), pp. 83-101.

Singh, S., Parkash, B., Awasthi, A.K., and Singh, T., 2012. Palaeoprecipitation record using O-isotope studies of the Himalayan Foreland Basin sediments, NW India. Palaeogeography, Palaeoclimatology, Palaeoecology, v. 331–332, pp. 39–49.

Smith, N.D., 1972. Some sedimentological aspects of planar cross-stratification in a sandy braided river. Journal of Sedimentary Petrology, v. 42, pp. 624–634.

Stattegger, K. and Morton, A.C., 1992. Statistical analysis of garnet compositions and lithostratigraphic correlation: Brent Group sandstones of the Oseberg field, northern North Sea. In: Morton, A.C., Haszeldine, R.S., Giles, M.R., Brown, S. (Eds.), Geology of the Brent Group. Geological Society of London, Special Publication, v. 61, pp. 245– 262.

Szulc, A.G., Najman, Y., Sinclair, H., Pringle, M., Bickle, M., Chapman, H., Garzanti, E., Ando, S., Huyghe, P., Mugnier, J.L., Ojha, T.P. and DeCelles, P.G. 2006, Tectonic evolution of the Himalaya constrained by detrital ^{40}Ar-^{39}Ar, Sm-Nd and petrographic data from the Siwalik foreland basin succession, SW Nepal. Basin Research, v. 18, pp. 375-391.

Tamrakar, N.K, Yokota, S. and Shrestha, S.D., 2003. Petrography of the Siwalik sandstones, Amlekhganj-Suparitar area, central Nepal Himalaya. Journal of Nepal Geological Society, v. 28, pp. 41-56.

Tandon, S. K. and Kumar, R., 1984. Discovery of tuffaceous mudstones in the Pinjor

formation of Punjab sub-Himalaya, India. Current Science, v. 53, pp. 982-984.

Tanaka, S. 1997. Uplift of the Himalaya and climate changes at 10.0 Ma evidence from records of the carbon stable isotopes and fluvial sediments in the Churia Group Nepal. Journal of Geological Society of Japan, v. 103(3), pp. 253–264.

Tauxe, L. and Opdyke, N.D., 1982. A time framework based on magnetostratigraphy for Siwalik sediments of Khaur area, northern Pakistan. Paleogeography, Paleoclimatology, Palaeoecology, v. 37, pp. 43-63.

Thio-Henestrosa, S. and Comas, M., 2011. CoDaPack v.2 USER's GUIDE (http://ima.udg.edu/CoDaPack)

Tokuoka, T., Takayasu, K., Yoshida, M. and Hisatomi, K., 1986. The Churia (Siwalik) Group of Arungg Khola area, west-central Nepal. Memorier Faculty of Science Shimane University, v. 22, pp. 135-210.

Tokuoka, T., Takayasu, K., Hisatomi, K., Yamasaki, H., Tanaka, S., Konomatu, M., Sah, R.B., and Roy, S.M., 1990. The Churia (Siwalik) Group of Tinau Khola-Binai Khola area, west-central Nepal. Memorier Faculty of Science, Shimane University, v. 24, pp. 71-88.

Tokuoka, T., Takayasu, K., Hisatomi, K., Tanaka, S., Yamasaki, H., Konomatsu, M., 1994. The Churia Siwalik Group in West Central Nepal. Himalayan Geology, v. 15, pp. 23–35.

Ulak, P. D. and Nakayama, K., 1998. Lithostratigraphy and evolution of the fluvial style in the Siwalik Group in the Hetauda-Bakiya Khola area, Central Nepal. Bulletin Department of Geology, Tribhuvan University, v. 6, pp. 1–14.

Ulak, P.D., Nakayama, K., 2001. Neogene fluvial systems in the Siwalik Group along Tinau Khola section, west central Nepal Himalaya. Journal of Nepal Geological

Society, v.25, pp. 111–122.

Upteri, B.N., 1999. An overview of stratigraphy and tectonics of the Nepal Himalaya. Journal of Asian Earth Science, v. 17, pp. 577–606.

Upreti, B.N. and Le Fort, P. 1999. Lesser Himalayan crystalline nappes of Nepal: problem of their origin. In:Macfarlame, A., Quade, J., and Sorkhabi, R. (des.), Himalaya and Tibet: Mountain root to tops, Geological Society of America, Special Paper, v. 328, pp. 225-238.

Van Der Beek, P., Robert, X., Mugnier, J.L., Bernet, M., Huyghe, P. and Labrin, E. 2006. Late Miocene-Recent exhumation of central Himalaya and recycling in the foreland basin assessed by apatite fission tract thermochronology of Siwalik Sediments, Nepal. Basin Research, v. 18, pp. 413-434.

Vannay, J-C. and Hodges, K.V. 1996. Tecnometamorphic evolution of the Himalayan metamorphic core between Annapurna and Dhaulagiri, central Nepal. Journal of Metamorphic Geology, v. 14, pp. 635-656.

Valdiya, K.S. 1995. Proterozoic sedimentation and Pan-African geo-dynamic development in the Himalaya. Precambrian Research v. 74, pp. 35-55.

Valdiya, K.S. 1998. In: Dynamic Himalaya. Universities Press (India) Ltd, Hyderabad pp. 178.

Von Eynatten, H., Barceló-Vidal, C. and Pawlowsky-Glahn, V., 2003. Modelling compositional change: the example of chemical weathering of granitoid rocks. Mathematical Geology, v. 35, pp. 231–251.

Weltje, G.J., 1994. Provenance and dispersal of sand-sized sediments: reconstruction of dispersal patterns and sources of sand-size sediments by means of inverse modeling techniques, PhD thesis, Geologicaa Ultraiectina.

Weltje, G.J., Meijer, X.D. and De Boer, P.L., 1998 Stratigraphi.c inversion of siliciclastic basin fills: a note on the distinction between supply signals resulting from tectonic and climatic forcing. In: Hovius, N., Leeder, M. (Eds.), Thematic Set on Sediment Supply to Basins. Basin Research, v. 10, pp. 129– 153.

Weltje, G.J., 2002. Quantitative analysis of detrital modes: statistically rigorous

confidence region in ternary diagrams and their use in sedimentary petrology. Earth Science Reviews, v. 57, pp. 211–253.

White, N.M., Pringle, M., Garzanti, E., Bickle, M., Najman, Y., Chapman, H. and Friend, P., 2002. Constraints on the exhumation and erosion of the High Himalayan Slab, NW India, from foreland basin deposits. Earth and Planetary Science Letters, v. 195, pp. 29-44.

Willis, B.J., 1993a. Ancient river systems in the Himalayan foredeep, Chinji village area, northern Pakistan. Sedimentary Geology, v. 88, pp. 1-76.

Willis, B.J., 1993b. Evolution of Miocene fluvial systems in the Himalayan foredeep through a two kilometer-thick succession in northern Pakistan. Sedimentary Geology, v. 88, pp. 77–121.

Yoshida, M. and Arita, K., 1982. On the Siwaliks observed along some routes in Central Nepal. Journal of Nepal Geological Society, v. 2, (Spec. Issue), pp. 51-58.

Young, S. W., 1976. Petrographic textures of detrital polycrystalline quartz as an aid to interpreting crystalline source rocks. Journal of Sedimentary Petrology, v. 46, pp. 595–603.

Zaleha, M.J., 1997. Intra-and extrabasinal controls on fluvial deposition in the Miocene Indo Gangatic foreland basin, northern Pakistan. Sedimentology, v. 44, pp. 369-390.

Zuffa, G.G., 1985. Optical analysis of arenites: influence ofmethodology on compositional results. In: Zuffa, G.G. (Ed.), Provenance of Arenites: North Atlantic Treaty Organization, Advanced Study Institute Series 148. Reidel, Dordrecht, pp. 165–189.